



FEDERAL UNIVERSITY OF PARÁ  
INSTITUTE OF GEOSCIENCES  
GEOPHYSICS GRADUATE PROGRAM

DOCTORATE THESIS

**On the well-to-seismic-tie analysis: effects of the  
borehole geometry and assumptions on wavelet  
estimation**

ISADORA AUGUSTA SANTANA DE MACEDO

Belém - Pará  
2019

ISADORA AUGUSTA SANTANA DE MACEDO

**On the well-to-seismic-tie analysis: effects of the  
borehole geometry and assumptions on wavelet  
estimation**

Doctorate thesis submitted to the Geophysics Graduate Program of the Geosciences Institute at Federal University of Pará for the obtainment of the title of PhD in Geophysics.

Area of study: Seismic Methods

Advisor: Prof. Dr. José Jadsom Sampaio de Figueiredo

Belém - Pará  
2019

**Dados Internacionais de Catalogação na Publicação (CIP) de acordo com ISBD  
Sistema de Bibliotecas da Universidade Federal do Pará  
Gerada automaticamente pelo módulo Ficat, mediante os dados fornecidos pelo(a) autor(a)**

---

- M141o      Macedo, Isadora Augusta Santana de.  
              On the well-to-seismic-tie analysis: effects of the borehole geometry and assumptions on wavelet  
              estimation / Isadora Augusta Santana de Macedo, . — 2019.  
              140 f. : il. color.
- Orientador(a): Prof. Dr. José Jadsom Sampaio de Figueiredo  
              Tese (Doutorado) - Programa de Pós-Graduação Geofísica, Instituto de Geociências, Universidade Federal  
              do Pará, Belém, 2019.
1. Método de reflexão sísmica Deconvolução. 2. Perfilagem geofísica de poços. 3. Inversão (geofísica). I.  
              Título.

CDD 550

---

ISADORA AUGUSTA SANTANA DE MACEDO

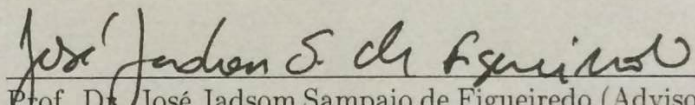
**On the well-to-seismic-tie analysis: effects of the borehole  
geometry and assumptions on wavelet estimation**

Thesis submitted to the Geophysics Graduate Program  
for the obtainment of the title of PhD in Geophysics.

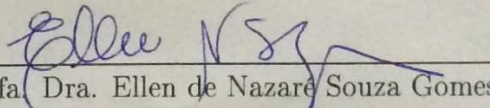
Approval Date: February 08, 2019

Grade: **10,0 (EXCELENTE)**

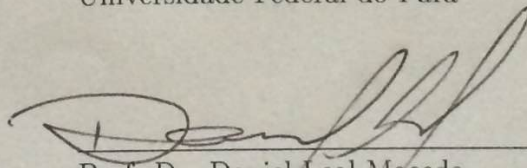
Comitte Members:



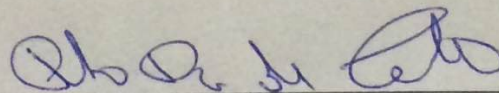
Prof. Dr. José Jadsom Sampaio de Figueiredo (Advisor)  
Universidade Federal do Pará



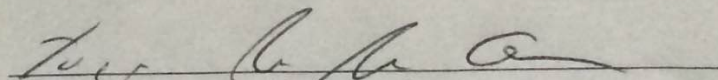
Prof. Dra. Ellen de Nazaré Souza Gomes  
Universidade Federal do Pará



Prof. Dr. Daniel Leal Macedo  
Universidade Federal do Pará



Prof. Dr. Paulo Roberto de Carvalho  
Universidade Federal Rural da Amazônia



Dr. Tiago Antonio Alves Coimbra  
Universidade de Campinas

To Zé Macedo, Deolinda and Bernardo.

## ACKNOWLEDGMENTS

I would like to express my sincere gratitude to the Federal University of Pará, especially to the Professors of the Faculty of Geophysics, who are responsible for my formation since the undergraduation.

I would like to thank Professor José Jadsom Sampaio de Figueiredo for all the knowledge shared, for his patience, assistance and motivation during the completion of this research, and to all the staff at the Post-Graduate Program of Geophysics.

I extend my sincere thanks to the comitte members for the valuable contributions to enhance the quality of this thesis.

I am also grateful to the institutions CAPES, CNPQ, INCT-GP for the financial support during this work.

## RESUMO

A amarração de dados de poço aos dados sísmicos - *well tie* - constitui uma etapa importante do processamento e interpretação sísmica uma vez que possibilita a conexão do dado sísmico com a geologia da subsuperfície. No entanto, no procedimento convencional de *well tie*, possíveis erros na aquisição dos dados de poço devido ao alargamento do diâmetro do poço não são levados em consideração e a modelagem do traço sísmico sintético é baseada nas premissas clássicas do modelo convolucional. Esta tese apresenta algumas ferramentas para melhorar a qualidade da amarração do *well tie* propondo 1) uma metodologia para corrigir os perfis de poço do efeito do alargamento do seu diâmetro durante a aquisição e uma abordagem para reduzir o ruído na refletividade através da distribuição de Benford 2) métodos de estimativa da wavelet sísmica que não supõe a refletividade como um processo aleatório e que não fazem suposições sobre a fase da wavelet. O foco deste trabalho é fornecer ferramentas que contornem algumas das objeções atualmente existentes no procedimento convencional de amarração de dados sísmicos aos dados de poço, possibilitando assim uma estimativa confiável das propriedades físicas da terra, etapa crucial da caracterização de reservatórios.

Palavras-chave: Método de reflexão sísmica - Deconvolução. Perfilagem geofísica de poços. Inversão (geofísica).

## ABSTRACT

The well-to-seismic-tie is a key step in seismic processing and interpretation since it provide the means to correctly connect the seismic data to the geology of the subsurface. It joins the information from the seismic surveys with the informations from the well log data. The conventional well-tie procedures, however, does not considers possible acquisition errors of well log data due to borehole enlargement, and the modelling of the synthetic trace is generally based on the classical premises of the convolutional model. This research present a few tools to enhance the quality of the well-to-seismic-tie by 1) proposing a form of correction of the density log for the borehole enlargement and a form to detect errors on the reflectivity through the Benford distribution 2) proposing wavelet estimations methods that does not imply a random process reflectivity or a minimum-phase wavelet. The focus of this study is to provide tools to circumvent some of the current objections to the conventional well tie procedure in order to have an accurate wavelet and a satisfactory seismic inversion, so that a reliable estimate of the Earth's physical properties can be made, which is crucial to the reservoir characterization.

Keywords: Seismic methods - Deconvolution. Well logging. Inversion (geophysics).

## LIST OF FIGURES

1.1	The research structure for the well-to-seismic-tie in this work: two articles - appended on Chapter 2 and Chapter 3 - related with the well log edition, and two articles - appended on Chapter 4 and Chapter 5 - related with wavelet estimation methods. . . . .	4
2.1	The research structure for the well-to-seismic-tie: the present article (in green), related with the well log edition. . . . .	6
3.1	The research structure for the well-to-seismic-tie: Chapter 2 and Chapter 3 (in green), related with the well log edition. . . . .	34
4.1	The research structure for the well-to-seismic-tie: Chapter 4 (in yellow), related with the wavelet estimation. . . . .	63
5.1	The research structure for the well-to-seismic-tie: Chapter 4 and Chapter 5 (in yellow), related with wavelet estimation. . . . .	85
6.1	Calculated reflectivity from well A, Viking Graben field and its conformity with Benford's law. a) Reflectivity without correction on density log for the borehole enlargement, mean absolute deviation around 0.0025. b) Reflectivity with correction on density log for the borehole enlargement, mean absolute deviation around 0.0023. . . . .	123
6.2	a) The recovered reflectivity from the seismic section near the well A when the regularization parameter that controls the sparsity of the solution is set to $\alpha = 0$ b) The Benford distribution of the estimated reflectivity from the seismic section for $\alpha = 0$ , a acceptable conformity with BL is achieved with a MAD of 0.0092. . . . .	125
6.3	a) The recovered reflectivity from the seismic section near the well A when the regularization parameter that controls the sparsity of the solution is set to $\alpha = 0.7$ b) The Benford distribution of the estimated reflectivity from the seismic section for $\alpha = 0.7$ , a close conformity with BL is achieved with a MAD of 0.0042. . . . .	126
6.4	a) The recovered reflectivity from the seismic section near the well B when the regularization parameter that controls the sparsity of the solution is set to $\alpha = 0$ b) The Benford distribution of the estimated reflectivity from the seismic section for $\alpha = 0$ , a acceptable conformity with BL is achieved with a MAD of 0.011. . . . .	127

6.5 a) The recovered reflectivity from the seismic section near the well B when the regularization parameter that controls the sparsity of the solution is set to  $\alpha = 0.1$  b) The Benford distribution of the estimated reflectivity from the seismic section for  $\alpha = 0.1$ , a close conformity with BL is achieved with a MAD of 0.0057. . . . . 128

# CONTENTS

1	INTRODUCTION	1
2	ARTICLE 1: USING THE BENFORD'S LAW ON SEISMIC REFLECTIVITY ANALYSIS	6
3	ARTICLE 2: DENSITY LOG CORRECTION FOR THE BOREHOLE EFFECTS AND ITS IMPACT ON SEISMIC-TO-WELL TIE: APPLICATION ON NORTH SEA DATASET	34
4	ARTICLE 3: ESTIMATION OF THE SEISMIC WAVELET THROUGH HOMOMORPHIC DECONVOLUTION AND WELL LOG DATA: APPLICATION ON WELL-TO-SEISMIC-TIE FROM NORTH SEA DATASET	63
5	ARTICLE 4: LINEAR INVERSION TO ESTIMATE THE SEISMIC WAVELET AND TO RECOVER THE REFLECTIVITY OF THE SEISMIC SECTION: WELL-TO-SEISMIC-TIE ON REAL DATASET FROM VIKING GRABEN, NORTH SEA.	85
6	DISCUSSION AND CONCLUSIONS	122
	Bibliography	130

# 1 INTRODUCTION

Establish a connection between the seismic data and the well log data is a fundamental step in seismic inversion and interpretation, which is called *well tie*. This is where key ambiguities that prevent the interpretation of a seismic image as band-limited reflectivity are resolved and is the best way to tie seismic data back to ground truth by comparison with well log data using synthetic seismogram. Through this tie, it is possible to guarantee that the seismic data is a reasonable estimate of the band-limited reflectivity of the subsurface, it is possible to estimate the source wavelet to be used in the inversion process or to be used as an input to the deconvolution to recover the reflectivity and correlate stratigraphic horizons. Also, if the final product from the seismic data processing is delivered in the depth domain, it provides very important seismic anisotropic information. The main essence of the well tie is the comparison of a synthetic trace with the real seismic trace from seismic surveys. The synthetic trace is the product of the convolution between the reflectivity series calculated from well logs with a wavelet, that must be estimated.

The required accuracy of a well-to-seismic-tie varies with the stage of using it. For regional mapping, the tie does not need to be very precise and the seismic data quality does not need to be high. It happens because the tie within 1 or 2 seismic cycles can map, for instance, a significant erosional unconformity or a flooding surface (Schroeder, 2006). In the exploration stage, where it is necessary to identify stratigraphic markers, it is required good seismic data quality and a high accuracy on the well-to-seismic-tie. In the exploitation stage of development and production, the shape of the real and synthetic seismic traces must be similar (Schroeder, 2006), and to achieve that, it is necessary a very good seismic data quality and a high accurate well-to-seismic-tie, to be possible to extract seismic attributes to predict rock and fluid properties and proper estimate the seismic wavelet to be used in the inversion to transform the seismic data into an estimate of the reflectivity or the rock's physical properties.

The connection between the well log and seismic data is done through the comparison between the real seismic trace and the synthetic seismic trace. This last is the product of the convolution between the seismic wavelet and the reflectivity series calculated from the sonic and velocity profiles. Well log measurements of velocity and density provide a link between seismic data and the geology of the substrata and the first set of assumptions that is used to build the forward model for the seismic trace follows (Yilmaz, 2000):

**Assumption 1:** the earth is made up with horizontal layers with constant velocity;

**Assumption 2:** the source generates a compressional wave that hits the interface of the reflector with a normal incidence angle.

The first assumption is violated in complex structurally areas when the layers of rocks plunge over others or areas with gross lateral velocity changes. The second assumption implies the unrealistic zero-offset recording situation. However, those assumptions allows the reflection coefficient of the interface between two different layers to be defined as:

$$r_i = \frac{\rho_{i+1} v_{i+1} - \rho_i v_i}{\rho_{i+1} v_{i+1} + \rho_i v_i}, \quad (1.1)$$

where  $\rho$  is the density from the well log measurements,  $v$  is the P-wave velocity from the sonic log and  $i$  represents the index of the samples in depth. The reflectivity  $r_i$  calculated in depth is placed in the time domain,  $r(t)$ , through the application of the correct time-depth relationship, that generally uses checkshot surveys or VSP data. The compressional wave generated by the impulsive source can be described as a band-limited wavelet of finite duration. As it propagates into the subsurface, its amplitude decays due to wavefront divergence and its frequency content suffers the effects of the attenuation. The non-stationarity of the wavelet, however, is not incorporated in the forward model for the seismic trace: it is considered to be stationary, which defines the third assumption.

**Assumption 3:** the seismic wavelet is stationary.

Based on the three assumptions above, the convolutional model can be written as:

$$x(t) = r(t) * w(t) + \eta(t), \quad (1.2)$$

where  $x(t)$  indicates the model seismic trace,  $r(t)$  is the earth's impulse response,  $w(t)$  is the stationary seismic wavelet and  $\eta(t)$  represents the random noise present on the seismogram. The random noise has two main characteristics: 1) a white amplitude spectrum and 2) an autocorrelation function small at all lags except at zero lag, which is a positive spike. For the equation (1.2) be solvable, the following assumptions are made:

**Assumption 4:** the noise component  $\eta(t)$  is zero;

**Assumption 5:** the wavelet  $w(t)$  is known.

With those new assumptions, the new equation to build the forward model for the seismic trace is:

$$x(t) = r(t) * w(t). \quad (1.3)$$

In order to have a successful well-to-seismic-tie, the seismic wavelet  $w(t)$  must be estimated. The literature concerning wavelet estimation methods fall largely into two categories: (1) purely statistical ways and (2) the use of well-log data (White and Simm, 2013), this last also referred as wavelet extraction or deterministic wavelet extraction. The deterministic methods require direct measurements of the source wavefield or the use of both real seismic trace and well log data (Oldenburg et al., 1981; Yilmaz, 2000). The statistical methods are based on mathematical tools to solve the problem of wavelet estimation using only the real seismic trace. For the conventional well-to-seismic-tie procedure, if the wavelet was not measured directly during seismic data acquisition, new assumptions must be made to solve equation (1.3):

**Assumption 6:** the earth's impulse response is a random process;

**Assumption 7:** the seismic wavelet is minimum-phase.

The earth's impulse response is not entirely a random process. It does not have the same characteristics as the random noise in the Fourier domain: its amplitude spectrum is not white and its autocorrelation function is not a spike at zero lag and approximately null at the other lags. The amplitude spectrum of the wavelet and the amplitude spectrum of the seismic trace, however, are similar, which suggests that if the amplitude spectrum of the earth's impulse response was white, one could use the amplitude spectrum of the real seismic trace, which is known, in the place of the amplitude spectrum of the seismic wavelet, which is unknown. The same happens with the autocorrelation function: by assuming a random process reflectivity, it is possible to use the autocorrelation of the seismogram in the place of the autocorrelation of the unknown seismic wavelet. A random process reflectivity and a minimum-phase wavelet allows the estimate of the wavelet through filtering in the Fourier domain and through a large class of deconvolution problems using the Wiener filtering technique, which is optimum in the least squares sense. However, taking assumptions (6) and (7) into account for the well-to-seismic-tie procedure to estimate the wavelet, are limiting factors that might contribute to damage the quality of the tie.

Since data processing is designed to estimate reflectivity, one might hope that well-tying would happen automatically with modern algorithms (Margrave, 2013). However, this is not generally observed to be the case. A few objections to the standard well-tie procedure can be highlighted, such as doubtful quality log information caused by washout zones or borehole enlargement that may not represent true values of formation density and velocity; available well log information might be insufficient for well tie; matching is usually done to primary reflectivity and there may be multiples in the seismic data;

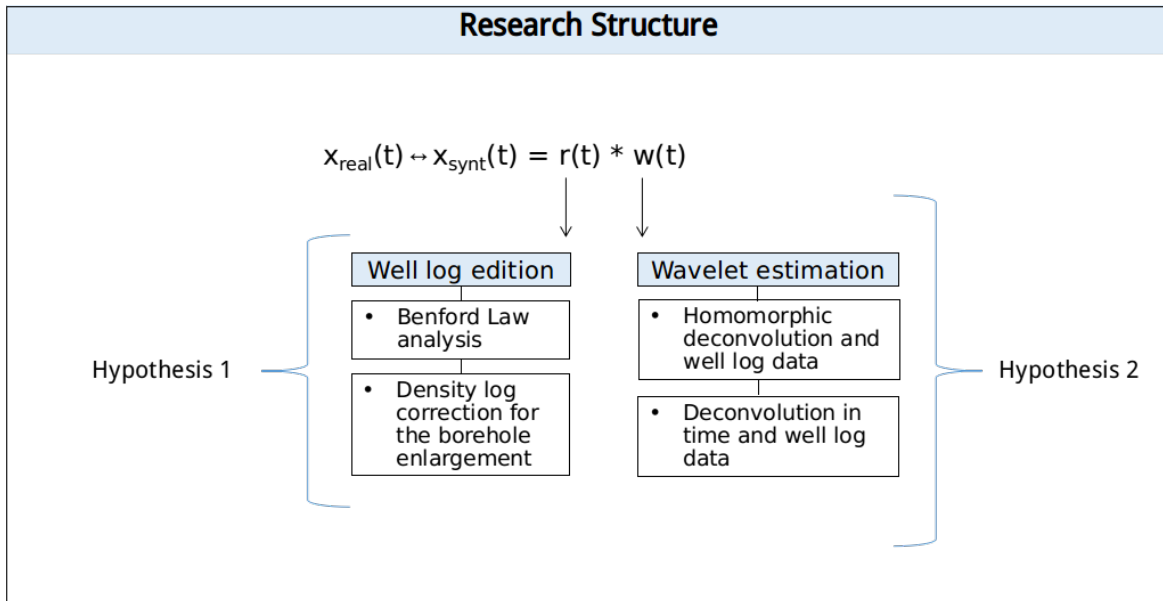


Figure 1.1: The research structure for the well-to-seismic-tie in this work: two articles - appended on Chapter 2 and Chapter 3 - related with the well log edition, and two articles - appended on Chapter 4 and Chapter 5 - related with wavelet estimation methods.

the synthetic trace may have been through a stretch-squeeze process to best fit the real seismic data which can produce a high correlation but is not recommended; when multiple wells are available, different wavelets are often obtained from each; the wavelet might have its accuracy compromised depending on the assumptions made to the method to estimate it; the data used to establish the time-depth relationship might be damaged and can compromise the well tie since time displaced events might be correlated one to the other.

Based on a well-to-seismic-tie on the real dataset from the Viking Graben field, in the North Sea (Macedo, I. A. S. de et al., 2017), two hypothesis guide this thesis:

**Hypothesis 1:** zones with poor well tie quality might be related with zones of washouts or borehole enlargement, indicated by anomalies on the caliper log. Errors related with borehole environment are not considered in the standard quality control of well logs for well-to-seismic-tie, since the habitual process of noise-despiking aims to eliminate only the environmental noise, but do not correct the tool physical properties measurements for the drilling mud invasion.

**Hypothesis 2:** methods to estimate the wavelet that assumes a random process reflectivity and a minimum-phase wavelet, characteristics of the classical assumptions of the convolutional model, might also affect the quality of the well-to-seismic-tie.

This thesis contains four articles appended on each chapter and its structure is illustrated on Figure 1.1. The articles of the Chapter 2 and Chapter 3 are related with the well log edition for the well-to-seismic-tie and the interference of the borehole enlargement; the articles of the Chapter 4 and Chapter 5 are related with wavelet estimation methods that does not imply a random process reflectivity or a minimum-phase wavelet. The Chapter 6 is dedicated to combining the methodologies proposed in each article, to show the improvement achieved on the quality of the well-to-seismic-tie at each step of this research, and also to discuss its future purposes. The goal we aim to reach is provide tools to circumvent some of the current objections to the conventional well tie procedure in order to have an accurate wavelet and a good seismic inversion, so that a reliable estimate of the Earth's physical properties can be made, which is crucial to the reservoir characterization.

## 2 ARTICLE 1: USING THE BENFORD'S LAW ON SEISMIC REFLECTIVITY ANALYSIS

Authors: Isadora Augusta Santana de Macedo, José Jadsom Sampaio de Figueiredo.

Published on *Interpretation*, August 2018.

<https://doi.org/10.1190/INT-2017-0201.1>

Presented at the 15th International Congress of the Brazilian Geophysical Society, Rio de Janeiro, Brazil, 31 July - 3 August 2017.

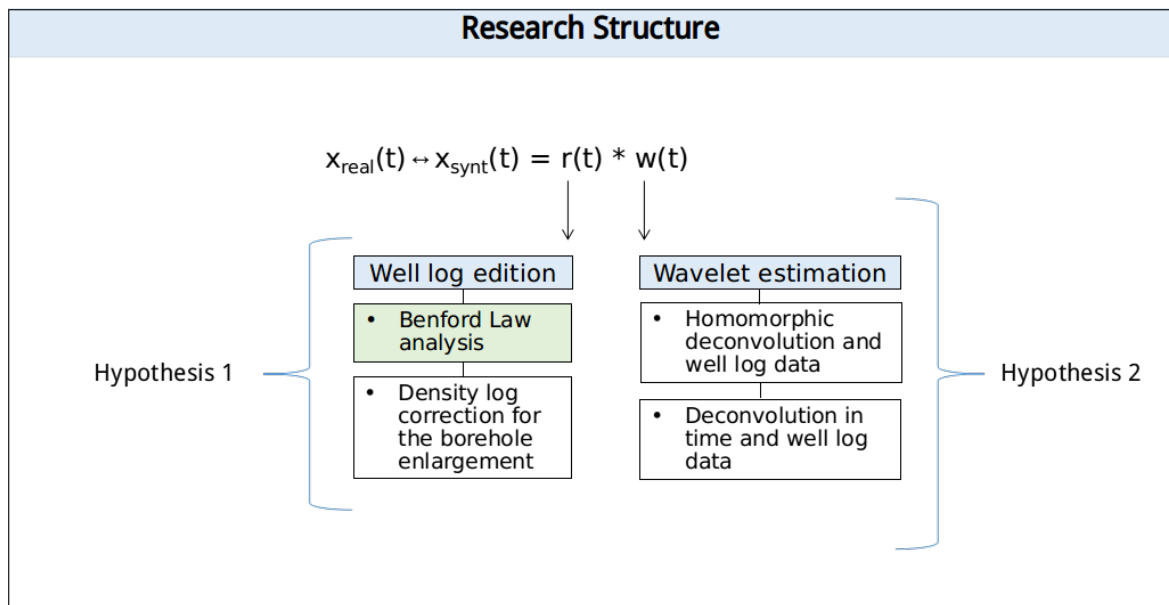


Figure 2.1: The research structure for the well-to-seismic-tie: the present article (in green), related with the well log edition.

The first goal of this study was to perform an analysis of Earth's reflectivity calculated from well log data, whose product resulted in the article appended in this chapter, entitled "Using the Benford's law on the seismic reflectivity analysis", published by the *Interpretation* journal in august 2018 (Macedo, I. A. S. de and J. J. S. de Figueiredo, 2018).

We show that the reflectivity calculated through well logs obeys the Benford's law, a phenomenological law used to detect errors and frauds in data sets of different natures, including data from geosciences (Sambridge et al., 2010; Geyer and J. Martí, 2012; Sottili et al., 2012).

Through the compliance of the Earth's reflectivity with Benford's law, we find an optimal coefficient for the despiking procedure of density and velocity log data. As well as Macedo, I. A. S. de et al. (2017) demonstrated that zones with a stable caliper profile

produce a better quality in the well tie, we show that zones with stable caliper profiles produce a reflectivity series with greater conformity with Benford's law, which encourages further studies of this law in geosciences and propose Benford as a tool to assist checking the quality of density and velocity well log data with respect to the profiling environment.

# Using Benford's law on the seismic reflectivity analysis

Isadora A. S. de Macedo <sup>\*†</sup> and J. J. S. de Figueiredo <sup>\*†</sup>

*\*UFPA, Faculty of Geophysics, Belém (PA), Brazil,*

*†National Institute for Petroleum Geophysics (INCT-GP), Brazil*

(May 15, 2018)

Running head: **Benford Law applied to well-log reflectivity**

## ABSTRACT

The Benford's Law (BL) is a mathematical theory of leading digits. This law predicts that the distribution of first digits of real-world observations is not uniform and follows a trend where measurements with lower first digit (1,2,...) occur more frequently than those with higher first digits (...8,9). Data set from Earth's geomagnetic field, estimated time in years between reversals of Earth's geomagnetic field, seismic P-wave speed of Earth's mantle below the southwest pacific and other geophysical data obey the BL. Although there are other statistical methods for analyzing data set, in this work, for the first time, we test the analysis of the seismic reflectivity through the Benford distribution point of view. We applied the BL on real reflectivity data from two wells from Penobscot field, and other two from Viking Graben field. In both data sets, the reflectivity was in conformity with the BL. Moreover, after analyzing the effect of sonic and density logs despiking on Benford's distribution through the BL, we found an optimum coefficient for the despiking process, which is a common procedure used to edit the well log data before its use on reservoir studies.

## INTRODUCTION

The Benford's Law (BL) (Benford, 1938) is a phenomenological law used in many branches of biological (Friar et al., 2012; Crocetti and Randi, 2016), economics (Sehity et al., 2005) and natural (Sambridge et al., 2010) sciences. It states that in many different data sets of real world observations without human interference, the probability of occurrence of the number 1 as the leading digit that represents the measurement of the data set is higher than the probability of occurrence of any other number as the leading digit that represents the measurement addressed.

The first person to observe this pattern was the American astronomer Simon Newcomb, who empirically derived what is known as the Benford's Law. Newcomb (1881) published those conclusions in 1881 in the "Note on the Frequency of Use of the Different Digits in Natural Numbers". The physician Frank Benford, in 1938, rediscovered this behavior of numbers on different data sets (Benford, 1938). He analyzed the digit patterns of different data sets with a total of 20,229 observations. The results showed that 30.6 percent of the numbers had a 1 as the first digit, 18.5 percent of the numbers had a 2 as the first digit, with 9 being the first digit only 4.7 percent of the time. This pattern of distribution of numbers was named after him and is commonly referred to as the *Benford Distribution*, *Benford's Law* or *The Power of One*, due to the high probability of occurrence of the number 1. The complete mathematical proof of the BL was published in 1995 by Theodore Hill on the paper "Base-invariance implies Benford's law" (Hill, 1995). Based on simulation evidence and measured datasets, studies showed that large classes of naturally occurring quantities (preferentially log-uniform distributed data) are expected to follow the BL. The literature on the BL in general either advances the existing mathematical and statistical theory behind

the law, or shows new practical applications in data sets never tested before.

BL was first used in the detection of human manipulation in reported data for auditing purposes (Nigrini, 1999), and became popular in the detection of fraud in finance data and tax returns because finance numbers follow the BL, and that human manipulation of such data shows up as anomalies in Benford distribution. Besides that, it also has been applied to natural science data. Sambridge et al. (2010) showed the conformity with the BL of several natural science datasets, such as the length of time between geomagnetic reversals, depths of earthquakes, models of Earth's gravity and geomagnetic and seismic structures. Sottili et al. (2012) applied the BL on approximately 17,000 seismic events in different geological contexts, and found that the deviation from a close conformity with the BL may be ruled by a periodical noise factor on those data, such as the effects of Earth tides on seismicity tuning. Nigrini and Miller (2007) applied the BL to hydrology data and found that the non-conformity with the BL may be due to data errors, inconsistencies and anomalies on the data set. Yang (2016) used the BL to characterize noise in airborne transient electromagnetic data. Geyer and Molist (2012) noticed that anomalies in volcanological data sets may be detected when comparing the data with Benford's law expected frequencies.

The potential utility of the BL on detecting errors on data sets is the first motivation behind this work. Regarding geophysical studies using well log data, the first step in any project is the well log audit and edits. In all cases the log data will require some editing (denoising, for example), normalization, and interpretation before they can be used in a reservoir study or well-seismic-ties applications. A key factor to the well profiles interpretation is the log corrections, which are necessary, assuming that there are many issues about the borehole conditions (Serra, 1994). An example of that is the interaction between the drilling fluid and the formations around the borehole, which is a relevant factor

for the in-depth acquisitions, especially concerning the density log whose precision is directly related to the well-tie response as described by Macedo et al. (2017).

We calculated several reflectivities series from density and sonic well logs from different geological settings and we show, for the first time, that the reflectivity calculated from well log data is in conformity with the Benford's Law, and we further test the potential utility of using the statistical BL on the seismic reflectivity analysis. We will show the results of the Benford's analysis on real data from two wells of the Penobscot field (located Canada-Scotian Shelf approximately 60 km to the southwest) and two wells of the Viking Graben field (located at North Sea), where we analyzed the effect of sonic and density logs despiking on the Benford's distribution, since it is a common procedure before its use on reservoir studies. The results on real data show that it is possible to find an optimum coefficient for the despiking process on the well logs according to the conformity of the BL on the reflectivity calculated from the well logs.

## METHODOLOGY

In this section, we describe our analysis on well-log reflectivity based on the BL. The following sections show how to calculate the conformity of a data set with the BL, and how to calculate the reflectivity. Then, we show how the optimum despiking factor is calculated followed by numerical experiments on the real data from the Penobscot and the Viking Graben fields.

## Benford's Law

The Benford's Law is also known as first digit law, and is an observation of the frequency distribution of leading digits in many sets of numerical data. The first digit of a number is the leftmost non-zero digit, where the minus sign and decimal points are ignored. Benford (1938) noticed the logarithmic pattern in the distribution of digits and derived the formulas for the expected frequencies of the digits:

$$P_D = \log_{10} \left( 1 + \frac{1}{D} \right), \quad (1)$$

where  $P_D$  is the probability of occurrence of the first digit (non-zero), and  $D=1, 2, 3, \dots, 9$ .

To measure the fit between the BL prediction with the values of the real distribution, we use the mean absolute deviation (MAD), because of its practical use in real world observations since it is not dependent on the number of records. The MAD test is described by:

$$MAD = \frac{\sum_{i=1}^K |AP - EP|_i}{K}, \quad (2)$$

where  $K$  represents the quantity of significant digits (which equals to 9 for the first digits),  $AP$  denotes the actual proportion - the actual occurrence of digits, and  $EP$  denotes the expected proportion - the occurrence of digits expected according to the BL.

Nigrini and Wells (2012) established the boundary values for the mean absolute deviation (MAD) that verify whether the data set is in conformity with the BL or not:

- MAD < 0.006 : close conformity;
- MAD < 0.012 : acceptable conformity;
- MAD < 0.015 : marginal conformity;
- MAD > 0.015 : non conformity.

We used those criteria to verify the conformity of the reflectivity calculated from the well logs with the BL.

## Sonic Reflectivity

The earth is composed of rock layers with different lithology and physical properties. From the seismic point of view, these layers are represented by different densities and velocities through which seismic waves propagate. The product of density and velocity is the seismic impedance and it is the impedance contrast between adjacent rock layers that causes the reflections that are recorded along a surface profile (Yilmaz, 2000).

We considered the classical assumptions of the convolutional model of the Earth to compute the reflectivity series. It is considered that the earth is made up of horizontally deposited layers of constant velocity and that an impulsive seismic source generates a compressional pressure wave (P-wave) that interacts on layer boundaries with normal incidence. The reflection coefficient  $R_c$  associated with the boundary between layers is defined as:

$$R_c(i) = \frac{\rho_{i+1}v_{i+1} - \rho_i v_i}{\rho_{i+1}v_{i+1} + \rho_i v_i}, \quad (3)$$

where  $\rho$  is the density,  $v$  is the interval velocity, the product  $\rho v$  is the acoustic impedance which can be directly calculated from the density and sonic logs, and  $i$  is the increment that represents each point in depth.

In order to analyze the reflectivity through the BL in this work, we first verify the minimum size required for the data to be in conformity with the BL, since this number varies according to the nature of the data. The second step is to find an optimum factor for the despiking process. The procedure to perform the despiking in this work is to set a limit value for the difference between the measured points at the same depth of the original log

and the smoothed log, as can be seen on Figure 1. This limit value represents the maximum possible difference between the highest and the lowest possible values of the log after the despiking at each depth point. In other words, if the difference at each point between the original log and the smoothed log is within this limit value, we assume that for this point, the original log is valid, and therefore we do not need to use the smoothed version. However, if the difference is beyond this limit value, we assume that for this point we are dealing with a noisy spike, and therefore we use the smoothed version of the log. Setting this limit value is a way to control the despike so it does not get underestimated, and an attempt to correct the noisy spikes but by using as much of the original log as possible. The smoothed log was obtained through the application of a moving average filter using a window with 100 points. We chose a window of 100 points because it maintains the general trend of the log and at the same time, it removes the noisy spikes. We recommend, however, to only use the measurements of this smoothed log when necessary in order to preserve as much as the original log information as possible.

## **NUMERICAL EXPERIMENTS ON REAL WELL-LOG DATA**

The first data analyzed was acquired in two wells from Penobscot field designated as B-41 and L-30 located in Canada. The second data set analyzed was two well logs designed as A and B from Viking Graben field, located in North Sea. The Penobscot field can be subdivided into two reservoir regions. The reservoir region south of the main Penobscot fault contains the L-30 well, which recovered oil and gas from several zones and two separate untested accumulations located to the north and northeast. The Verrill Canyon shales are believed to be the source rock for the Penobscot structure. The main fault system exhibits evidence of early movement within the Jurassic period. This early movement may have

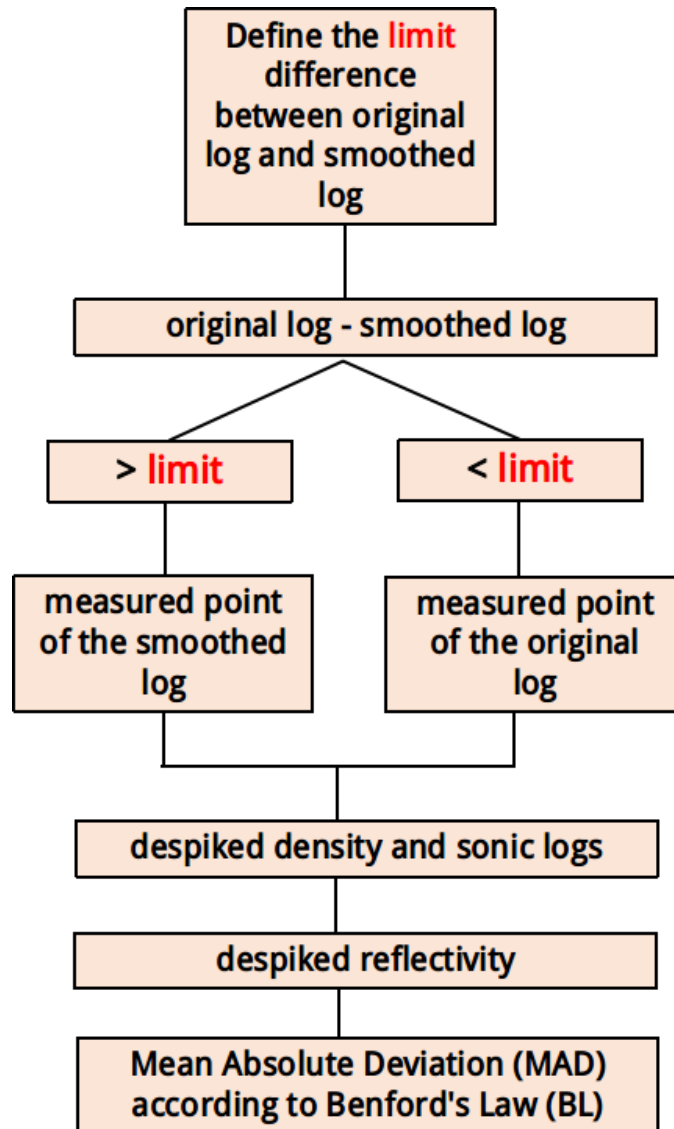


Figure 1: Flowchart describing the despiking procedure used in this work as well as the process to find its optimum limit. The limit (in red) is the maximum possible difference between the original log and the smoothed log. It is possible to find this optimum limit value based on the Benford analysis.

created a conduit for the migration of generated hydrocarbon fluids into the system (Clack and Crane, 1992).

The North Viking Graben was formed as a result of late Permian to Triassic rifting; extensional episodes and accompanying sedimentation continued through the Jurassic into the Early Cretaceous. The extensional episode in the beginning of Jurassic causes the Pangea to break into two continents, Gondwana and Laurasia. During this period the sea level rose. The burial of algae and bacteria below the mud of the seafloor resulted in the formation of the oil and gas in the North Sea (Macedo et al., 2017). The Jurassic was a period of active faulting; hydrocarbon traps are usually fault-bounded structures, but some are associated with stratigraphic truncation at the unconformity at the base of the Cretaceous (Keys and Foster, 1998).

Figures 2 and 3 show the original and the despiked density, compressional velocity ( $V_P$ ) and reflectivity data using the BL as a criteria to define the maximum possible difference between the original and smoothed logs to perform the despiking. For the Viking Graben field, the maximum possible difference between the original and the smoothed log - also referred as *limit difference* between the logs - to perform the despiking is 145 for well log A and 225 for well log B. For the Penobscot field the limit difference between the original and the smoothed log for the despiking process is 165 for well log B-41 and 225 for well log L-30. These limit values produced despiked densities and velocities logs that generated reflectivities series in closest conformity with the BL. Figure 4 shows the results of the frequency distribution of the reflectivity series for all the data sets.

Assuming that the synthetic random noise can represent the nature of the noise present in the real borehole environment, we show that this kind of noise does not follow the Benford

distribution while the correct data itself does. The reflectivity (original and despiked with our limit difference criteria) for both data sets follows the trend of the Benford distribution. Assuming that where the caliper log is unstable the noise level rise due to acquisition problems, we expect that the reflectivity on those specific segments lose conformity with the Benford distribution, as we will show later. To define the degree of conformity with the BL we used the mean absolute deviation criteria described by equation (2).

### **Data size and despiking analysis**

As the number of samples in the data have a significant influence on the Benford distribution (Nigrini, 1999), we generate a curve to analyze how many samples of data are necessary to have the reflectivity series in close conformity (mean absolute deviation lower than 0.006) with the Benford distribution. It is important to highlight that for the random noise data, even if we increase the number of samples, it is still in non conformity with the BL. The results shows that the conformity with the BL increases with the number of samples, but the number of samples varies for different datasets, as shown on the Figure 5. We believe that the number of samples required for the data set to be in conformity with the BL is related to the measurement errors and the nature of noise that are specific of each borehole, and are also related to the geology in the vicinity of the well. This might be the reason why different number of samples of reflectivity are required even when we are dealing with wells that are close to each other: different boreholes imply different scenarios of measurements, and although the wells are close, they do not represent exactly the same lithology. For the logs from the Penobscot field, the reflectivity is in close conformity with BL when reaching 4700 samples for both B-41 and L-30 logs. For the Viking Graben field, the reflectivity is in close conformity with BL when log A reaches 5700 samples and log B reaches 3900 samples.

Figure 6 shows that it is possible to find an optimum limit value for the difference between the original log and the smoothed log when performing the despiking process as described in the flowchart on Figure 1. This is feasible because the random noise does not follow the Benford trend while the real reflectivity measurements do. The procedure to perform the despiking in this paper is to set a maximum limit value for the difference between the original and smoothed logs for density and sonic profiles. If the difference between the points of the original and the smoothed logs, for a measurement at the same depth, exceeds that maximum limit, the value of the smoothed log is used. However, if the difference of the measured points does not exceed that limit, the value of the original log is used. Some important considerations must be made in this step. Firstly, we used the sonic and density logs together to find the optimum limit. Therefore, the same limit value for the difference of spikes is used in both logs. Secondly, in order to do so, it is necessary that both logs are in the same unit system: the sonic log in  $m/s$  and the density log in  $kg/m^3$ , so that the same factor can be used to despike both logs with consistency.

For all curves of MAD versus limit value for the difference between original log and smoothed log, there was a local minimum (the limit value for the difference between original and smoothed log), which indicates the best limit value to use in the despiking process since it has the closest conformity with the BL (MAD lower than 0.006). For all our testing data, this local minimum were geologically consistent. By geologically consistent we mean that the limit value found for the despike process did not produce a despiked density or sonic log that underestimated or overestimated values for the rocks we know. In Figure 6a for the logs of the Penobscot field, it is possible to notice that for the well B-41, the limit value for the spikes is 165 ( $m/s$  or  $kg/m^3$ ) and it produced a reflectivity with a close conformity with the BL, with a MAD of 0.003032. For the well L-30, the limit value for the spikes is

195( $m/s$  or  $kg/m^3$ ) and it produced a reflectivity in close conformity with the BL, with a MAD of 0.001548. Regarding the Viking Graben field, the limit for the spikes for well A was 145 ( $m/s$  or  $kg/m^3$ ) and for the well B was 225 ( $m/s$  or  $kg/m^3$ ). Those limit values produced a reflectivity in close conformity with the BL with a MAD of 0.003143 for well A and 0.00199 for well B.

### **Caliper analysis**

Macedo et al. (2017) suggested that well-logs acquisition during drilling may create anomalies in the density and velocity measurements which can be verified in caliper log. This may lead to a low correlation in the well-to-seismic-tie in the Viking Graben dataset. Therefore, in this study we checked on the data from the Viking Graben field if the portions where the caliper log is unstable, the conformity with the BL decreases. The results are shown in Figure 7. We made this test only on well A of the Viking Graben field that has portions of unstable caliper log because the caliper log of well B is reasonably stable throughout the whole profile as can be seen in Figure 3b.

On the previous sections we showed that the data set requires a minimum number of samples to be in conformity with the BL and that this number varies according to the data set. At this point of our work, to analyze the stability of the caliper log with the Benford distribution, we segmented the reflectivity in different portions by grouping a certain number of samples obeying the minimum number of samples we found earlier. Moreover, in order to isolate the influence of the caliper stability criteria on BL, the segmented portions of reflectivity have the same number of samples. This is the reason why we choose not to isolate the stable and unstable portions of the reflectivity according to the caliper only: our

previous results have already shown that the number of samples affects the mean absolute deviation.

Macedo et al. (2017) showed that the well-to-seismic-tie has a better quality on the portions where the caliper log is stable. Our result shows that the conformity with the BL is higher on the portions of reflectivity where the caliper log is stable as well. On segment 1 of the Viking Graben data set where the caliper is unstable, the mean absolute deviation from BL was 0.0062, which is an acceptable conformity. On segments 2 and 3, where the caliper log is well behaved, the results showed a close conformity with the BL, with a MAD of 0.0033 and 0.0059 respectively.

Figure 8 shows that the segment with the lower correlation coefficient  $c_1 = 0.409$  corresponds to the zone where the caliper log is unstable, which directly affects the sonic and density measurements and, consequently, affects the quality of the well-to-seismic-tie directly. Keys and Foster (1998) mentioned about the problems on the Viking Graben data set acquisition along the well A, which might be related with this anomalous zone on the caliper log. This first segment is associated with the lithology of the formation above the Cretaceous unconformity at 1.97s. The Paleocene and Cretaceous rocks above the unconformity are deep water clastic sediments. Since they are deposited in a slope in the basin, the formation contain turbidites. In the second segment where  $c_2 = 0.805$ , and third segment where  $c_3 = 0.839$ , it is possible to note that when the caliper log gets more stable, the correlation increases although the shale content also increases due to the Jurassic rocks associated with deepwater shales. The correlation coefficient of the well-to-seismic-tie is calculated through the cross-correlation, which measures the similarity of two random vectors as function of the displacement of one to the other. In general, when dealing with synthetic seismic traces, the shale content contributes to decreasing the correlation.

In order to verify whether our methodology is coherent, we also test the conformity of the reflectivity affected by the caliper anomalies seen in the well logs from the Penobscot field. Figures 9a and 9b show the results. We segmented the reflectivity according to the caliper in three different portions. These wells have two different caliper logs, one related to the density tool and another related to the sonic tool. The expected geometry of the borehole is a cylinder of radius size similar to the drill bit, with a smooth inner surface. Irregularities along the borehole due to unconsolidated formations affect the signals recorded by the logging tool, which in this situation are more related to the drilling mud than to the formation. The stability of the caliper log is related to whether or not there was a difference in the diameter of the borehole along the acquisition, and to possible noisy spikes that may appear on the caliper log.

For the well B-41 (see Figure 2a), the sonic caliper is unstable throughout the entire profile. In the first segment the diameter of the borehole increased, and in the other segments it is contaminated with noisy spikes. Both situations indicate the instability of the tool during the acquisition. The density caliper for the same well is stable only in the segment 2. For the well L-30 (Figure 2b), the opposite happens: the density caliper is unstable throughout the entire profile while the sonic caliper is stable only in segment 2. The segments 1 and 3 in both well logs have noisy and unstable calipers that suggest instability during the drilling that might affect the measurements of the density and velocity logs.

The results on the Penobscot field follows the previous conclusions: the conformity with the BL is higher in terms of the mean absolute deviatio where the caliper is stable. The results for the wells from the Penobscot field show that on the segments where one of the caliper logs are unstable, the reflectivity moves away from the Benford distribution while on the segments where both caliper logs are stable, the reflectivity gets in close conformity with

the BL. Well B-41 segment 2, which has a stable density caliper, has the highest conformity with a MAD of 0.0026. Well L-30 segment 2, which has a stable sonic caliper, is the one with the highest conformity with the BL with a MAD of 0.0034. For all the tests we made, we used the despiked reflectivity using our optimum limit value for the difference between the original and the smoothed measured points (see Figures 2 and 3) to show that the despiking itself does not correct for the borehole enlargement or collapse especially for the cases of well-to-seismic-tie, and that the BL might be used as an indicator of compromised measurements on the logs.

## CONCLUSIONS

In this work we show for the first time that the BL has a potential utility on the analysis of the seismic reflectivity. Based on our test, the reflectivity from both real data sets were in close conformity with BL. Moreover, from our tests, it was noticed that the number of samples necessary for the reflectivity to follow the BL is of the order of thousands. For the Penobscot field it is around 4700 samples and for the Viking Graben field, it is around 5700 for well log A and 3900 for well log B. Using the BL we show that it is possible to find a optimum limit difference between original and smoothed logs when performing the despiking process. For Viking Graben field, the optimum limit for the despiking was 145 for well A, and 225 for well B; for the Penobscot field, it was 165 for well B-41 and 195 for well L-30.

For all the curves MAD X limit value of the difference between the original and the smoothed logs, we show that there exists a local minimum indicating the optimum difference value to be used for the despiking process, and this local minimum for all the tests we have performed is geologically consistent. In addition, our results show that on the portions

where the caliper log is unstable, the measurements of densities and velocities are compromised, and it affects the conformity of the reflectivity with the BL. We showed, based on the BL, that the despiking itself does not correct for the borehole enlargement or collapse because on the portions where the caliper log is unstable, the conformity of the reflectivity with the BL decreases.

For future works, the authors suggest developing an algorithm to find the optimum limit value for the difference between logs that use the density log and the sonic log individually, since in this paper, this optimum limit was found considering both logs at the same time. It would be also interesting to analyze if a correction on the reflectivity series for the enlargement or collapse of the borehole affects the Benford distribution. Finally, our analyses encourage the application of the BL in different geophysical data sets due its coherent results with a simple and direct implementation.

## ACKNOWLEDGMENTS

The authors would like to thank the Exxon Mobil for providing the Viking Graben dataset and the Nova Scotia Department of Energy for providing the Penobscot dataset. This work was kindly supported by the Brazilian agencies CAPES, INCT-GP and CNPQ. We would like to thank Rodrigo Portugal by the important discussions on BL. Also, We also would like to thank the Associate Editor Dr. Gaurav Dutta, and to Yunfei Yang and other two anonymous reviewers for many helpful comments and suggestions.

## REFERENCES

- Benford, F., 1938, The Law of Anomalous Numbers \ Logarithm: Proceedings of the American Philosophical Society, **78**, 551–572.
- Clack, W. J. F., and J. D. T. Crane, 1992, Penobscot prospect: geological evaluation and oil reserve estimates: Report for Nova Scotia Resources (Ventures) Ltd.
- Crocetti, E., and G. Randi, 2016, Using the Benford’s Law as a First Step to Assess the Quality of the Cancer Registry Data: *Frontiers in Public Health*, **4**.
- Friar, J. L., T. Goldman, and J. Pérez-Mercader, 2012, Genome Sizes and the Benford Distribution: *PLoS ONE*, **7**.
- Geyer, A., and J. M. Molist, 2012, Applying Benford’s law to volcanology: *Geology*, **40**, 327–330.
- Hill, T. P., 1995, Base-invariance implies benford’s law: Proceedings of the American Mathematical Society, **123**.
- Keys, R. G., and D. J. Foster, 1998, Comparison of seismic inversion methods on a single real data set, open file publications: Society of Exploration Geophysics, 233.
- Macedo, I. A. S., C. B. da Silva, J. J. S. de Figueiredo, and B. Omoboyac, 2017, Comparison between deterministic and statistical wavelet estimation methods through predictive deconvolution: Seismic to well tie example from the North Sea: *Journal of Applied Geophysics*, **136**, 298–314.
- Monroe, J. T., J. J. S. de Figueiredo, and L. K. Santos, 2015, Seismic attributes analysis for the identification and characterization of hydrocarbon reservoirs - revisiting the viking graben dataset: 893–897.
- Newcomb, S., 1881, Note on the frequency of use of the different digits in natural numbers: Proceedings of the American Mathematical Society, **4**, 39–40.

- Nigrini, M., 1999, I've got your number: *Journal of Accountancy*, **187**, 79.
- Nigrini, M., and S. J. Miller, 2007, Benford's Law Applied to Hydrology Data—Results and Relevance to Other Geophysical Data: *Mathematical Geology*, **39**, 469–490.
- Nigrini, M., and J. T. Wells, 2012, Benford's law: Applications for forensic accounting, auditing, and fraud detection: Wiley.
- Parsley, J. A., 1990, North sea hydrocarbon plays, in glennie, k. w., ed., introduction to the petroleum geology of the north-sea: Blackwell Scientific Publications.
- Sambridge, M., H. Tkalcic, and A. Jackson, 2010, Benford's law in the natural sciences: *Geophysical Research Letters*, **22**, L22301.
- Sehity, T., E. Hoelzl, and E. Kirchler, 2005, Price developments after a nominal shock: Benford's Law and psychological pricing after the euro introduction: *International Journal of Research in Marketing*, **22**, 471–480.
- Serra, O., 1994, Fundamentals of well logging interpretation - 1. the aquisition of logging data: Elsevier, volume **15A** of *Development in Petroleum Science*.
- Sottili, G., D. M. Palladino, B. Giaccio, and P. Messina, 2012, Benford's Law in Time Series Analysis of Seismic Clusters: *Mathematical geosciences*, **44**, 619–634.
- Yang, D., 2016, Characterization of noise in airborne-transient electromagnetic data using benford's law: *SEG Technical Program Expanded Abstracts*, 1043–1047.
- Yilmaz, O., 2000, *Seismic data analysis: processing, inversion, and interpretation of seismic data*: SEG Books.

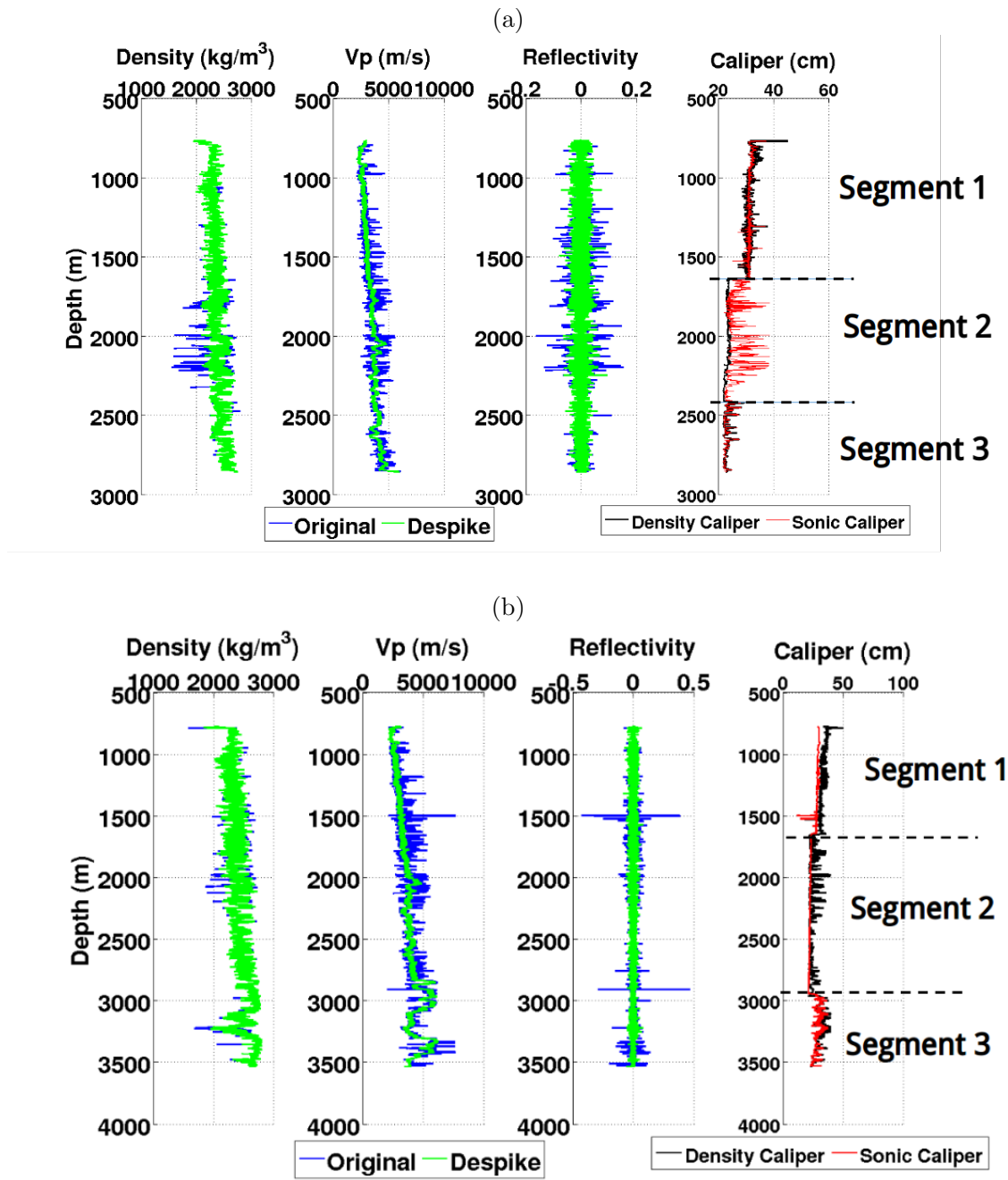


Figure 2: Well logs (a) B-41 and (b) L-30 from Penobscot field used in the Benford analysis. The segmentation of the caliper logs is to analyze how the reflectivity behaves in relation to the Benford distribution according to the stability of the caliper log. The despiking operation was done using the optimum limit value for difference between the original log (in blue) and the despiked log (in green) according to the BL.

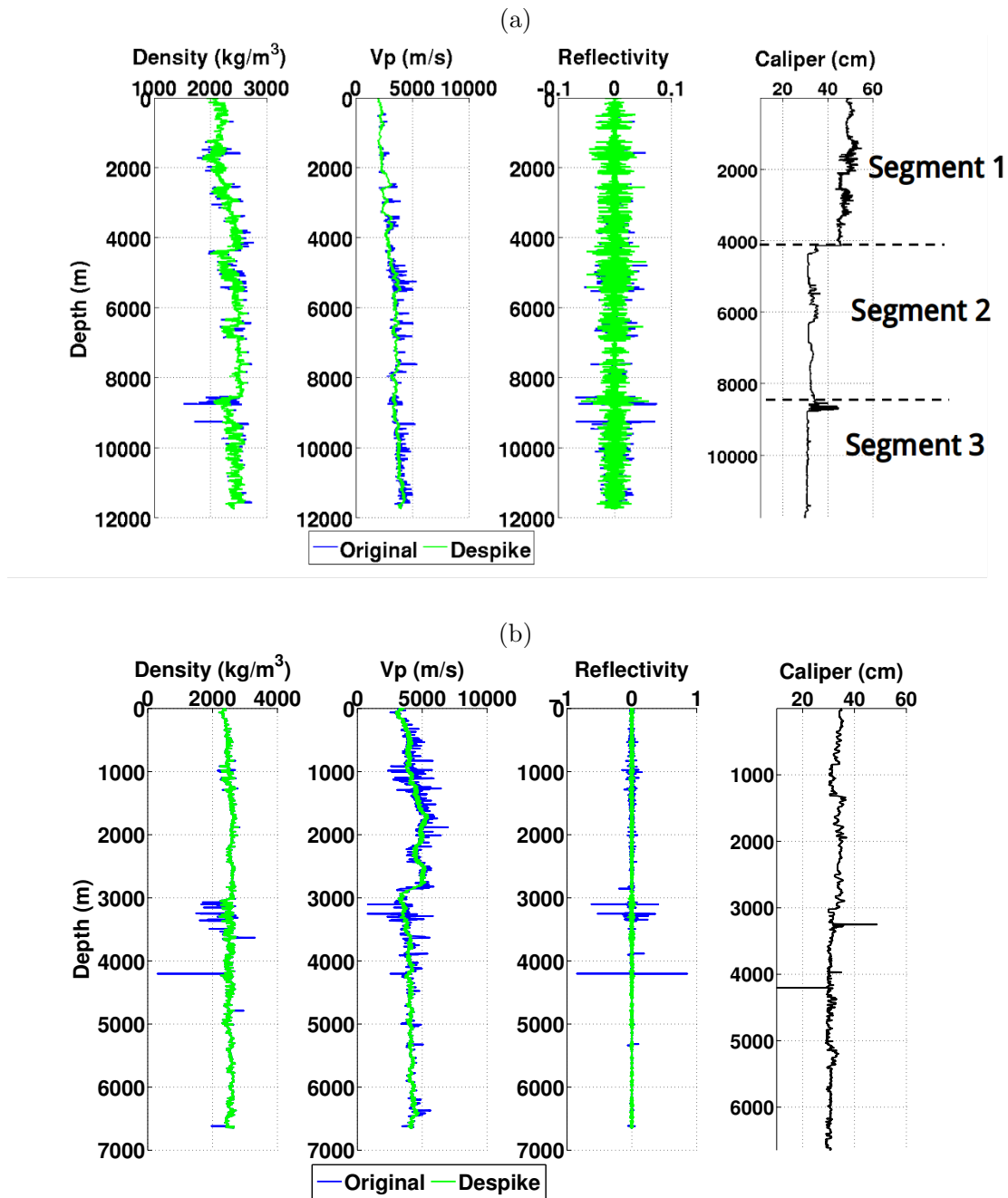


Figure 3: Well logs (a) A and (b) B from Viking Graben field used for Benford analysis and the density caliper logs. The segmentation of the caliper log in the well A is to analyze how the reflectivity behaves in relation to the Benford distribution according to the stability of the caliper log. As the caliper log of the well B is reasonably stable throughout the hole profile, it is not segmented. The despiking operation was done using the optimum limit value for difference between the original log (in blue) and the despiked log (in green) according to the BL.

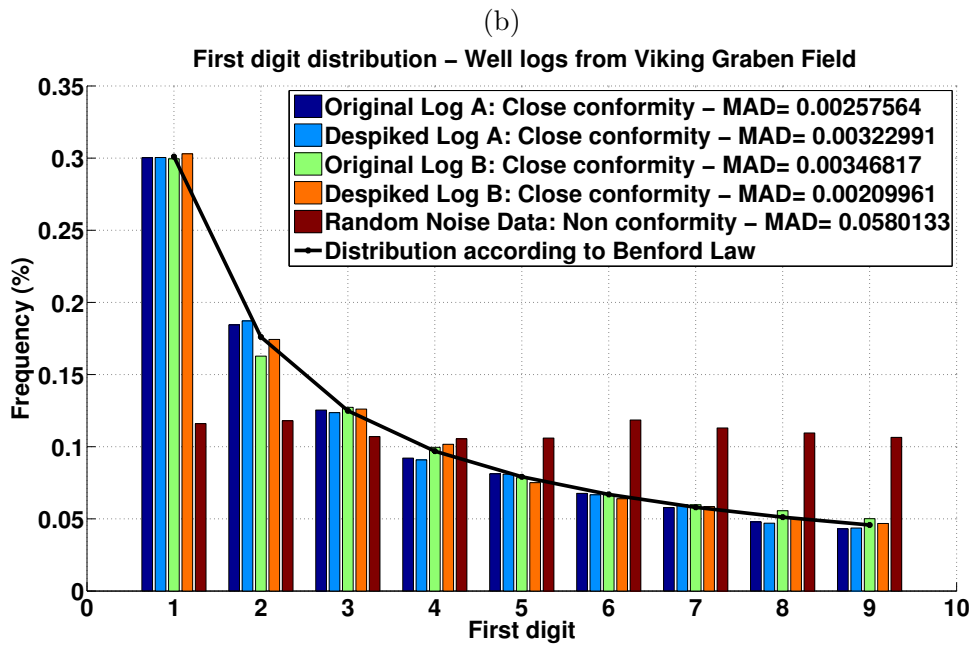
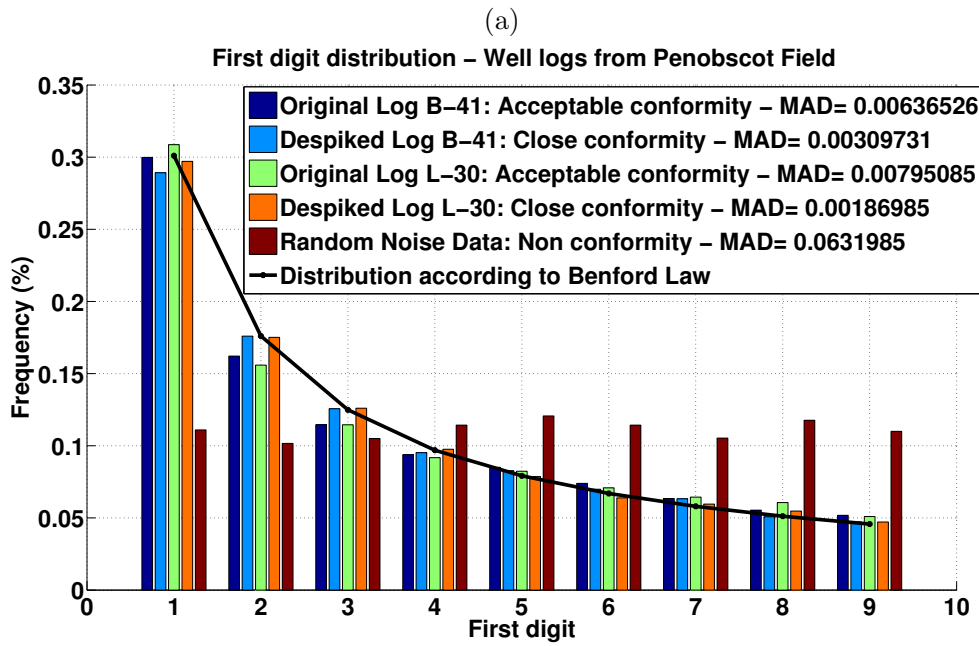


Figure 4: Frequency distribution of the first digits of the reflectivity series. (a) Well logs from Penobscot field and (b) Well logs from Viking Graben field.

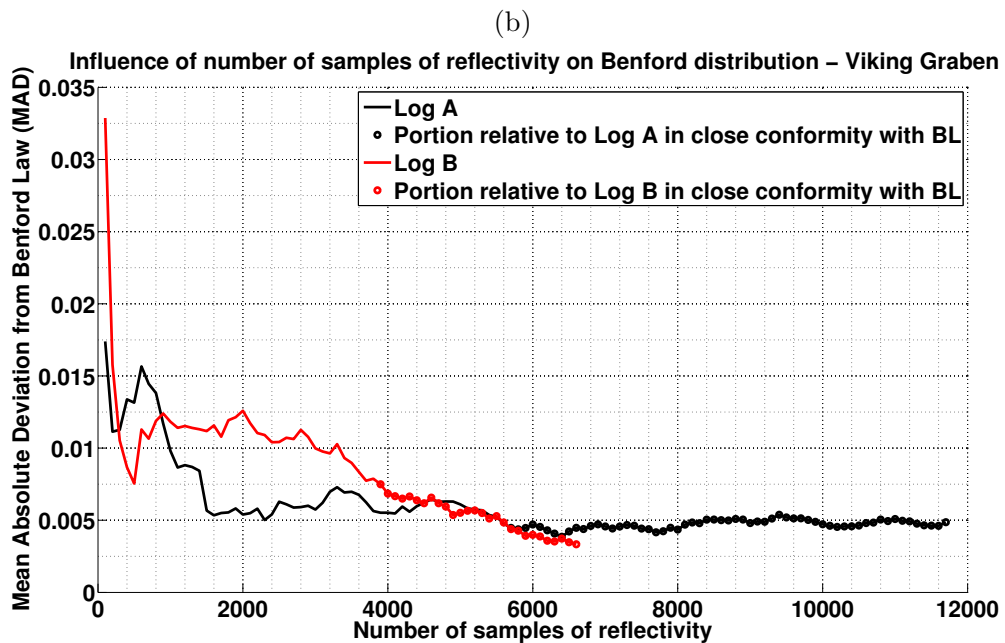
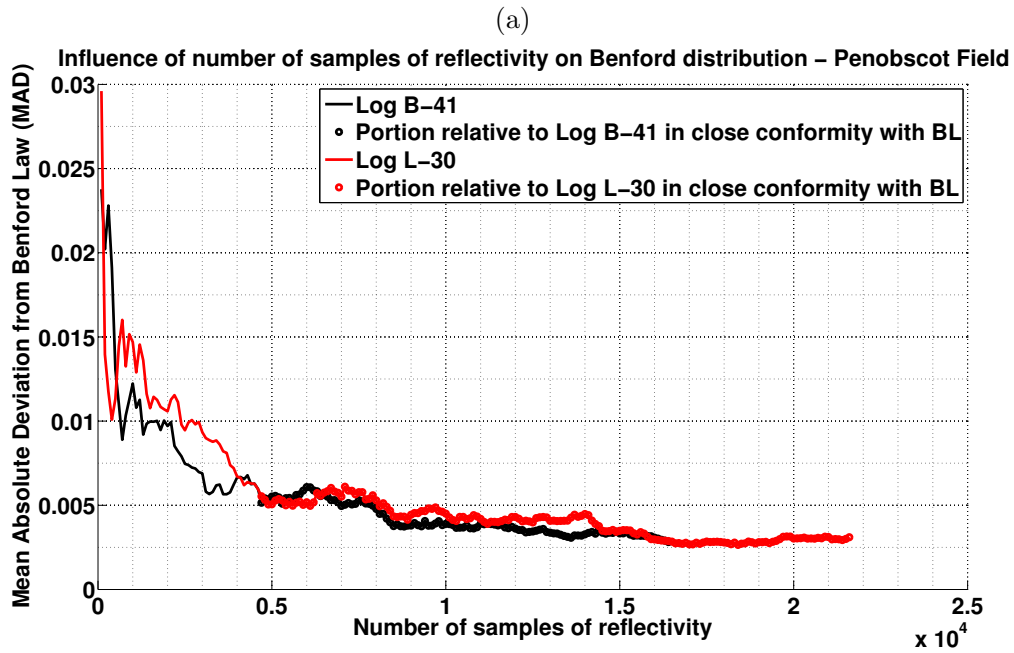


Figure 5: Curves indicating the influence of the number of samples of reflectivity on Benford distribution. It shows the minimum number of samples from which the mean absolute deviation stays stabilized below 0.006 - close conformity. a) Well logs from Penobscot field: the reflectivity is in close conformity with BL when reaching 4700 samples for both B-41 and L-30 logs b) Well logs from Viking Graben field: the reflectivity is in close conformity with BL when log A reaches 5700 samples and log B reaches 3900 samples.

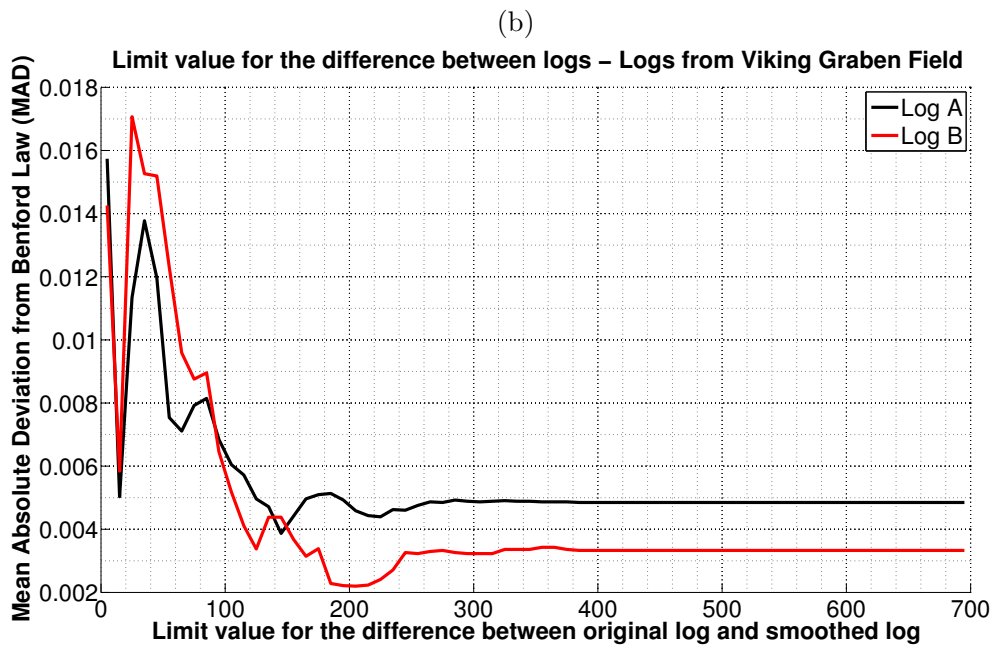
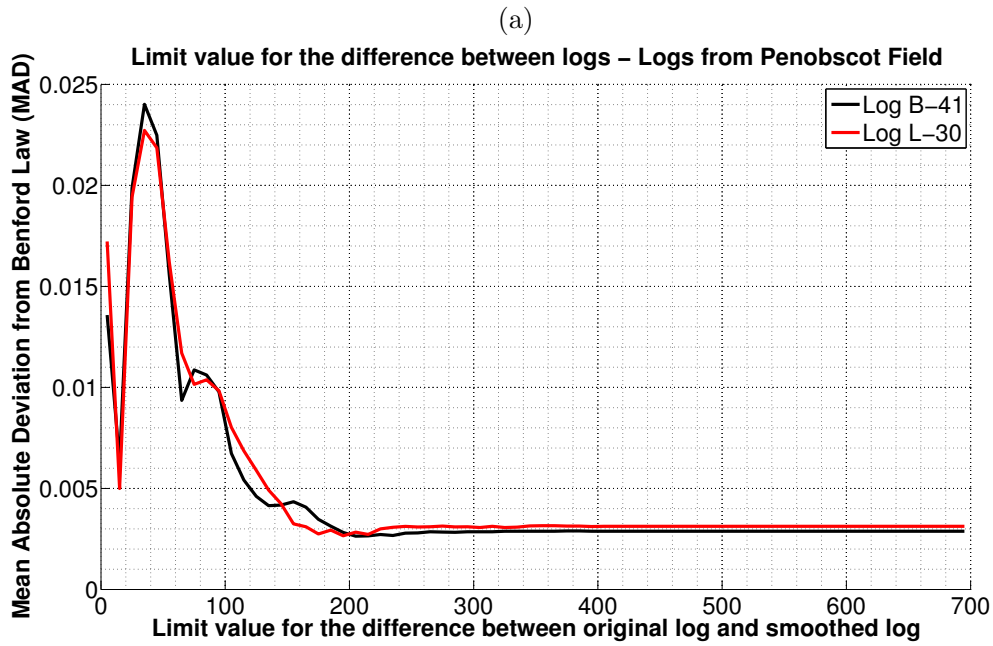


Figure 6: Curves indicating which limit for the spikes on the logs produces the higher conformity of reflectivity with the BL in terms of the mean absolute deviation (MAD) a) Well logs from Penobscot field. Log B-41: limit value of 165 and MAD 0.003032. Log L-30: limit value of 225 and MAD 0.001548. b) Well logs from Viking Graben field. Log A: limit value of 145 and MAD 0.003143. Log B: limit value of 225 and MAD 0.00199.

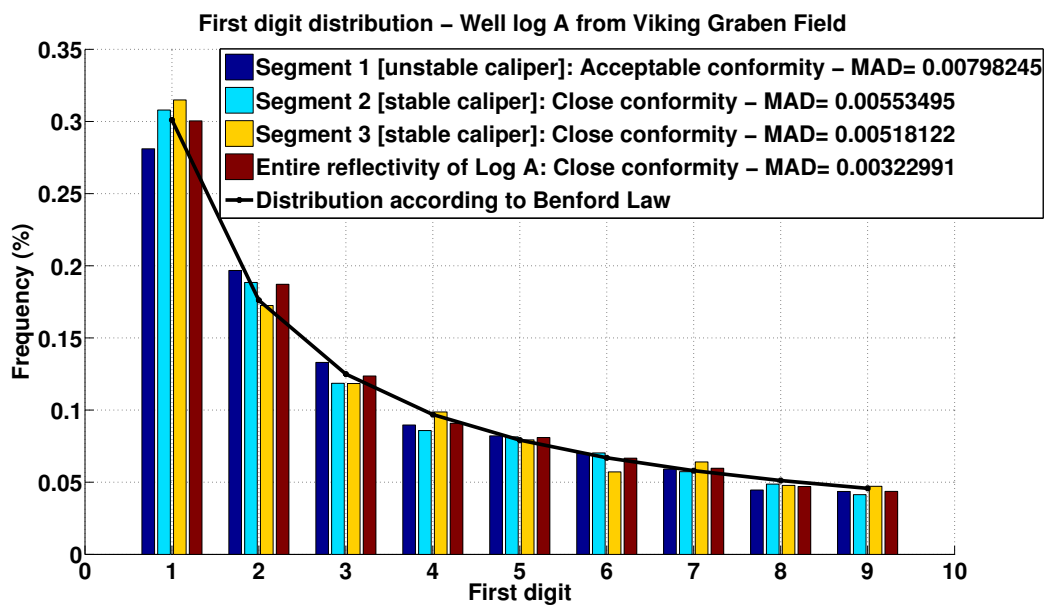


Figure 7: The Benford distribution for each segment of reflectivity (see Figure 3) according to the caliper response of Well A from the Viking Graben field.

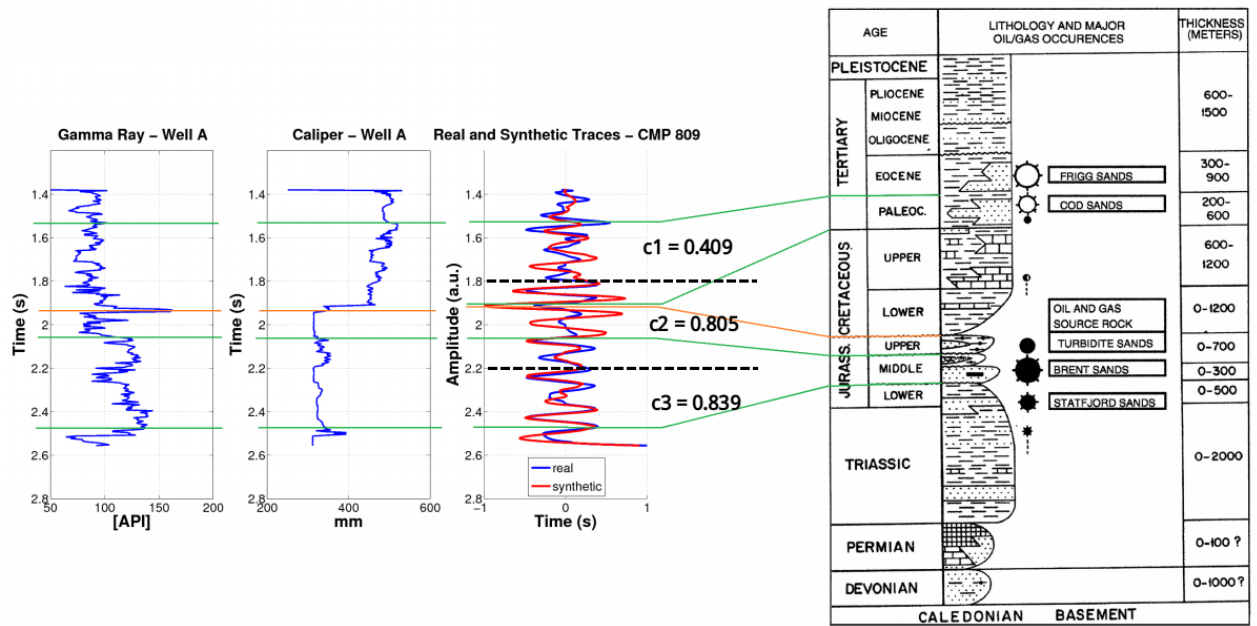


Figure 8: Well-to-seismic-tie for the synthetic trace from well A with correspondent trace of migrated seismic section shown in Monroe et al. (2015) and Macedo et al. (2017). Stratigraphic column for northern North Sea from (Parsley, 1990). The best estimated wavelet was obtained by deterministic estimation in Macedo et al. (2017).

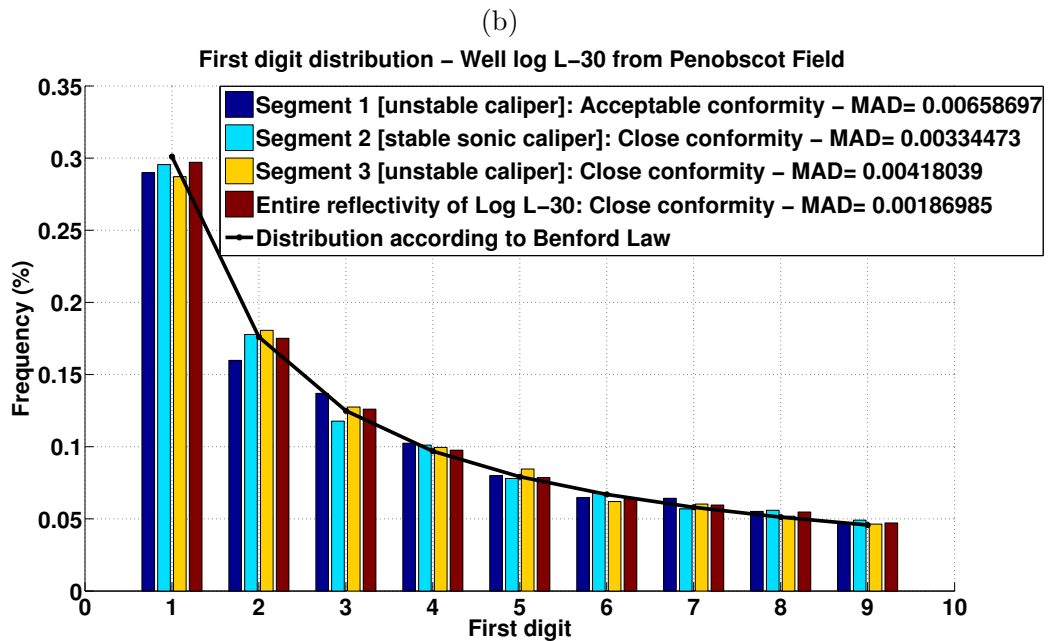
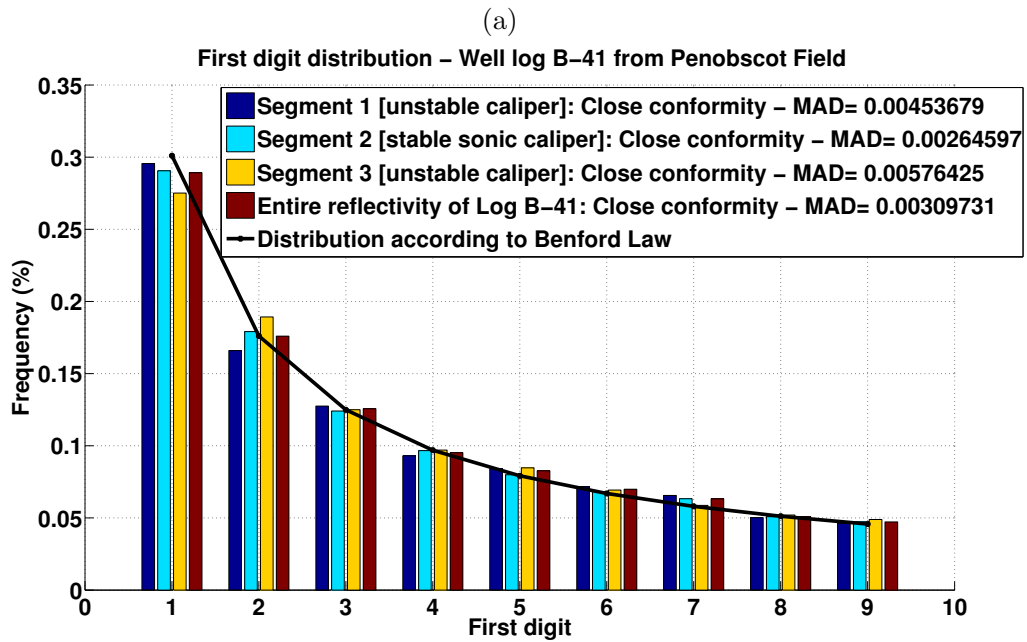


Figure 9: The Benford distribution for each segment of reflectivity according to the caliper response on the logs of the Penobscot field for logs a) B-41 and b) L-30.

### 3 ARTICLE 2: DENSITY LOG CORRECTION FOR THE BOREHOLE EFFECTS AND ITS IMPACT ON SEISMIC-TO-WELL TIE: APPLICATION ON NORTH SEA DATASET

Authors: Isadora Augusta Santana de Macedo, Matias Costa de Sousa , Murillo José de Sousa Nascimento, José Jadsom Sampaio de Figueiredo.

Under revision at the Interpretation journal

Presented at the 15th International Congress of the Brazilian Geophysical Society, Rio de Janeiro, Brazil, 31 July - 3 August 2017.

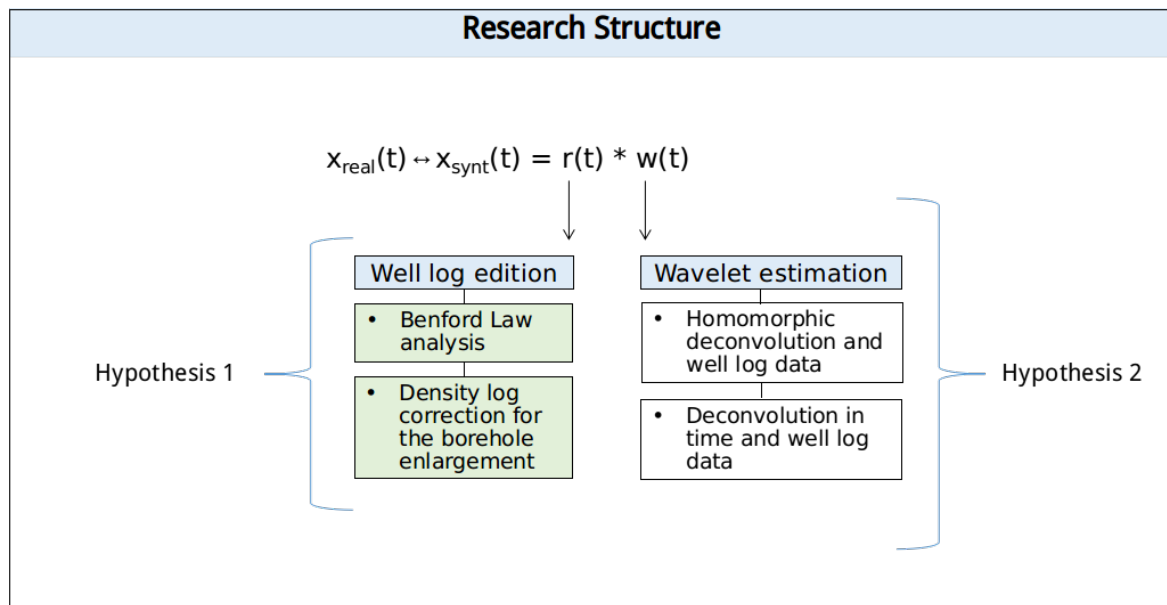


Figure 3.1: The research structure for the well-to-seismic-tie: Chapter 2 and Chapter 3 (in green), related with the well log edition.

The second part of this work consists in proposing a way to correct the density tool measurement for the borehole enlargement or shrink, followed by the verification of the correction effect on well-to-seismic-tie. The result of this approach is in the article entitled "Density log correction for the borehole effects and its impact on seismic-to-well tie: application on North Sea data set".

When the cave ins occurs along the borehole, it is assumed that the medium around the well is composed of the mud filtrate and the formation. As in Doll's geometric factor theory for the induction tool, it can be inferred that each concentric region around the well have a different weight and a different density value, so that the density measured by the tool is the sum of the individual contribution of each concentric zone. By establishing

these weights (named  $G_{mud}$  in the article) from priori informations and properties relative to the depth of investigation of the tool, we correct the density profile for each point in depth and then perform well-to-seismic-tie. Our results show that the accuracy of the tie in terms of correlation increase when the corrected density log is used.

# Density log correction for the borehole effects and its impact on seismic-to-well tie: application on North Sea data set

Isadora A. S. de Macedo <sup>\*†</sup>, Matias C. de Sousa <sup>\*†</sup>, Murillo José de Sousa Nascimento <sup>\*†</sup> and J. J. S. de Figueiredo <sup>\*†</sup>

*\*UFPA, Faculty of Geophysics, Belém (PA), Brazil,*

*†National Institute for Petroleum Geophysics (INCT-GP), Brazil*

## GEO-Example

Running head: **Density log correction and its impact on seismic-to-well tie**

## ABSTRACT

The reservoir characterization require accurate elastic logs. It is necessary to guarantee that the logging tool is stable during the drilling process in order to do not compromise the measurements of the physical properties in the formation in the vicinity of the well. Irregularities along the borehole may happen specially if the drilling device is passing through unconsolidated formations, which affects the signals recorded by the logging tool, and the measurement may be more related with the drilling mud than the lithology. The caliper log indicates the change in the diameter of the borehole with depth and might be an indicator of the quality of other logs whose data may be degraded by the enlargement or shrink of the borehole wall. Damaged well log data, specially density and velocity profiles, might affect the quality and accuracy of the well-to-seismic tie. Although corrections on density log sometimes are neglected, meaningful improvements on the correlation of the seismic-to-well tie can be achieved by performing proper rectifications. In order to investigate the impacts of borehole enlargement on the well-to-seismic tie, an analysis on density log correction was performed. This approach uses the Doll's geometric factor to correct the density log for wellbore enlargement using the caliper readings. Since the wavelet is an important factor on well tie, we tested our methodology with a statistical and a deterministic wavelet estimation. For both cases, the results on the real dataset from the Viking Graben field - North Sea, show a meaningful improvement on the correlation of the well-to-seismic tie

when compared to the case where no corrections on the density log are made.

## INTRODUCTION

The well-to-seismic-tie is an important tool in seismic inversion and interpretation since it can joint the vertical resolution of the well logs with the horizontal resolution of the seismic data, enabling the identification of stratigraphic markers on the seismic section and the correct estimate of the wavelet to be used to invert the seismic data to reflectivity or impedance. In general, the basic principle behind a well tie is to compute a synthetic seismic trace and further compare it with the real seismic trace. The convolutional model is the basis for the most well tie procedures, since it establishes a relationship between the reflectivity function calculated from the well log data, the seismic wavelet and the synthetic seismic trace. According to White and Simm (2003), the methods to estimate the seismic wavelet are divided in two categories: deterministic and statistical. The first require direct measurements of the source wavefield or the use of the well log data (Oldenburg et al., 1981; Yilmaz, 2000). Statistical methods estimate the wavelet from the seismic trace itself and depending on the approach used, might require assumptions about the characteristics of the wavelet (Buland and Omre, 2003; Lundsgaard et al., 2015), such as its amplitude spectrum or phase. The main factors controlling the accuracy of the well-to-seismic-tie are the seismic wavelet, a coherent time-depth relationship to be applied on the reflectivity, and the accuracy of the elastic well log data to compute the reflectivity series.

An accurate well tie or characterization of any reservoir require accurate elastic logs. The in-depth information provided by the wireline procedures, when tied properly to the data acquired by surface surveys, allows the interpreters to verify whether their geological conclusions about the seismic background are suitable to the observed lithology parameters (White and Hu, 1998). A central matter to the well profiles interpretation are the log corrections, which are necessary, assuming that there are many issues about the borehole conditions (Serra, 1994). The size of the borehole is one of the most obvious factors of environmental effect on the well measurements, whose corrections must be applied to preserve the meaning of the log values (Ellis and Singer, 2007). Although the stability of the wellbore is controlled during the drilling process, non-predicted occurrences of formation collapsing might change the distribution of the physical property of interest around the

wellbore, causing a logging distortion that can be solved by correcting the data segments that have anomalous caliper values. This borehole effect implies log distortions, including density irregular measures that result from the formation original components combined to the mud filtrate (Liu and Zhao, 2015). This interaction of the drilling fluid and the formations around the wellbore is a relevant factor to be concerned for the in-depth acquisitions, especially regarding the density log, whose precision is directly related to the well-to-seismic-tie response, a central matter of this study. An expanded borehole or an irregular wellbore wall may affect the density log curve so markedly that the curve drops precipitously, and the measured density value is much lower than the true density value (Yong and Zhang, 2007).

Macedo et al. (2017) analyzed the influence of the stability of the borehole diameter during acquisition on the well-to-seismic-tie and showed that anomalies on the caliper logs can directly affect the quality of the tie and consequently, the estimated wavelet. Within this scenario, the present paper aims to analyze the well-to-seismic-tie response when the proper corrections on the density log for the wellbore enlargement are made. These corrections are based on Doll's geometric factor. To verify the feasibility of our proposed methodology, we performed well-to-seismic tie on the real dataset from the Viking Graben field - North Sea with and without density log correction. We also appraise the response of the well-to-seismic tie for two different methods of wavelet estimation, deterministic and statistical, this last, made through the predictive deconvolution and based on the classical assumptions of the convolutional model of the earth.

## THEORY

### Well-to-seismic-tie procedure

To perform the well-to-seismic-tie, it is necessary to calculate the synthetic seismic trace; therefore, it is necessary to calculate the reflectivity series generated by changes of impedance  $I = \rho V_p$  within the earth and then convolve it with a wavelet. The reflectivity

is created directly from the sonic log and bulk density curves, according to equation 1

$$R_c(i) = \frac{\rho_{b_{i+1}}v_{i+1} - \rho_{b_i}v_i}{\rho_{b_{i+1}}v_{i+1} + \rho_{b_i}v_i}, \quad (1)$$

where  $i$  represents the index of a sample in depth,  $R_c$  is the reflectivity,  $v$  is the P-wave velocity and  $\rho_b$  is the bulk density.

The reflectivity 1 calculated in depth through the well logs needs to be in the time domain to be convolved with the seismic wavelet, and it can be achieved by the application of the proper time-depth relationship, which can be done by checkshot surveys or VSP data. The next step is to convolve the reflectivity and the seismic wavelet to create the synthetic seismogram, according to equation 2, where  $s(t)$  is the synthetic trace,  $w(t)$  is the estimated wavelet and  $r(t)$  is the reflectivity in time.

$$s(t) = w(t) * r(t). \quad (2)$$

## Density Log Measurements

As shown by equation 1, the acquisition of the bulk density curve is of paramount importance to calculate the contrast of acoustic impedance. Therefore, a good sense of when a density measurement can be trusted is necessary. The density estimated by the logging tool is based on back-scattering (from Compton scattering) gamma radiation emitted by a radioactive source, such as  $Cs^{137}$  or  $Co^{60}$ . The gamma rays emitted from a source will interact with the electrons of the formation. The higher the electron density of the formation the higher the number of collisions of the gamma-rays with the electrons and, consequently, the lower the intensity of gamma-rays detected by the sensor. The intensity of gamma-rays detected is expressed by:

$$I = I_o e^{-\mu\rho_e L}, \quad (3)$$

where  $I$  is the intensity of gamma-rays detected by the scintillometer,  $I_o$  is the intensity of gamma-rays at the source,  $\mu$  is a constant that depends on the geometry of the tool,  $\rho_e$  is the density of electrons of the formation, and  $L$  is the distance between the source and the

detector. The electron density ( $\rho_e$ ) and the bulk density ( $\rho_b$ ) of the formation are related through the following equation:

$$\rho_e = \rho_b \frac{Z}{A} N, \quad (4)$$

where  $Z$  is the atomic number,  $A$  is atomic mass and  $N$  is the Avogadro number ( $6.023 \times 10^{23}$ ). Since for the majority of the formations ( $\frac{Z}{A} \approx \frac{1}{2}$ ), equation 4 becomes

$$\rho_e = \rho_b \frac{N}{2}. \quad (5)$$

By substituting 5 in equation 3 the intensity of detected gamma-rays becomes

$$I = I_o e^{-\mu \frac{\rho_b N}{2} L}. \quad (6)$$

Taking the logarithm of both sides of equation 6, we have the density of formation  $\rho_b$  in terms of the intensity of the gamma-ray detected by the sensor in the logging tool:

$$\rho_b = \frac{2[LnI_o - LnI]}{\mu N L}. \quad (7)$$

The lower the source-detector distance, the lower the depth of investigation, which makes the density formation values more influenced by the borehole enlargement. Moreover, the depth of investigation also decreases with the increase in the density of the formation.

The first one detector density tools measurements suffered from the effects of mud-cake and were marketed in the mid 1950s (Labo, 1987; Serra, 1994). The second generation tool employs a two-detector system that compensates for near-borehole problems (Labo, 1987). According to Serra (1994), the effect of the borehole is more severe for uncompensated density logs but less so for the compensated. The author also states that if the borehole wall is not smooth, the Formation Density Compensated (FDC) pad is not correctly applied to the formation and isolates zones full of mud, which strongly affect the measurement. Therefore, even if the tool has a compensation system to mitigate the rugosity of the borehole wall, if the borehole enlargement is severe, it will still affects the density log values: the media within the range of detection by the density logging tool can be assumed to be

composed of drilling mud and the rocks of the formation, and the density value measured by the tool is the contribution of the density of the formation and the density of the drilling mud. The traditional correction schemes for density has some limitations since beyond some thickness ( $\approx 1$  in.), depending on the tool design details that control, in part, the depth of investigation, the compensation scheme breaks down and the estimate of the bulk density will be in doubt (Ellis and Singer, 2007). According to Ellis and Singer (2007), the auxiliary measurement that is most helpful to indicate suspicious density readings is the caliper. Motivated by those reasons, we tested the Doll's geometric factor as a possible form to correct the density log for the effects of severe borehole enlargement, that might be indicated by the anomalies on the caliper log.

## METHODOLOGY

### Correcting the density log for the borehole enlargement

In order to correct the density log for the borehole enlargement through the caliper log readings we use the Doll's geometric factor. Doll (1949) developed the apparent geometric factor theory for the induction logging, which was created to measure formation resistivity in boreholes containing oil-based muds and in air-drilled boreholes because electrode devices could not work in these non conductive boreholes. For the induction logging, the theory states that the voltage at the receiver is the sum of the contribution of a large number of infinitesimal rings of Foucault current. The geometric factor of each coaxial cylindrical area would represent the fraction of contribution of this singular area to the entire signal, assuming a uniform conductivity within each zone.

The presence of unconsolidated formations compromise the signals recorded by the logging tool. When the formation in the vicinity of the well is homogeneous and there is no washout zones, the density measured by the logging tool is similar to the true density of the formation. However, when the formation is heterogeneous, the apparent density measured by the tool represents a combination of the densities of the different formations that exists around the well. The influence of each formation can be considered separately and

the signal measured is represented by the sum of each individual signal generated by each formation.

To properly use the apparent geometric factor theory for the density logging, it is necessary to establish the geometry of the borehole environment we are assuming to deal in our methodology. The first assumption is that the different regions around the well are concentric and, therefore, have a rotation symmetry. We also assume that the geometry of the borehole is a cylinder of radius size similar to the drill bit, and that it maintained its size during the drilling.

When borehole enlarges it is correct to assume that the media around the borehole is now composed of mud and formation rock. As well as proposed by Doll (1949) for the induction logging, the density measurement can also be obtained from a weighted average of mud and formation densities 9 as a consequence of the apparent geometric factor that satisfy the condition 8.

$$G_b + G_{mud} = 1, \quad (8)$$

$$\rho_a = G_b \rho_b + G_{mud} \rho_{mud}, \quad (9)$$

where  $G_b$  is the coefficient for the formation rock,  $0 \leq G_b \leq 1$ ;  $G_{mud}$  is the coefficient for the mud,  $0 \leq G_{mud} \leq 1$ ;  $\rho_a$  is the apparent density ( $g/cm^3$ );  $\rho_b$  is bulk density ( $g/cm^3$ ); and  $\rho_{mud}$  is mud density ( $g/cm^3$ ). If there is significant borehole diameter expansion, all values are represented by mud density, according to equations (8) and (9),  $G_{mud} = 1$ ,  $G_b = 0$ ,  $\rho_a = \rho_{mud}$ ; in contrast, if the logging tool keeps contact with a regular wellbore wall, then  $G_{mud} = 0$ ,  $G_b = 1$ ,  $\rho_a = \rho_b$ . Therefore, in terms of error estimation due to borehole expansion,  $G_{mud}$  and  $\rho_{mud}$  are fundamental parameters that needed to be investigated.

To determine the true values of density that represent the subsurface formations, we derive from equations 8 and 9 the following expression:

$$\rho_b = \frac{\rho_a - G_{mud} \rho_{mud}}{1 - G_{mud}}, \quad (10)$$

which indicates the corrected value of bulk density, in terms of apparent density, mud density

and apparent geometry factor of mud. The method we used to analyze how the borehole effect affects the well-to-seismic tie results consists in explore a semi-quantitative application of  $G_{mud}$  and  $\rho_{mud}$ , using equation 10 to investigate the proper values of formation density ( $\rho_b$ ).

We performed the correction on the density log at each point in depth by creating a linear relationship between the minimum and maximum values of the caliper log with the minimum and maximum values of the apparent geometric factor of the mud  $G_{mud}$ . From equation 9 one can note that when  $G_{mud} = 0$ , the corrected bulk density is equal to the measured bulk density. The choice of the maximum value of  $G_{mud}$ , related with the maximum value of the caliper log, must be based on prior information and the sensitivity of the density logging tool.

In order to create a log of  $G_{mud}$  values in depth to proceed with the correction of the bulk density log at each point in depth, a linear relationship between the caliper log and the  $G_{mud}$  values was established according to the equations described below and the graphic from Figure 1.

As the diameter of the borehole increases, the density log value decreases; on the contrary, density log values increase as borehole diameters approach normal levels. It means that on the portions of the density log that occurs the enlargement of the borehole, the density log values are underestimated. Hence, the correction for the geometry of the wellbore should increase the values of the density log on those portions. To correct the density log for the geometry of the borehole, we calculate the slope and intercept of the line of Figure 1:

$$m = \frac{Cal_{max} - Cal_{min}}{G_{max} - G_{min}}, \quad (11)$$

$$b = Cal_{min} - m G_{min}, \quad (12)$$

where  $Cal_{max}$  and  $Cal_{min}$  represents the maximum and minimum value of the caliper log, and  $G_{max}$  and  $G_{min}$  represents the maximum and minimum value of the apparent geometric factor of the mud  $G_{mud}$ , with the minimum value being zero and the maximum value depending upon the geology and the logging tool. For the Viking Graben data set

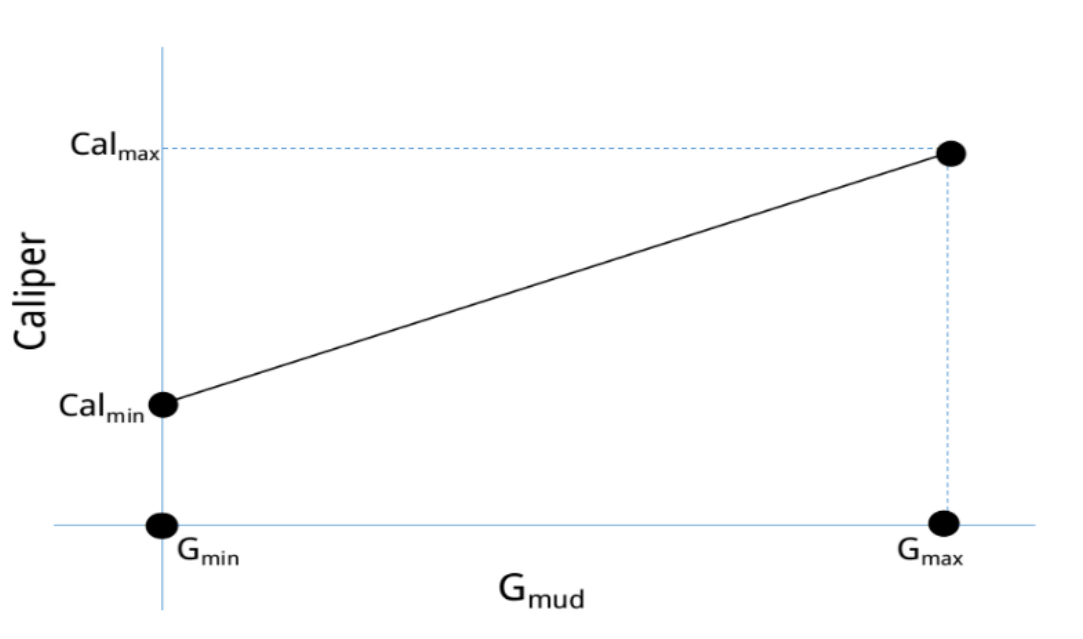


Figure 1: The linear relationship between the apparent geometric factor  $G_{mud}$  and the caliper log, according to its maximum and minimum values.

(the real data used in this paper) we set  $G_{max} = 0.4$ .

Accordingly, the  $G_{mud}$  log is created through equation:

$$G_{mud} = \frac{Cal - Cal_{min}}{m} + G_{min}, \quad (13)$$

where  $Cal$  represents each value of the caliper log in depth and  $G_{mud}$  is each value of  $G_{mud}$  created along the depth axis. By applying the relation 13 in equation 10, we generate the relation that we used to correct the bulk density value for each point in depth 14:

$$\rho_b = \frac{\rho_a - [(Cal - Cal_{min})/m + G_{min}] \rho_{mud}}{1 - [(Cal - Cal_{min})/m + G_{min}]}. \quad (14)$$

In the situation where there are no enlargement of the borehole (when the caliper log is stable),  $m = 0$  and equation 14 turns into:

$$\rho_b = \frac{\rho_a - G_{min} \rho_{mud}}{[1 - G_{min}]}. \quad (15)$$

Also in this situation, the minimum value of the apparent geometric factor of the mud is  $G_{min} = 0$ . Hence, when the caliper log is stable and the diameter of the borehole maintains its bit size during the drilling, there is no need to correct the measured bulk density since  $\rho_b = \rho_a$ . The procedure to perform the correction on the density log is shown on the flowchart of Figure 2, and the complete procedure to perform the correction and the well-to-seismic tie are described in the following steps and on charts on Figures 2 and 3:

1. Edit the sonic and density logs to do not deal with noisy spikes;
2. Establish the range of possible values of  $\rho_{mud}$ ;
3. Establish the value of  $G_{max}$  and set  $G_{min} = 0$ ;
4. Create the  $G_{mud}$  log in depth according to equation 13;
5. Perform the correction on the measured density log using the  $G_{mud}$  log and equation 14;

6. Calculate the reflectivity series with the corrected density log using equation 1;
7. Estimate the seismic wavelets through the deterministic and statistical approaches;
8. Convolve the reflectivity series with the estimated wavelets to calculate the synthetic seismic trace;
9. Compare the synthetic seismic trace with the real seismic trace through the cross-correlation;
10. Compare the correlation of the well-to-seismic tie without correction on the density log with the correlation of the well-to-seismic tie with the correction on the density log.

### **Estimation of the wavelet**

The estimation of the wavelet is a key feature on the well-to-seismic tie. We used in this study wavelets estimated by two different approaches: a statistic estimation through the predictive deconvolution using the optimum Wiener filter, and a deterministic extraction by building a filter, using both the seismic trace and well log data. In order to verify only the influence of the corrected density log, we used the same wavelet for both well-ties, with and without correction on density log. For the traditional deterministic wavelet estimation, however, since it depends on the well log data, different wavelets are extracted for each well tie case. The application of the predictive deconvolution to estimate the wavelet was also used on Macedo et al. (2017).

The predictive deconvolution is a special case of the Wiener filtering, which requires the

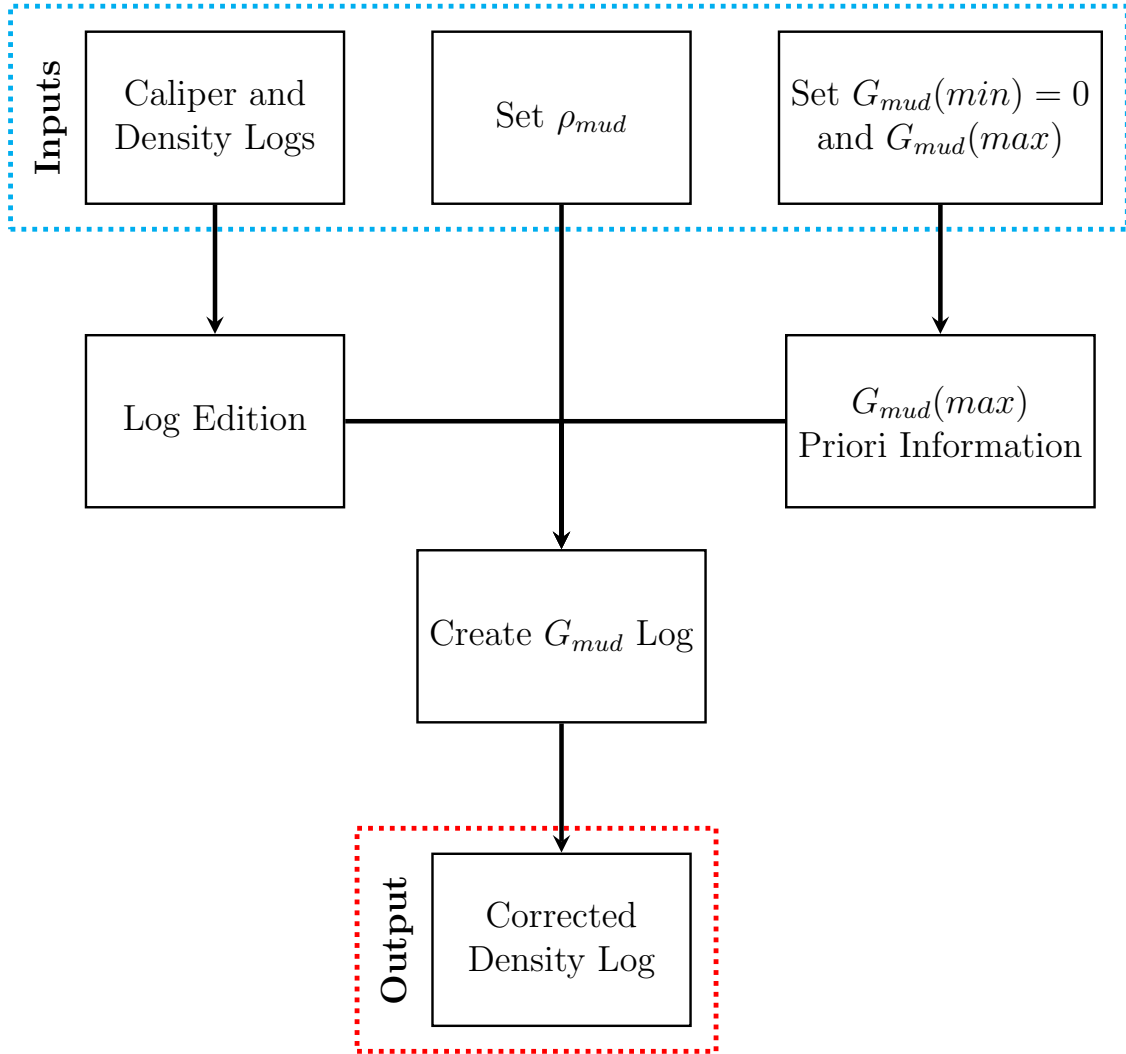


Figure 2: The fluxogram indicating the procedure to correct the density log for the borehole enlargement. The first steps are the log editions for despiking and to remove null values, set a usual value for the  $\rho_{mud}$ , set the minimum value of  $G_{mud}$  as zero and set the maximum value of  $G_{mud}$  according to the priori information and depth of investigation of the tool. With those information it is possible do create the  $G_{mud}$  log that will be used to correct the density log for the borehole enlargement for each point in depth.

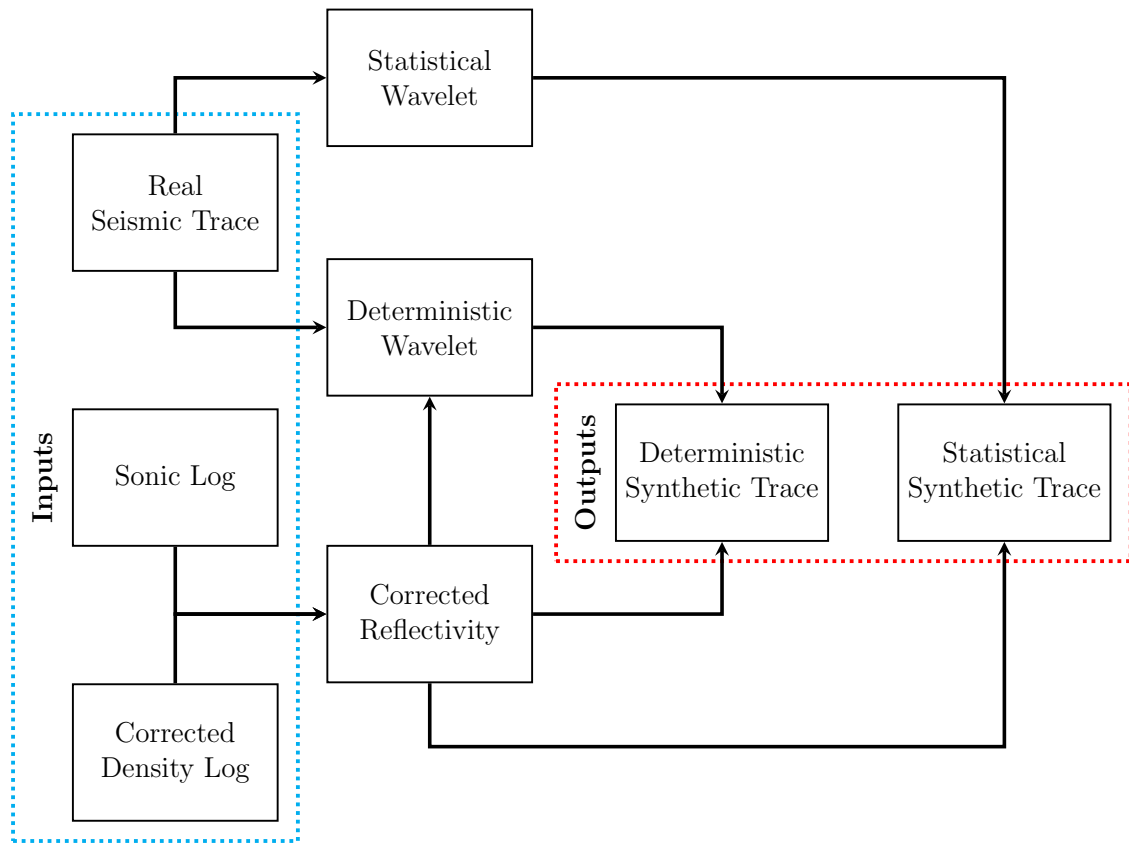


Figure 3: The fluxogram indicating the procedure to perform the well-to-seismic-tie after the correction on density log. The corrected reflectivity is calculated and two wavelets are estimated: a statistical wavelet through the predictive deconvolution, which uses only the real seismic trace; a deterministical wavelet, from both the corrected reflectivity and the real seismic trace. The convolution of those wavelets with the corrected reflectivity will produce the statistical synthetic trace and the deterministic synthetic trace, respectively.

solution of the normal equations:

$$\begin{pmatrix} r_0 & r_1 & r_2 & \cdots & r_{n-1} \\ r_1 & r_0 & r_1 & \cdots & r_{n-2} \\ r_2 & r_1 & r_0 & \cdots & r_{n-3} \\ \vdots & \vdots & \vdots & \ddots & \vdots \\ r_{n-1} & r_{n-2} & r_{n-3} & \cdots & r_0 \end{pmatrix} \begin{pmatrix} a_0 \\ a_1 \\ a_2 \\ \vdots \\ a_{n-1} \end{pmatrix} = \begin{pmatrix} g_0 \\ g_1 \\ g_2 \\ \vdots \\ g_{n-1} \end{pmatrix} \quad (16)$$

where  $r_i$  represents the autocorrelation lags of the input wavelet,  $a_i$  are the Wiener filter coefficients and  $g_i$  are the cross-correlations lags of the desired output with the input wavelet. The prediction process is assumed when the desired output on the normal equations is a time-advanced form of the input series. In the case of the predictive deconvolution, given an input series  $x(t)$ , the goal is to predict its value at some future time  $x(t + \alpha)$ , where  $\alpha$  is the prediction lag. Using the normal Wiener equations to build a filter to estimate  $x(t + \alpha)$  (the new desired output that must be cross-correlated with the input  $x(t)$ ), it gives:

$$\begin{pmatrix} r_0 & r_1 & r_2 & \cdots & r_{n-1} \\ r_1 & r_0 & r_1 & \cdots & r_{n-2} \\ r_2 & r_1 & r_0 & \cdots & r_{n-3} \\ \vdots & \vdots & \vdots & \ddots & \vdots \\ r_{n-1} & r_{n-2} & r_{n-3} & \cdots & r_0 \end{pmatrix} \begin{pmatrix} a_0 \\ a_1 \\ a_2 \\ \vdots \\ a_{n-1} \end{pmatrix} = \begin{pmatrix} r_\alpha \\ r_{\alpha+1} \\ r_{\alpha+2} \\ \vdots \\ r_{\alpha+n-1} \end{pmatrix} \quad (17)$$

That is the case for a  $n$ -long prediction filter and a  $\alpha$ -long prediction lag. The prediction filter requires only the autocorrelation of the input series, which configures a statistical estimation of the wavelet. According to Enders A. Robinson (2008), the canonical representation of the seismic trace is the convolution of an all-pass filter - with a flat magnitude spectrum - and a minimum-delay wavelet. Both the trace and the wavelet have the same non-flat magnitude spectrum. The predictive deconvolution separates the components of the trace on the basis of the criteria of minimum-delay and white: the error series of the

predictive deconvolution yields the white components of the seismic trace (all pass filter and the reflectivity), and the prediction filter yields the predictable components of the seismic trace, which is the minimum-delay component that constitute the minimum-phase estimated wavelet. Therefore, we selected a segment of the trace that we believed to be a result of a reflector and deconvolved that segment in order to separate the white-components from the minimum-phase component, by choosing a prediction lag and operator length. For a single segment in time of the real seismic trace, we selected a range of prediction-lag and a range of operator length and performed the deconvolution to estimate the wavelet. The algorithm returns the prediction lag and operator length that produces the best wavelet that match the synthetic trace and the real trace.

The deterministic extraction of the wavelet is made by the building of a filter that when convolved with the reflectivity produces the best match between the synthetic trace (produced by the convolution of the filter coefficients and the reflectivity), with the real seismic trace. The inputs to the deterministic wavelet extraction are the reflectivity series, the seismic trace, the length of the filter (wavelet) and the increment in time, which corresponds to the best shift between the reflectivity series and the real seismic trace. For a given range of length of filter and increment, the algorithm returns the best parameters that produces the wavelet that best match the synthetic trace and the real seismic trace.

## RESULTS ON VIKING GRABEN DATASET

### Geological Background

The Viking Graben is located in the North Sea Basin and is the product of a rifting occurred during the late Permian to the Triassic. The formation of the oil and gas of the North Sea is related to a extensional episode in the beginning of Jurassic, which causes the Pangea to break into the continents Gondwana and Laurasia. Details regarding the stratigraphy of the Viking Graben might be found on Madiba and McMechan (2003); Keys and Foster (1998); Macedo et al. (2017). The dataset used in this study was the subject of a 1994 SEG workshop on comparison of seismic inversion methods (Keys and Foster, 1998).

We used a 2D seismic line, oriented east-west, with 2142 CMPs separated by 12.5m, each one with 1501 samples and a sample rate of 0.004s. The well log information is from two wells named Well A and Well B. Macedo et al. (2017) performed well-tie procedures using these logs and the same seismic section, verifying that the best match to the well data is the CMP 809 for the Well A, which we also used as a real seismic trace. Due to unrecorded points and noises in the density and sonic logs, it was necessary to edit them in order to not deal with wrong values.

## Numerical Experiments and Discussion

In this section we present our results of the well-to-seismic-tie applied on the Viking Graben dataset with the correction on the density log for the borehole enlargement. We used two different ways to estimate the seismic wavelet: the deterministic approach and the statistical approach, through the predictive deconvolution Macedo et al. (2017). For the deterministic seismic wavelet estimation, we perform the correction on the density log in two ways: the first is correcting the entire density log and the second is performing the correction only on the segments of the density log where the corresponding caliper log is unstable. We did that because the deterministic wavelet estimation is dependent on the reflectivity series. Therefore, different corrections produce different reflectivity series and, therefore, produce different deterministic estimated wavelets. We wanted to verify how the correction on the density log affects the estimated wavelet and the correlation of the well-to-seismic-tie: if a correction only where the caliper indicates a severe borehole enlargement will be enough to provide a better tie or if a correction on the entire density log is necessary to yield a better tie. The statistical wavelet estimation is dependent only on the seismic wavelet, therefore different types of corrections on the density log will not change the wavelet estimated, only the reflectivity series to be used on the tie, which does not have a meaningful impact (less than 1%) on the final correlation between the synthetic seismic trace and the real seismic trace.

Figure 4 shows the well logs from the real dataset from the Viking Graben field used for the well-to-seismic-tie. The despiking procedure was applied to remove the noisy spikes.

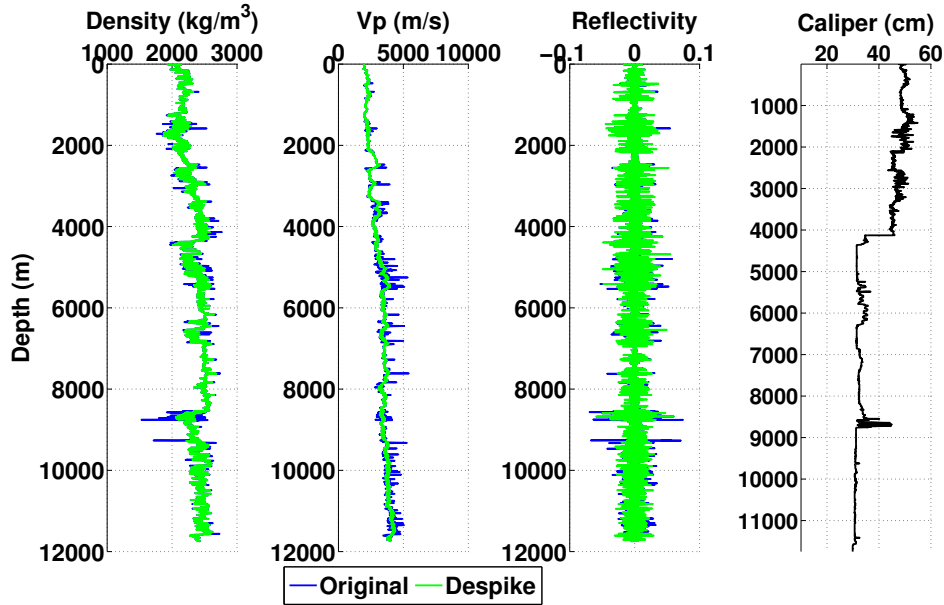


Figure 4: Real well log data from the Viking Graben field used on the well-to-seismic-tie without the proper corrections on the density log, only with the despiking to remove the noisy spikes.

Figure 5 shows the caliper readings, the original and corrected density log and the correction applied on the original density log, that was produced through our methodology using the Doll's geometric factor.

We used the maximum value of  $G_{mud}$  of 0.4, which means that the minimum value that the geometric factor of the formation  $G_b$  might assume is 0.6. The value of the geometric factor of the formation  $G_b$  is related with the depth of investigation of the logging tool. In the case of the density tool, the depth of investigation is small due to the short penetration of the gamma-ray into the formation. According to Ellis and Singer (2007), 90% of the response of the density logging tool is influenced by the first 4 inches of depth of investigation, which means that there is a strong sensitivity of the tool to the near-borehole zone presumed to be invaded by the drilling mud. Because of that, it is necessary to add more weight on the zones farther from the borehole, where the true value of density could be measured, in order to

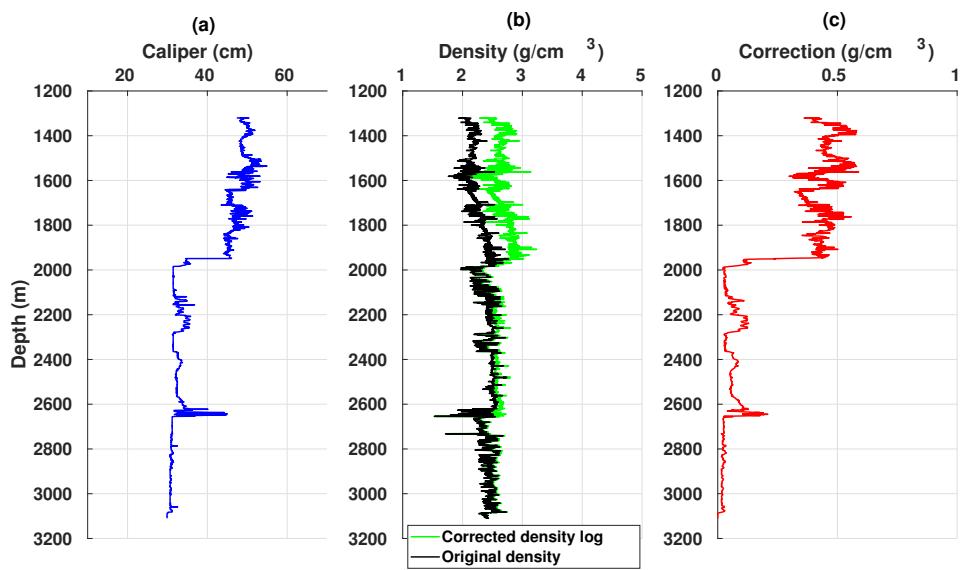


Figure 5: a) Caliper log used to calculate the correction to be applied on the density log. b) Original and corrected density log for the borehole enlargement. c) The calculated correction applied to the original density log.

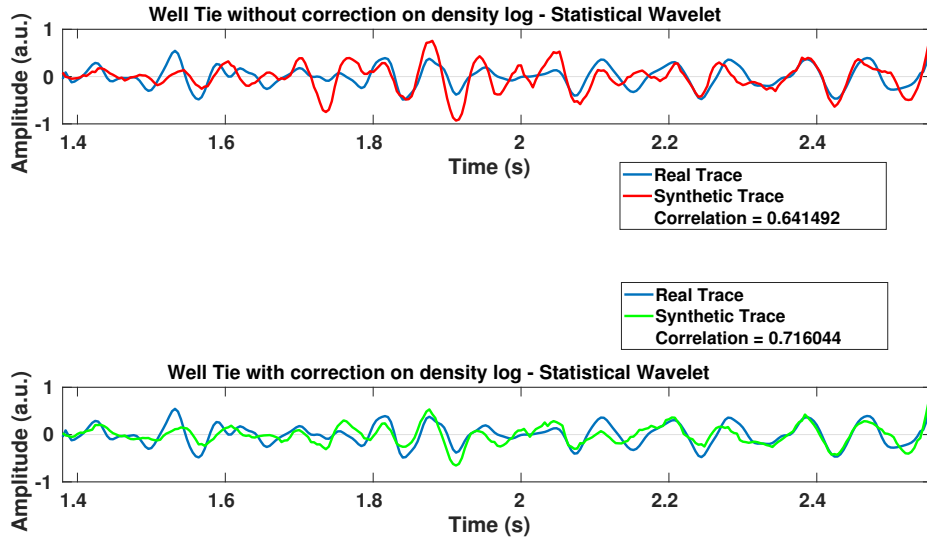


Figure 6: Well-to-seismic-tie using a statistical wavelet estimation and a correction on the density log only where the caliper indicates a severe borehole enlargement. The correlation improved from 0.64 to 0.71 when performing the correction.

obtain a proper measure. Thus, the geometric factor of the formation  $G_b$  will vary from 0.6 to 1, weights that are maintained larger than the weight of the mud, in order to compensate for the sensibility of the tool to the near-borehole zone. Moreover, by establishing those weights, we ensure that the corrected density log maintain its geological consistency: the corrected density log measurements are not underestimated nor super-estimated.

Figures 6 and 7 show the results of the well-to-seismic-tie for the CMP 809 of the Viking Graben field, with and without the correction on the density log. The results are divided in three sections: 1) well-to-seismic-tie using a statistical wavelet estimation and a correction on the density log only where the caliper indicates a severe borehole enlargement; 2) well-to-seismic-tie using a deterministic wavelet estimation and a correction on the entire density log; and 3) well-to-seismic-tie using a deterministic wavelet estimation and a correction on the density log only where the caliper indicates a severe borehole enlargement.

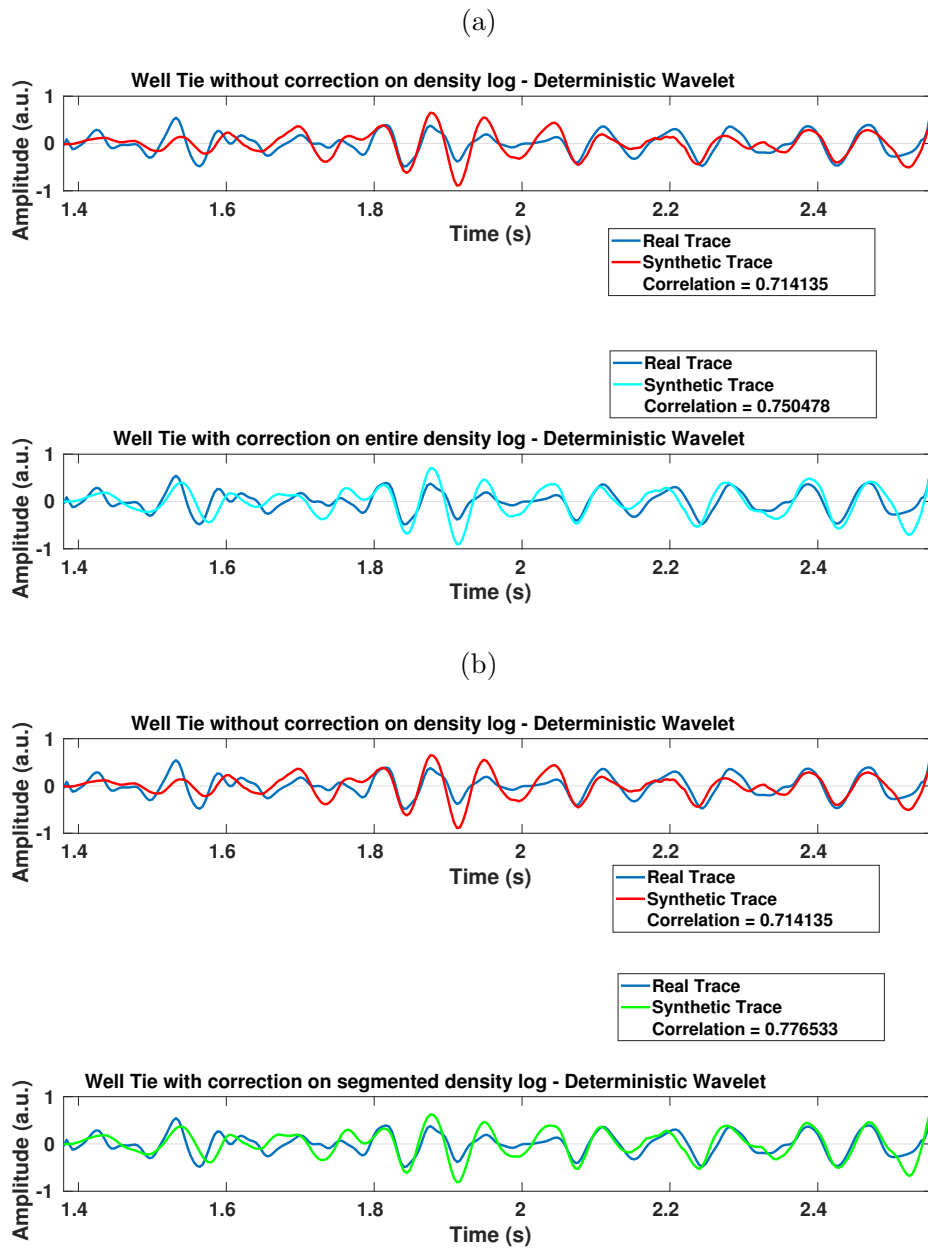


Figure 7: a) Well-to-seismic-tie using a deterministic wavelet estimation and a correction on the entire density log. The correlation improved from 0.71 to 0.75 when performing the correction. b) Well-to-seismic-tie using a deterministic wavelet estimation and a correction on the density log only where the caliper indicates a severe borehole enlargement. The correlation improved from 0.71 to 0.77 when performing the correction.

The results show that for the three cases, the correlation improved after the correction. The best improvement was achieved for the statistical case, a raise of 7% on the correlation between the real and synthetic seismic traces. In this case, as the statistical estimation of the wavelet through the predictive deconvolution does not require the reflectivity series as an input, the same wavelet is used for the original well-to-seismic-tie and for the corrected well-to-seismic-tie. The wavelet was estimated by the predictive deconvolution of the segment from 1.38 s to 1.6 s of the real seismic trace, using the optimum parameters returned by the semi-automatic algorithm Macedo et al. (2017), with a prediction lag  $\alpha = 13$  and filter length  $N = 14$ .

The well-to-seismic-tie using the deterministic estimation of the wavelet show that the best correlation was achieved when the correction on the density log is performed only on the segment where the caliper indicates a severe borehole enlargement and the rest of the density log remains as the original, with a improvement of 6% on the correlation between the real and the synthetic seismic traces. As in this case a different density log (because of the correction) results in different reflectivity series, and the deterministic estimation of the wavelet require the reflectivity series as an input, different wavelets are extracted. The wavelets used for the deterministic case are shown in Figure 8.

Although the density of the drilling mud is a known factor during the completion of the well, and its density varies according to the conditions of the borehole, we analyzed how the  $\rho_{mud}$  affects the correlation between the real and synthetic seismic traces after the correction on the density log. We used a range from  $\rho_{mud} = 1.10g/cm^3$  to  $\rho_{mud} = 1.30g/cm^3$  to contemplate the usual values for the density of the drilling mud. The results are shown in Figure 9.

It is observed that the greatest influence of  $\rho_{mud}$  on the well-to-seismic-tie was for the case where a correction on the anomalous segment of the caliper log is made, and using the deterministic wavelet, where a change from  $\rho_{mud} = 1.10g/cm^3$  to  $\rho_{mud} = 1.30g/cm^3$ , causes the correlation to drop around 1.5%. For all the other cases, the change in  $\rho_{mud}$  causes a change of less than 1% on the correlation between the real and synthetic seismic traces.

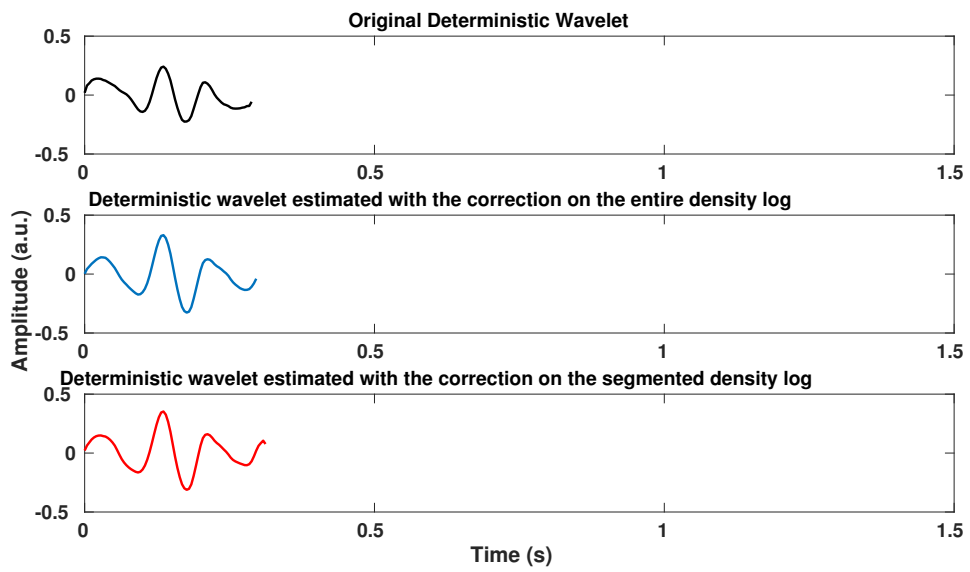


Figure 8: The extracted deterministic wavelets used on the well-to-seismic-tie in Figure 7. a) The original wavelet. b) The wavelet used on the case of correction on the entire density log. c) The wavelet used on the case of correction on the segment where the caliper is unstable.

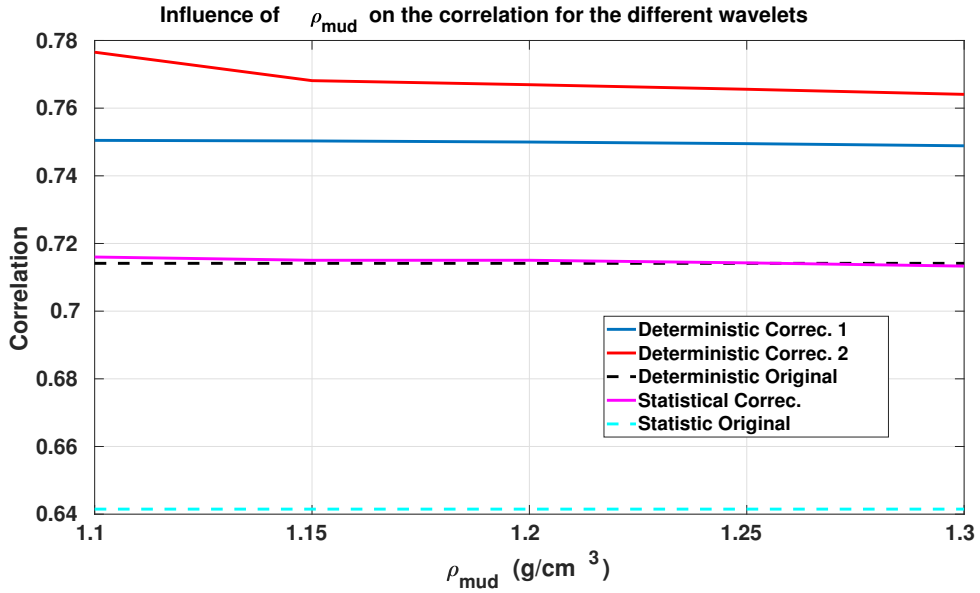


Figure 9: The influence of  $\rho_{mud}$  on the correlation between the real and synthetic seismic traces. Deterministic correction 1 (in blue) indicates the correlation for the case where the correction is made on the entire density log using the deterministic wavelet; Deterministic correction 2 (in red) indicates the correlation for the case where the correction is made on the segment where the caliper is unstable using the deterministic wavelet; Deterministic original (in black) indicates the original correlation of the well-to-seismic-tie when no corrections are made using the deterministic wavelet; Statistical correction (in pink) indicates the correlation for the case where the correction is made on the segment where the caliper is unstable using the statistical wavelet; Statistic original indicates the original correlation of the well-to-seismic-tie when no corrections are made using the statistical wavelet.

## CONCLUSIONS

We have proposed a method to correct the density log for the borehole enlargement at each point in depth using the Doll's geometrical factor theory, in order to obtain a more accurate well-to-seismic-tie, for the real dataset from the Viking Graben, North Sea. The first step is to set the minimum and maximum values of  $G_{mud}$  and associate them to the caliper readings to generate the  $G_{mud}$  profile according to priori information and the depth of investigation of the logging tool. The  $G_{mud}$  log represents the geometric factor relative to the density of the drilling mud that interacts with the formation on the washout zones. This procedure makes it possible to associate the geometric factor of the mud with the segments where there are enlargement of the borehole diameter. Those specific areas have their density log corrected, and then we performed the well-to-seismic-tie. We estimate the seismic wavelet through a statistical and a deterministic approach: for the statistical case through the predictive deconvolution only the seismic trace is used, for the deterministic case both the seismic trace and the reflectivity - calculated with the corrected density log - are used. Our analysis agrees with previously published works, that a anomalous segment of caliper contributes to lower the correlation on the well-to-seismic-tie. The results showed that both ties had their correlations increased with the correction on the density log. However, precaution on setting the  $G_{mud}$  maximum value is a need since its maximum value is related with the minimum geometric factor of the formation. Because the density logging tool is more sensitive to the near-borehole zones, it is recommended that the geometric factor of the formation far from the borehole be higher than the weight of the washout zone in order to avoid unrealistic densities values. Further work, may be worthwhile to apply this methodology of correction on density log on other dataset that also have an anomalous caliper due to severe enlargement of the borehole. Moreover, we also suggest to verify how this methodology of correction behaves on the well-to-seismic-tie with other statistical and deterministic methods of estimative of the wavelet, specially the ones that does not imply a random process reflectivity and a minimum-phase wavelet.

## REFERENCES

- Buland, A., and H. Omre, 2003, Bayesian wavelet estimation from seismic and well data: *Geophysics*, **68**.
- Doll, H. G., 1949, Introduction to induction logging and application to logging of wells drilled with oil base mud: *Journal of Petroleum Technology*, **1**, 148–162.
- Ellis, D. V., and J. M. Singer, 2007, *Well logging for earth scientists*, 2 ed.: Springer.
- Enders A. Robinson, S. T., 2008, *Digital imaging and deconvolution: The abcs of seismic exploration and processing*: SEG Books.
- Keys, R. G., and D. J. Foster, 1998, Comparison of seismic inversion methods on a single real data set, open file publications: *Society of Exploration Geophysics*, 233.
- Labo, J., 1987, *in* *A Practical Introduction to Borehole Geophysics (An Overview of Wireline Well Logging Principles for Geophysicists)* — 8. Density Log Principles, **10.1190/1.9781560802587**.
- Liu, Z., and J. Zhao, 2015, Correcting hole enlargement impacts on density logs for coalbed methane reservoirs: *The Open Petroleum Engineering Journal*, **8**, 72–77.
- Lundsgaard, A. K., H. Klemm, and A. J. Cherrett, 2015, Joint bayesian wavelet and well-path estimation in the impedance domain.: *Geophysics*, **80**.
- Macedo, I. A. S., C. B. da Silva, J. de Figueiredoa, and B. Omoboyac, 2017, Comparison between deterministic and statistical wavelet estimation methods through predictive deconvolution: Seismic to well tie example from the North Sea: *Journal of Applied Geophysics*, **136**, 298–314.
- Madiba, G. B., and G. A. McMechan, 2003, Processing, inversion, and interpretation of a 2d seismic data set from the North Viking Graben, North Sea: *Geophysics*, **68**, 837–848.
- Oldenburg, D., S. Levy, and K. Whittal, 1981, Wavelet estimation and deconvolution: *Geophysics*, **46**.
- Serra, O., 1994, *Fundamentals of well logging interpretation - 1. the aquisition of logging data*: Elsevier, volume **15A** of *Development in Petroleum Science*.
- White, R., and R. Simm, 2003, Tutorial: Good practice in well ties: *First Break*, **21**.
- White, R. E., and T. Hu, 1998, How accurate a well tie can be?: *The Leading Edge*, **17**,

1065–1071.

Yilmaz, O., 2000, *Seismic data analysis: processing, inversion, and interpretation of seismic data*: SEG Books.

Yong, S. H., and C. M. Zhang, 2007, *Logging Data Processing and Interpretation*: Petroleum University Press: Dongying, 59–61.

# 4 ARTICLE 3: ESTIMATION OF THE SEISMIC WAVELET THROUGH HOMOMORPHIC DECONVOLUTION AND WELL LOG DATA: APPLICATION ON WELL-TO-SEISMIC-TIE FROM NORTH SEA DATASET

Authors: Isadora Augusta Santana de Macedo, José Jadsom Sampaio de Figueiredo.  
**Under revision at the Geophysical Prospecting journal**  
 Submitted to 81st EAGE Conference Exhibition, London, 3-6 June 2019

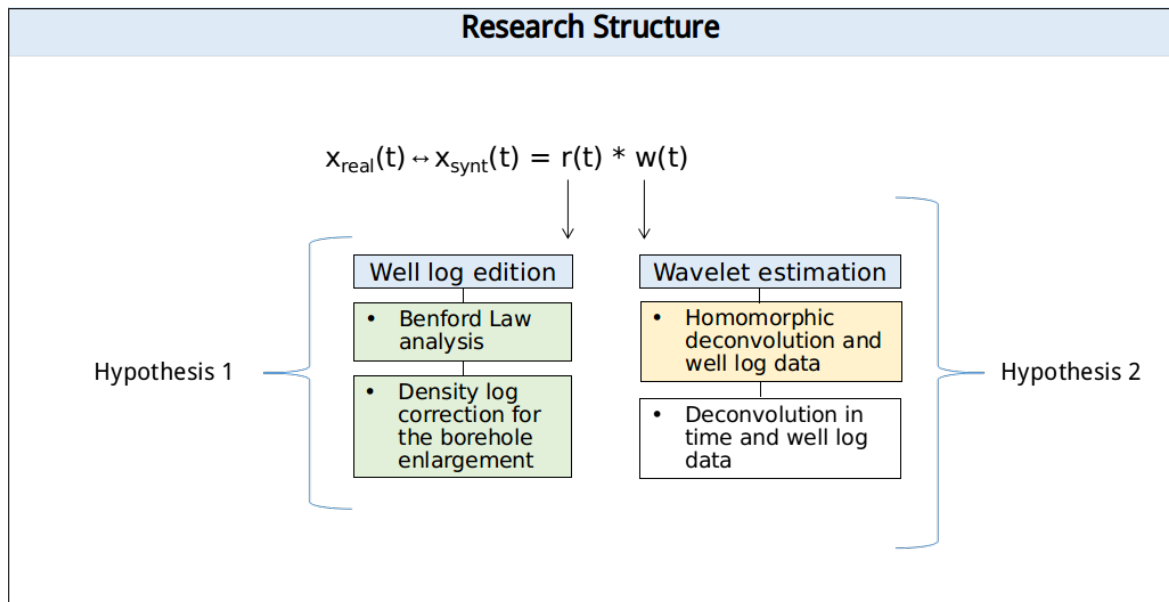


Figure 4.1: The research structure for the well-to-seismic-tie: Chapter 4 (in yellow), related with the wavelet estimation.

The deconvolution methods to recover the reflectivity of the seismic data, in general uses the classical assumptions of the convolutional model of the Earth, which involve, among other factors, the premise that the seismic wavelet is of minimum phase and that the reflectivity is a random process. By doing that, it is possible to use the autocorrelation of the seismic trace as the autocorrelation of the seismic wavelet. Aiming to produce a high quality well-to-seismic-tie, the last part of this study is devoted to deconvolution wavelet estimation methods that does not imply the randomness of the reflectivity or assumptions regarding the wavelet's phase, going against the commonly used Wiener filtering techniques.

On chapter 4, the article "Estimation of the seismic wavelet through homomorphic deconvolution and well log data: application on well-to-seismic-tie from North Sea dataset",

show the results obtained with an approach to estimate the seismic wavelet using the homomorphic deconvolution (a statistical method) and the well log information, which makes our proposal a deterministic wavelet estimation approach. The advantage of homomorphic deconvolution is due the fact it does not infer assumptions about the reflectivity or the wavelet's phase, which makes it a more precise statistical method, but dependent on the construction of a filter capable to separate the wavelet and the reflectivity components. In our case, the homomorphic deconvolution is followed by the use of the reflectivity calculated from well logs to build a linear filter in the cepstral domain, aiming to achieve a more accurate wavelet when compared to the standard deconvolution methods of wavelet estimation.

# Estimation of the seismic wavelet through homomorphic deconvolution and well log data: application on well-to-seismic-tie procedure

Isadora A. S. de Macedo <sup>\*†</sup> and J. J. S. de Figueiredo <sup>\*†</sup>

<sup>\*</sup> UFPA, Faculty of Geophysics, Petrophysics and Rock Physics Laboratory - Prof. Dr.

*Om Prakash Verma, Belém, PA, Brazil.*

<sup>†</sup> National Institute of Petroleum Geophysics (INCT-GP), Brazil.

Running head: **homomorphic deconvolution on well-to-seismic-tie**

## ABSTRACT

Wavelet estimation as well as well-tie procedures are important tasks in seismic processing and interpretation. Deconvolutional statistical methods to estimate the proper wavelet in general are based on the assumptions of the classical convolutional model, which implies a random process reflectivity and a minimum-phase wavelet. The homomorphic deconvolution, however, does not take these premises into account. In this paper we propose an approach to estimate the seismic wavelet using the advantages of the homomorphic deconvolution and the deterministic estimation of the wavelet, which uses both seismic and well log data. The feasibility of this approach is verified on well-to-seismic-tie from a real dataset from Viking Graben Field, North Sea, Norway. The results show that the wavelet estimated through this methodology produced a higher quality well tie when compared to methods of estimation of the wavelet that consider the classical assumptions of the convolutional model.

## INTRODUCTION

In order to collect seismic informations about the subsurface, a seismic source emits a pulse that is transmitted from the surface. The contrast of acoustic impedance between the rock's layers causes the reflections that are registered in the surface by an array of receivers. Generally, the assumption that the seismic pulse is stationary, which means that it does not change with its propagation throughout the subsurface layers, is taken into account, as well as the assumption of a random process reflectivity. The recorded seismic trace can be modeled as a convolution between the seismic wavelet and the reflectivity series. One way to separate the components of the convolution, is through the deconvolution process, in which the reflectivity - or the earth's impulse response - can be obtained if the source wavelet is known. Most modern seismic inversion methods require the wavelet information, which is also the key input to the well-to-seismic-tie (Bo et al., 2013). The solution of the inversion, which is not unique, can be constrained by comparing the seismic traces with synthetic traces constructed from the convolution between the inversion model and the wavelet (Bo et al., 2013).

The wavelet can be measured directly during seismic data acquisition, but its measurement requires special acquisition techniques (Bo et al., 2013). The use of controlled-phase acquisition and processing strategies can help control seismic phase (Trantham, 1994), but mismatches between recorded seismic data and synthetic traces constructed from well-log data occur very frequently (Edgar and Van der Baan, 2011). The wavelet estimation methods fall largely into two categories: (1) purely statistical ways and (2) the use of well-log data (White and Simm, 2003). The statistical methods estimates the wavelet using the amplitude spectrum or the autocorrelation functions of the recorded seismic data (Bo et al.,

2013), but is unable to determine the phase of the wavelet without further assumptions, such as assuming that the wavelet has a minimum phase. When it occurs, the autocorrelation of the wavelet can be derived from the autocorrelation of the seismic trace. The reflectivity series computed from sonic and density logs can be used to estimate the wavelet with proper amplitude and phase spectra (Dey and Lines, 1998).

In this study we aim to estimate the seismic wavelet for well-to-seismic-tie purposes using the homomorphic deconvolution and we also make the proper analysis of its advantages and disadvantages. The homomorphic deconvolution configures a statistical filtering process applied to geophysical data to recover the reflectivity or estimate the source signature, through separation of components on the cepstrum domain. The accuracy of the homomorphic deconvolution is determined by the ability of a filter, or other method, to separate the reflectivity and the seismic wavelet components. We propose, for the seismic wavelet estimation through the homomorphic deconvolution, the use of the reflectivity series in the time domain in order to design a filter to separate the components in the cepstral domain. Since we are using the well log data to calculate the reflectivity, there is no need to perform the phase unwrapping. Our results show that this methodology improved the correlation on the well-to-seismic-tie in comparison with methods that assume the premises of the classical convolutional model, suggesting a more accurate way to correlate stratigraphic horizons and a more accurate wavelet for the inversion of seismic data to reflectivity or impedance.

## THEORETICAL BACKGROUND

Homomorphic systems are a class of linear systems that satisfy the principle of superposition and are useful in the separation of signals generated by convolutions. The seismic trace ( $x(n)$ ) is generally given as a convolution between the source pulse wavelet ( $w(n)$ ) and

the reflectivity series ( $h(n)$ ) of the Earth subsurface. Mathematically, this relation can be described by

$$x(n) = w(n) * h(n). \quad (1)$$

In the frequency domain, this equation can be expressed as:

$$X(w) = W(w)H(w), \quad (2)$$

where  $X(w)$  and  $W(w)$  are the Fourier transforms of  $x(n)$  and  $w(n)$ , respectively. A signal can be transformed from the time domain to the complex-valued cepstral domain by Fourier transformation followed by a log operation Herrera and Van Der Baan (2012):

$$\hat{X}(w) = \log\{X(w)\} = \log\{|X(w)| \exp^{i\arg(X(w))}\}. \quad (3)$$

The cepstral transform of  $x(n)$  is given by inverse Fourier transform of  $\hat{X}(w)$ , i.e.,  $x(n) = iFFT\{\hat{X}(w)\}$ . The convolutional model described in 1 can be transformed into an addition in the cepstral domain according to:

$$\hat{x}(n) \approx \hat{w}(n) + \hat{h}(n). \quad (4)$$

The output  $\hat{x}(n)$  is called complex cepstrum of the input  $x(n)$  and it contains both informations of phase and amplitude of the seismic signal. It is important to emphasize, however, that the complex cepstrum of a real input series is also a real output series. The analysis of the convolution of two different series through a homomorphic system, depends on the ability to build a linear operator on the cepstral domain that can recover the cepstrum of each component of the convolution individually, which in the cepstral domain are represented by an addition. Therefore, the homomorphic deconvolution is useful for signals that have their complex cepstrum components separated. The assumption that must be made is that the components of the signal occupy different separated ranges in the cepstral domain. This assumption is valid to a wide variety of signals in which one pulse

has a smooth spectrum and the other has a sequence of periodic pulses with minimum or maximum-phase. Such properties make the homomorphic deconvolution an interesting technique for wavelet estimation, since the seismic wavelet may be recovered without any prior assumptions regarding the structure of the wavelet or the reflection series. The seismic wavelet is not assumed minimum-phase as it happens with the predictive deconvolution, nor the reflection series is assumed uncorrelated as it happens with Wiener filtering techniques Tribolet and Oppenheim (1977). Those two last deconvolutional approaches, as methods of wavelet estimation, were already tested on the same real dataset of this study, and the well-to-seismic-tie was also performed. The correlation results of the well tie comparing those deconvolutional techniques are described in the table .

## METHODOLOGY

In this paper, we aim to estimate the seismic wavelet by transforming the real seismic trace in time domain to the cepstral domain in order to separate the components of the wavelet and the reflectivity series. Our approach is to use a linear inverse filter in the cepstral domain to separate the components of the convolution. We use the reflectivity series calculated from well log data to isolate the complex cepstrum of the wavelet. The main advantage of this methodology is the direct implementation that does not require a high computational cost. Moreover, as we are using the reflectivity from well logs, there is no need to perform the phase unwrapping, since the estimation of the wavelet is not purely statistical: we are using both the real seismic trace and the well log data, therefore, we are dealing with a form of deterministic wavelet estimation.

The use of the complex cepstrum of the reflectivity takes place in the process of building a filter in the cepstral domain. The complex cepstrum of a seismogram can be described

as:

$$\hat{x}(n) = \hat{w}(n) + \hat{h}(n), \quad (5)$$

where  $\hat{x}(n)$ ,  $\hat{w}(n)$ ,  $\hat{h}(n)$  are the complex cepstrum of the real seismic trace, the wavelet, and the reflectivity, respectively. In this domain, we aim to build a filter  $l(n)$  that applied to the real seismic trace, separates the component of the wavelet  $\hat{w}(n)$  from the component of the reflectivity  $\hat{h}(n)$ . Therefore:

$$l(n).\hat{x}(n) = \hat{w}(n). \quad (6)$$

Our choice is to build  $l(n)$  as an inverse linear filter. If we have the reflectivity series calculated from the well log data, it is possible to transform it to the time domain by the correct time-depth relationship used on the well-to-seismic-tie, and to calculate a new complex cepstrum of the reflectivity,  $\hat{h}'(n)$ , which transforms the equation 5 into:

$$\hat{x}(n) = \hat{w}(n) + \hat{h}'(n). \quad (7)$$

Therefore, the inverse linear filter  $l(n)$  is described as:

$$l(n).\hat{x}(n) = \hat{x}(n) - \hat{h}'(n), \quad (8)$$

$$l(n) = \frac{\hat{x}(n) - \hat{h}'(n)}{\hat{x}(n)}, \quad (9)$$

$$l(n) = 1 - \frac{\hat{h}'(n)}{\hat{x}(n)}. \quad (10)$$

By applying the filter 10 in the complex cepstrum of the real seismic trace 6, we have:

$$\hat{w}(n) = \hat{x}(n)\left\{1 - \frac{\hat{h}'(n)}{\hat{x}(n)}\right\}, \quad (11)$$

which represents the complex cepstrum of the seismic wavelet isolated in the cepstrum domain. The next step is to bring back the cepstrum of the wavelet to the time domain, in order to estimate the wavelet. Therefore:

$$\hat{W}(w) = FFT\{\hat{w}(n)\}, \quad (12)$$

$$W(w) = FFT\{\hat{W}(w)\}, \quad (13)$$

$$w(n) = iFFT\{W(w)\}. \quad (14)$$

The equation 14 represents the estimated wavelet in the time domain through the homomorphic deconvolution using the well log data. The flowchart 1 illustrates the procedure. The steps necessary to perform the well-to-seismic-tie with this approach of wavelet estimation is described below.

1. Edit the sonic and density logs to remove noisy spikes and null values
2. Calculate the reflectivity series in depth
3. Apply the time-depth relationship on the reflectivity series to have it in the same time segment of the real seismic trace
4. Calculate the complex cepstrum of the real seismic trace
5. Calculate the complex cepstrum of the reflectivity series in the time domain
6. Apply the inverse filter to isolate the complex cepstrum of the wavelet
7. Perform the inverse operations to transform the complex cepstrum of the wavelet to the time domain
8. Convolve the wavelet estimated with the reflectivity series
9. Calculate the correlation between the real seismic trace and the synthetic trace

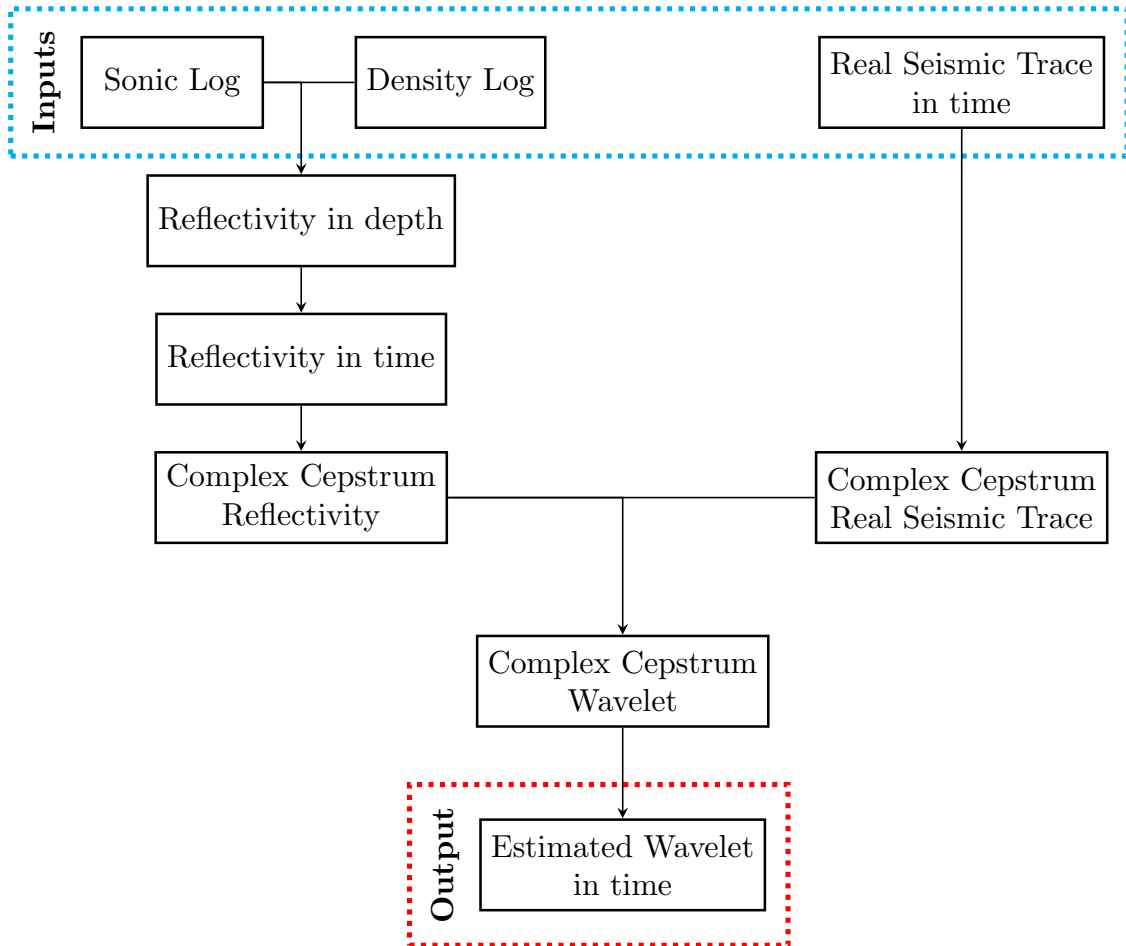


Figure 1: Flowchart illustrating the steps of the algorithm to estimate the wavelet through the homomorphic deconvolution. The inputs are the sonic and density logs to calculate the reflectivity and the real seismic trace, which configures a deterministic method to estimate the wavelet.

## RESULTS

We have applied our methodology of wavelet estimation on a synthetic model and on two well-logs from the Viking Graben on North Sea. Then, we performed the well-to-seismic-tie in order to verify the feasibility of our approach. We used the correlation between the real and synthetic traces as a measure of coherence.

### Application on synthetic data

This section shows the results of the well-to-seismic-tie and the estimation of the wavelet for a synthetic scheme, in order to validate our algorithm and our methodology. Figure 2 shows the layered model used to generate the impedance log and, therefore, the reflectivity series. The Figure 3 shows the convolutional model for the proposed synthetic scheme. The reflectivity in time domain, is convolved with the original wavelet, which in this case is a causal pulse with a peak frequency of 20Hz. The resampling procedure introduce additional spikes on the reflectivity. To avoid the Gibbs effect, a low-pass filter was applied.

We followed the same methodology described previously, and calculated the complex cepstrums of the seismic trace and of the reflectivity, in order to build the linear filter applied in the cepstral domain to separate the complex cepstrum of the wavelet. We performed this process for both seismic traces with and without the white noise, to verify how the noise affects this methodology of wavelet estimation. Figures 4 and 5 show the well-to-seismic-tie and the estimated wavelets for the synthetic case. It is possible to notice that the homomorphic deconvolution produced excellent results for the wavelet estimation and well-to-seismic-tie. For the case without noise, the wavelet was entirely recovered and the correlation between the real and calculated traces was 1. For the case with noise, the main

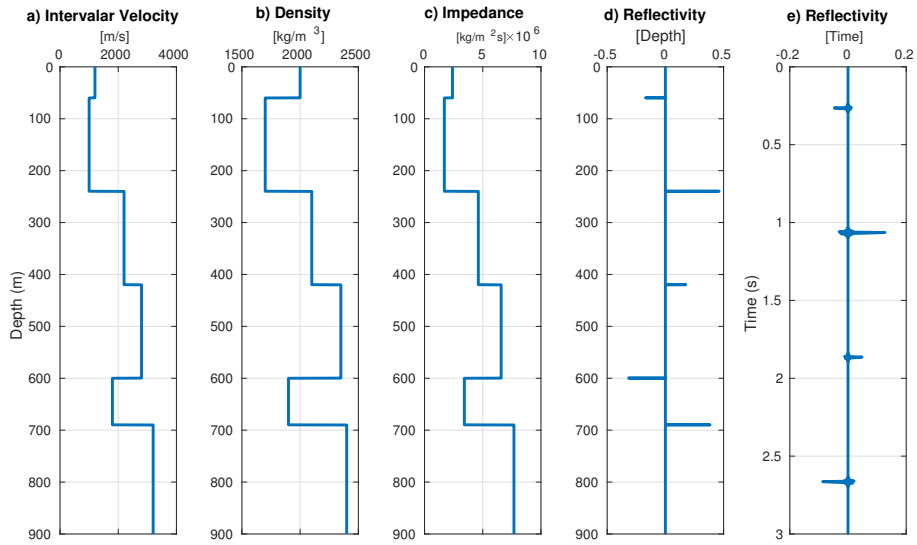


Figure 2: The layer model (constituted of 5 interfaces) used to generate the impedance profile and, therefore, the reflectivity series.

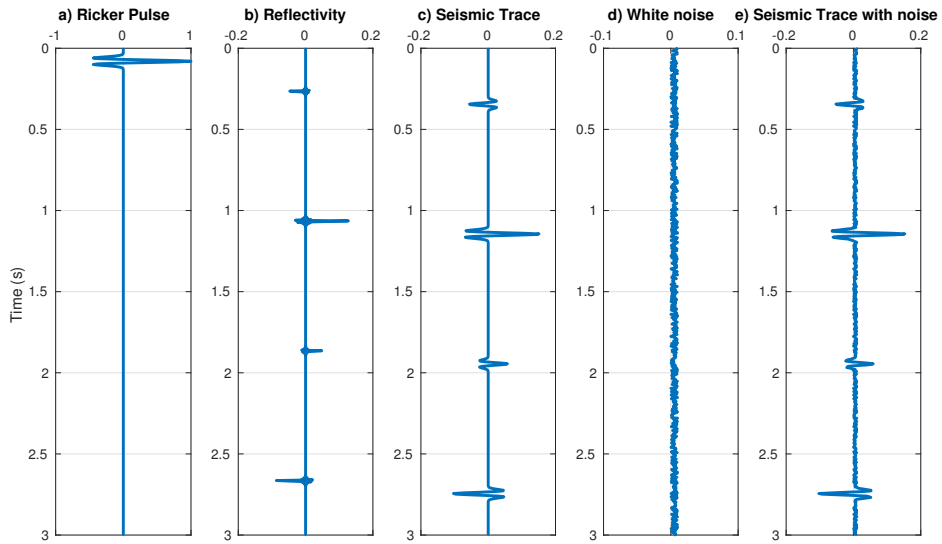


Figure 3: The convolutional model for the synthetic scheme: the reflectivity, the original wavelet (which in this case is the Ricker pulse), and the both seismic traces generated, with and without the white noise.

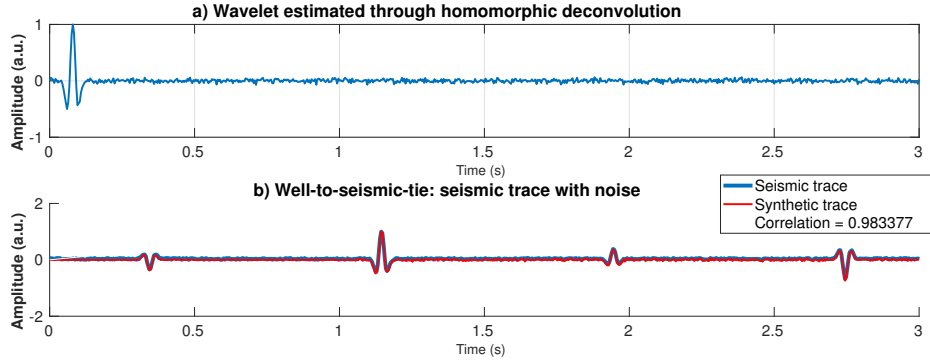


Figure 4: The wavelet estimated through the homomorphic methodology and the well-to-seismic-tie for the case with noise. The correlation is 0.98, with the main signal of the wavelet entirely recovered but with mismatches along the portions contaminated with noise.

signal of the wavelet was entirely recovered, but there were mismatches along the portion with noise. Nevertheless, the correlation between the traces was 0.98.

## Results on Viking Graben data set

The Viking Graben dataset comes from the North Sea basin and a detailed description of its geological background and of its seismic and well logs data acquisition can be found on Madiba and McMechan (2003) and Keys (1998). We used the 2D seismic section - which contains 2142 CMPs with 1501 samples separated by 0.004ms - available on the dataset and two well logs placed on the seismic line, named well A (located on CMP 808) and well B (located on CMP 1572). One of the main geological features of this dataset is an unconformity (referred as BCU) located above the Jurassic sediments and under the Cretaceous sediments, that is approximately at 1.9s in well A and at 2.4s in well B. We followed the steps described before in both synthetic and real schemes. The input parameters of this methodology is the complex cepstrum of the real seismic trace and the

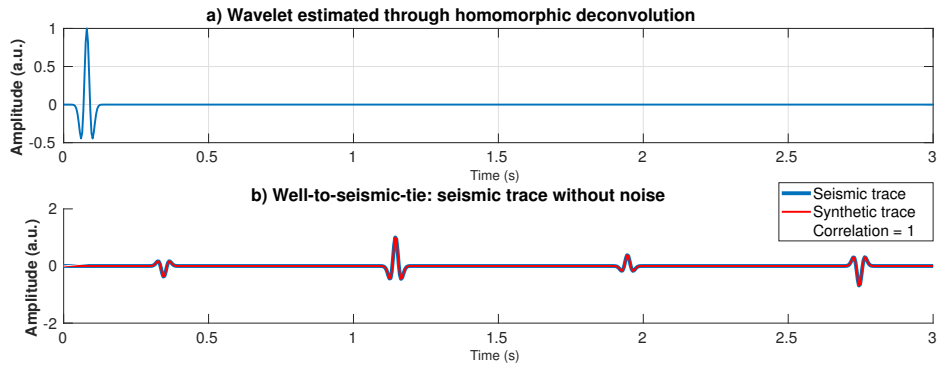


Figure 5: The wavelet estimated through the homomorphic methodology and the well-to-seismic-tie for the case without noise. The correlation is 1, with the wavelet entirely recovered.

complex cepstrum of the reflectivity calculated from the well logs, after the application of the time-depth relationship. The output of the algorithm is the seismic wavelet in the time domain, as a result of the application of the linear filter in the complex cepstrum domain.

### *Discussion and Results of the well to seismic tie*

This section shows the results of the well-to-seismic-tie using our approach for the estimation of the wavelet for the two well logs of the Viking Graben field. Those results might be compared with the ones obtained by Macedo et al. (2017), since the only factor that differentiates the well-ties is the estimation of the wavelet. Figure 6 shows the input data of the algorithm to perform the estimation of the wavelet: the real seismic trace and the reflectivity in time domain calculated from well logs. The complex cepstrum of those parameters are used to build the linear filter that must be applied to the real seismic data to isolate the complex cepstrum of the wavelet, and then transform it to the time domain. Figure 7 illustrates the general form of the linear filter for both wells of the Viking Graben, and the product of the application of the filter, the estimated wavelet. In order to clarify how the components of the wavelet and the reflectivity compose the seismic trace in the cepstrum domain, Figure 8 shows the influence of each component in the composition of the entire cepstrum of the real seismic data.

Figure 9 shows the estimated wavelets and the result of the well-to-seismic-tie, revealing a high degree of correlation for both cases. For the well A, the correlation is 0.749 and for well B the correlation is 0.866. Comparing those results with the ones obtained by Macedo et al. (2017) it is possible to notice that this methodology of estimation of the wavelet produce better results. The use of both seismic and well log data to build the linear filter properly estimate the phase of the seismic wavelet, and the homomorphic deconvolution process does not imply the conventional assumptions adopted by the classical convolutional model, such as a random process reflectivity and a minimum-phase wavelet. We believe that these two factors and the ability of the homomorphic systems to describe a signal as

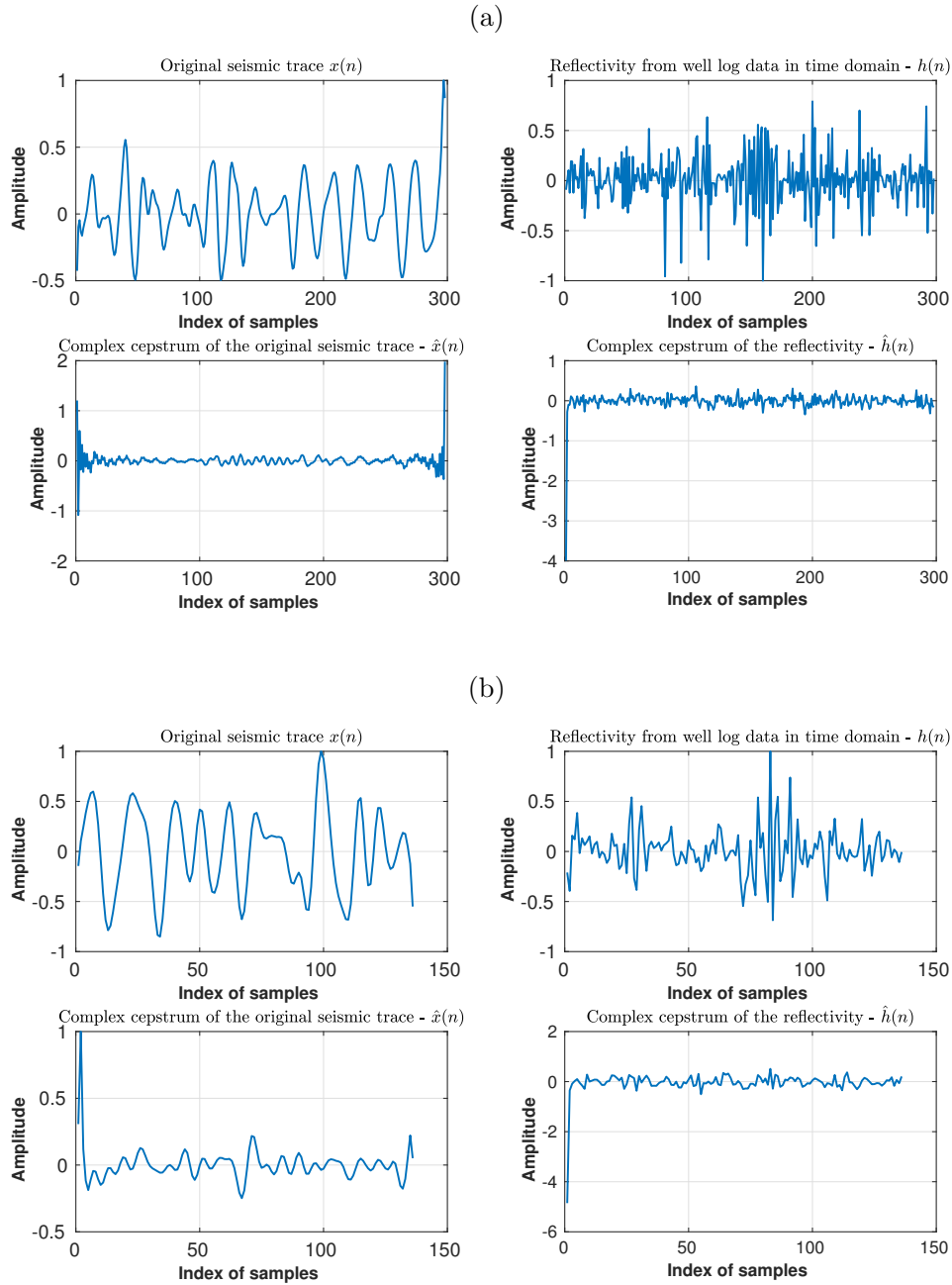


Figure 6: The inputs of the algorithm to estimate the wavelet through the homomorphic deconvolution and well log data: The original seismic trace, the reflectivity calculated from well logs in the time domain and their corresponding complex cepstrum. a) Real seismic trace from the CMP 809 of the Viking Graben migrated seismic section and the reflectivity from well log A b) Real seismic trace from the CMP 1573 of the Viking Graben migrated seismic section and the reflectivity from well log B.

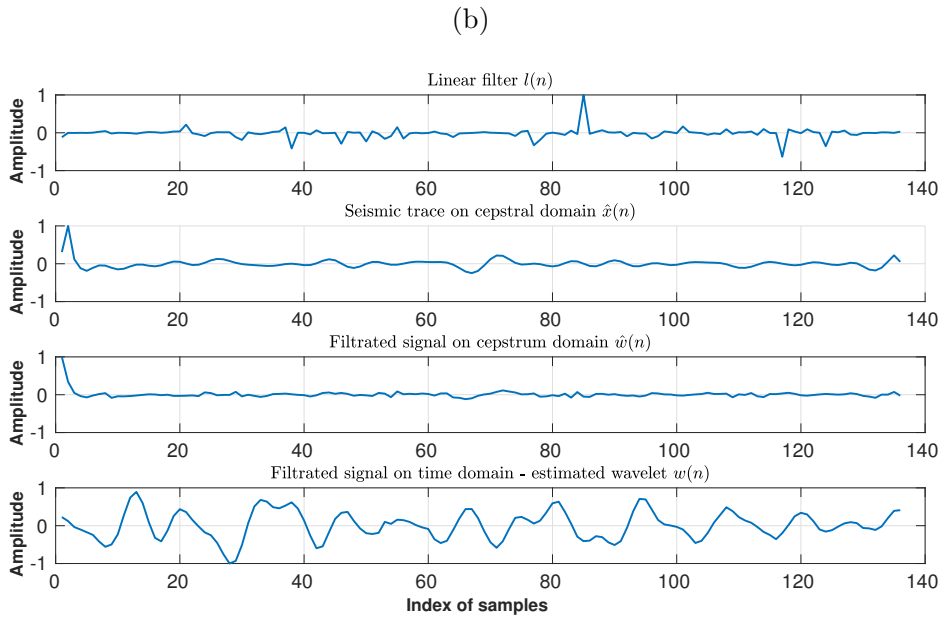
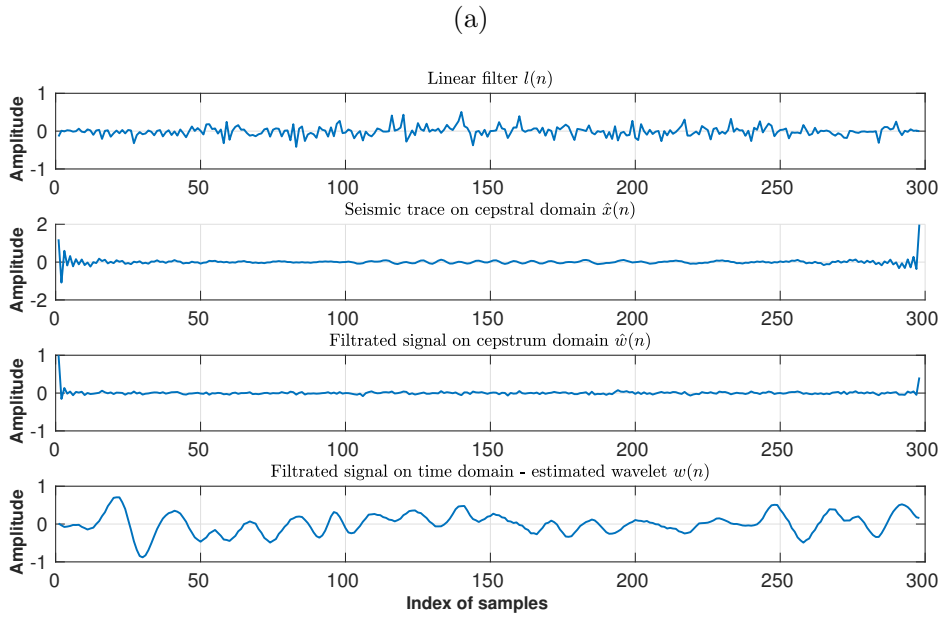


Figure 7: The linear filter applied to separate the components of the convolution, the complex cepstrum of the real seismic trace, the complex cepstrum of the product of the application of the filter and the product of the filtration in the time domain. a) Using the real seismic trace from CMP 809 b) Using the real seismic trace from CMP 1573.

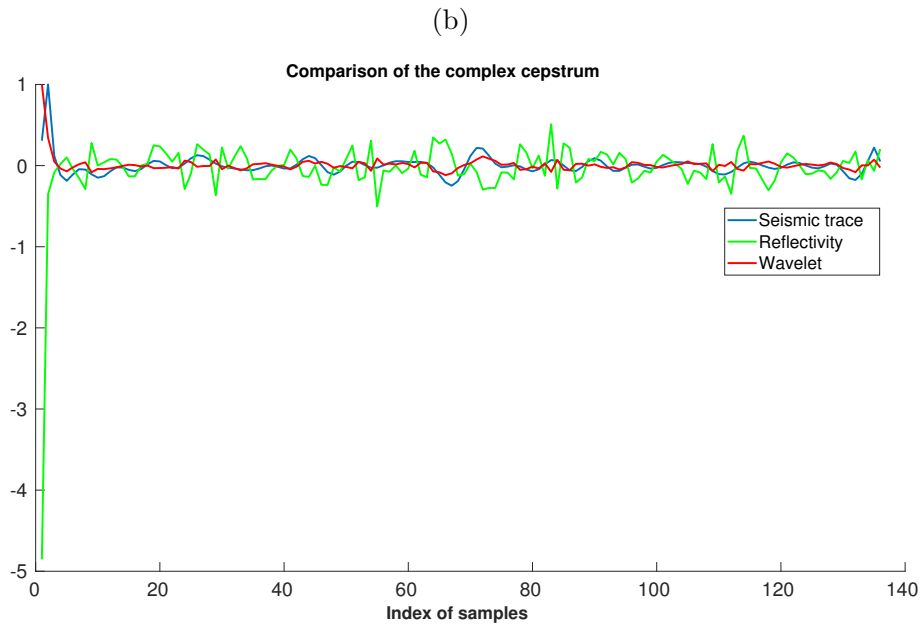
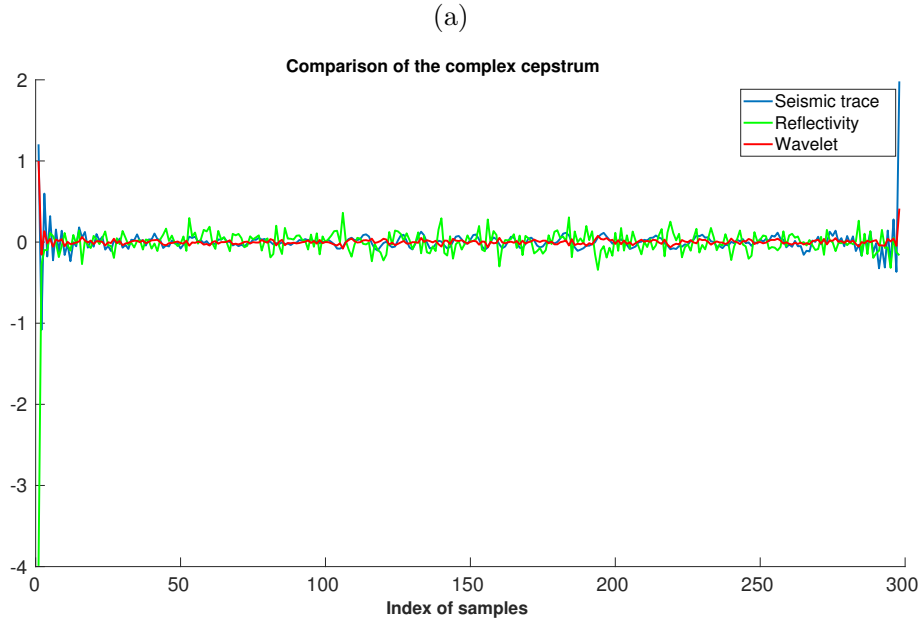


Figure 8: Comparison of the complex cepstrum of each component of the convolution (reflectivity and wavelet) together with the real seismic trace. a) Using the data relative to the well log A and CMP 809 b) Using the data relative to the well log B and CMP 1573.

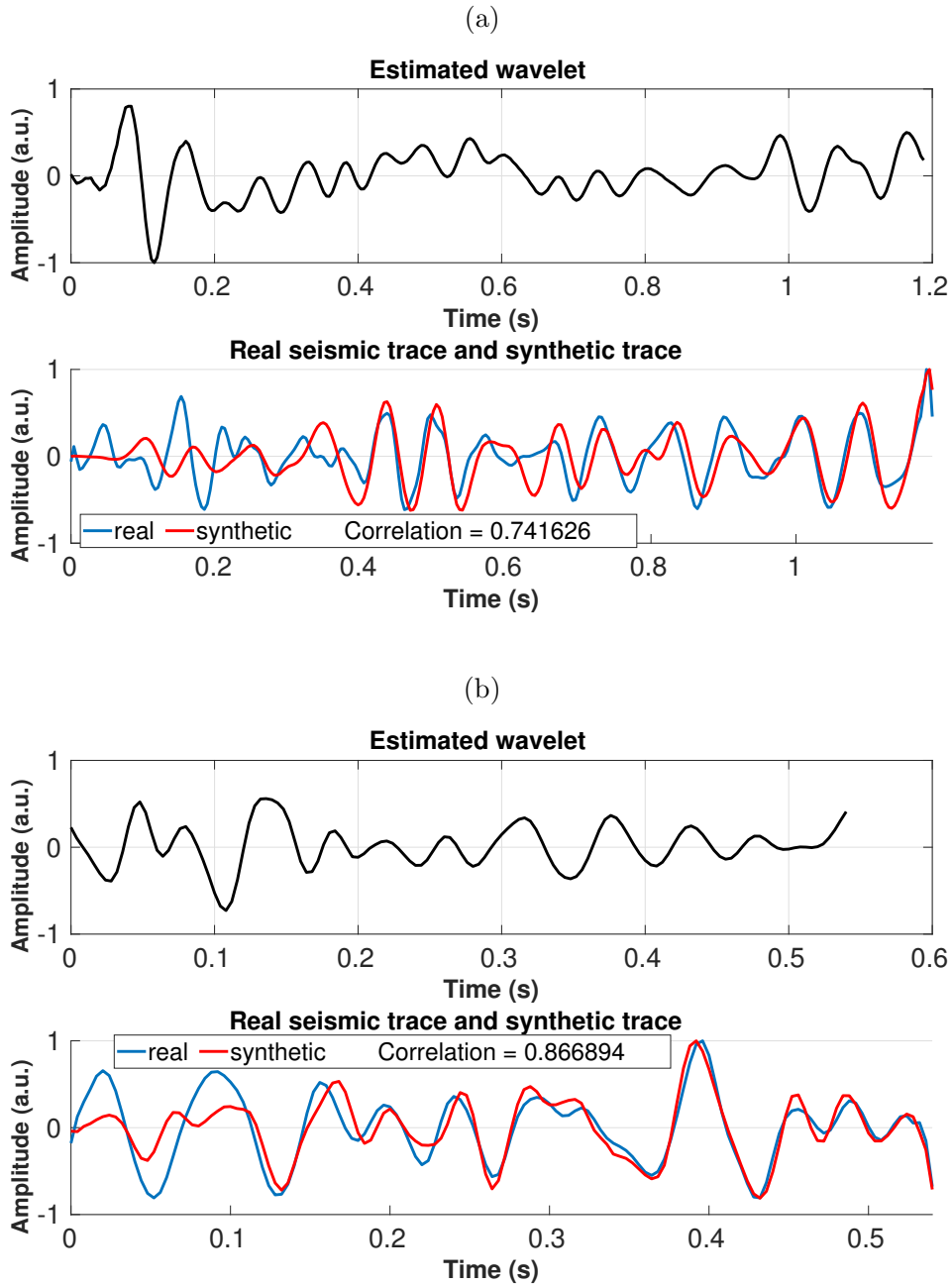


Figure 9: The result of the application of our new approach to estimate the wavelet on the well-to-seismic-tie a) Estimated wavelet and well-to-seismic-tie of the CMP 809 and well log A b) Estimated wavelet and well-to-seismic-tie of the CMP 1573 and well log B.

an addition made possible to estimate a good wavelet in a direct way, as long as an accurate time-depth relationship is available. For comparison purposes, the correlation obtained by Macedo et al. (2017) using the classical assumptions of the convolutional model for the well A was 0.65 using the predictive deconvolution, and 0.712 using the deterministic estimation of the wavelet through the Wiener filtering technique. For well B, the correlation was 0.74 using the predictive deconvolution and 0.81 using the deterministic approach. Our previous results of deconvolution as a method of wavelet estimation for the well-to-seismic-tie are summarized in the table , which shows the correlation between the real and the synthetic seismic trace when only the method to estimate the wavelet is changed.

METHOD OF WAVELET ESTIMATION					
		Predictive Deconvolution (Macedo et al., 2017)	Average Predictive Deconvolution (Macedo et al., 2017)	Deterministic Wiener Filter (Macedo et al., 2017)	Homomorphic Deconvolution
<b>SYNTHETIC DATA</b>	With noise	0.911	X	0.981	0.983
	Without noise	0.956	X	1	1
<b>VIKING GRABEN DATASET</b>	Well A	0.658	0.674	0.712	0.749
	Well B	0.741	0.734	0.811	0.866

Table 1: Correlation values achieved on the well-to-seismic-tie using different approaches to estimate the wavelet. The first three methodologies assume a minimum-phase wavelet.

## CONCLUSIONS

In this paper we propose an approach to estimate the seismic wavelet that uses the advantages of the homomorphic deconvolution and the advantages of the deterministic wavelet estimation, using both seismic and well data. Our results showed that this methodol-

ogy produces higher values of correlation for the well-to-seismic-tie when compared with a methodology that consider the classical assumptions of the convolutional model. For the well A of the Viking Graben Field, we obtained a correlation of 0.749, and for the well B, we obtained a correlation of 0.866.

Although the homomorphic deconvolution configures a statistical approach to estimate the wavelet, since originally the linear filter building considers only mathematical tools, our approach might be considered deterministic because we use both real seismic and well log data to build the linear filter and then estimate the wavelet in the time domain. Because the homomorphic procedure does not imply a minimum-phase wavelet, and describe the convolution as an addition, the ability to separate the components is dependent upon the building of an efficient filter. The need to use the reflectivity in the time domain as an input to the filter in our algorithm makes this methodology strongly dependent on an accurate time-depth relationship, therefore, attention must be taken in order to do not produce a reflectivity shifted in time.

For future studies, we suggest to verify how this approach behaves with different kinds of filters applied on the cepstral domain and how it behaves with errors or corrections on the time-depth relationship, in order to establish its dependence to those criteria.

## **ACKNOWLEDGMENTS**

The authors would like to thank the Exxon Mobil for providing the Viking Graben dataset. This work was kindly supported by the Brazilian agencies INCT-GP, CAPES and CNPq from Brazil and the Geophysics Graduate Program at Federal University of Par.

## REFERENCES

- Bo, Y. Y., G. H. Lee, H.-J. Kim, H.-T. Jou, D. G. Yoo, B. J. Ryu, and K. Lee, 2013, Comparison of wavelet estimation methods: *Geosciences Journal*, **17**, 55–63.
- Dey, A. K., and L. R. Lines, 1998, Seismic source wavelet estimation and the random reflectivity assumption, *in* SEG Technical Program Expanded Abstracts 1998: Society of Exploration Geophysicists, 1088–1091.
- Edgar, J. A., and M. Van der Baan, 2011, How reliable is statistical wavelet estimation?: *Geophysics*, **76**, V59–V68.
- Herrera, R. H., and M. Van Der Baan, 2012, Revisiting homomorphic wavelet estimation and phase unwrapping: arXiv preprint arXiv:1205.3752.
- Keys, R. G., 1998, Comparison of seismic inversion methods on a single real data set, open file publications: Society of Exploration.
- Macedo, I. A. S., C. B. d. Silva, J. J. S. d. Figueiredoa, and B. Omoboyac, 2017, Comparison between deterministic and statistical wavelet estimation methods through predictive deconvolution: Seismic to well tie example from the North Sea: *Journal of Applied Geophysics*, **136**, 298–314.
- Madiba, G. B., and G. A. McMechan, 2003, Processing, inversion, and interpretation of a 2d seismic data set from the North Viking Graben, North Sea: *Geophysics*, **68**, 837–848.
- Trantham, E. C., 1994, Controlled-phase acquisition and processing, *in* SEG Technical Program Expanded Abstracts 1994: Society of Exploration Geophysicists, 890–894.
- Tribolet, J. M., and A. V. Oppenheim, 1977, Deconvolution of seismic data using homomorphic filtering: Technical report, MASSACHUSETTS INST OF TECH CAMBRIDGE RESEARCH LAB OF ELECTRONICS.
- White, R., and R. Simm, 2003, Tutorial: Good practice in well ties: *First Break*, **21**.

# 5 ARTICLE 4: LINEAR INVERSION TO ESTIMATE THE SEISMIC WAVELET AND TO RECOVER THE REFLECTIVITY OF THE SEISMIC SECTION: WELL-TO-SEISMIC-TIE ON REAL DATASET FROM VIKING GRABEN, NORTH SEA.

Authors: Isadora Augusta Santana de Macedo, José Jadsom Sampaio de Figueiredo.  
 Submitted to Geophysics journal

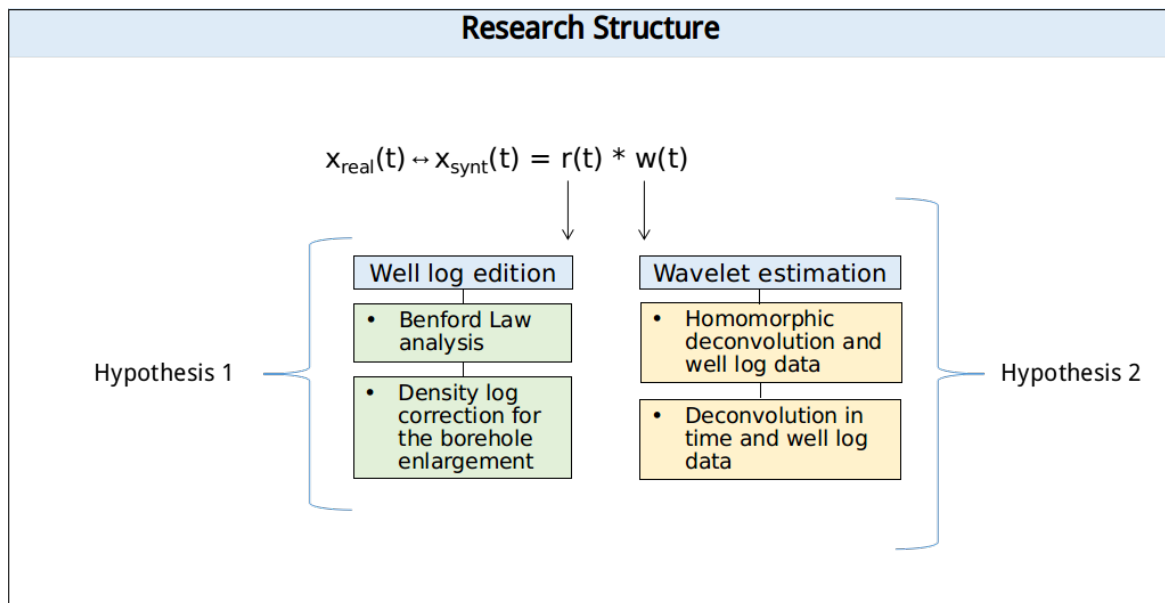


Figure 5.1: The research structure for the well-to-seismic-tie: Chapter 4 and Chapter 5 (in yellow), related with wavelet estimation.

The present chapter shows the results obtained with a deconvolution in time as a method to estimate the seismic wavelet. The deconvolution in time, which can be seen as an linear inverse problem, does not require a random reflectivity or assumptions about the wavelet's phase. For the wavelet estimation, we used a least-squares minimization with a zero order quadratic regularization. In the article "Linear inversion to estimate the seismic wavelet and to recover the reflectivity of the seismic section: well-to-seismic-tie on real dataset from Viking Graben, North Sea", we show that the wavelet estimated through this methodology produce a high quality well tie, suitable for the exploitation stage. Moreover, the estimated wavelet is quite similar to the one obtained through the deterministic homomorphic deconvolution, which suggests the feasibility of both approaches, since their formulations are essentially different. Using the estimated wavelet as input, we recover the reflectivity of the seismic section near the borehole through a

sparse-spike deconvolution algorithm, which is also a least-squares minimization but with a L1 norm regularization. We used known stratigraphic markers as reference to check the reliability of the inversion.

**Linear inversion to estimate the seismic wavelet and to  
recover the reflectivity of the seismic section:  
well-to-seismic-tie on real dataset from Viking Graben,  
North Sea.**

**Isadora A. S. de Macedo <sup>\*†</sup> and J. J. S. de Figueiredo <sup>\*†</sup>**

*\* UFPA, Faculty of Geophysics, Petrophysics and Rock Physics Laboratory - Prof. Dr.*

*Om Prakash*

*Verma, Belém, PA, Brazil.*

*† National Institute of Petroleum Geophysics (INCT-GP), Brazil.*

Running head: **deconvolution in time on well-to-seismic-tie**

**ABSTRACT**

The well-to-seismic-tie is an important step in seismic processing and interpretation. Deconvolutional statistical methods to estimate the proper wavelet in general are based on the assumptions of the classical convolutional model, which implies a random process reflectivity and a minimum-phase wavelet. In this study we aim to estimate the wavelet for well-to-seismic-tie purposes through least squares minimization with zero order quadratic regularization and compare with the results obtained from the deterministic homomorphic deconvolution. Both methods does not make any assumptions regarding the wavelet's phase or the reflectivity. The best estimated wavelet was used as input to the sparse-spike deconvolution to recover the reflectivity near the well location. Our results show that the wavelets estimated from both deconvolutions are similar, which suggests their feasibility. The reflec-

tivity of the seismic section was recovered according to known stratigraphic markers present in the real dataset from the Viking Graben field, Norway.

## INTRODUCTION

The impulse response of the Earth can be considered as a connection between the geology and the seismic data, since the contrast of acoustic impedance between the rock's layers causes the impulses that, when convolved with a seismic wavelet, generates a reflection that is recorded by an array of receivers. Another way of promoting this connection between the seismic and the geology, is through the well-to-seismic-tie: a procedure in which the synthetic traces calculated from well log data are compared with the real seismic traces from the seismic acquisition survey. Temporal resolution of the seismic data limits the accuracy of detailed mapping of geology, which is quite important in mapping of thin reservoirs for hydrocarbon exploration (Ursin and Holberg, 1985). The well-to-seismic-tie joints the vertical resolution that comes from the well logs with the horizontal resolution of the seismic data and makes it possible to identify stratigraphic horizons on the seismic section and estimate the proper wavelet to be used in the inversion for the reflectivity or acoustic impedance.

The key of the well-to-seismic-tie is the comparison of the synthetic seismogram - calculated through the sonic and density profile - with the real recorded seismogram in the vicinity of the well location. The synthetic seismogram is the product of the convolution of the seismic wavelet with the reflectivity. In order to do so, it is necessary to convert the reflectivity series calculated from the well log data in depth, to the time domain. A time-depth relationship can be obtained from seismic recordings such as checkshot surveys or zero offset Vertical Seismic Profiles (VSPs), measured in the vicinity of the well (White, 2003). The seismic wavelet used in the convolution with the reflectivity series can be estimated by different approaches. Generally, the methods to estimate the wavelet fall largely

into two categories: (1) purely statistical ways and (2) the use of well-log data (White and Simm, 2003). The reflectivity series computed from sonic and density logs can be used to estimate the wavelet with proper amplitude and phase spectra (Dey and Lines, 1998). The use of controlled-phase acquisition and processing strategies can help control seismic phase (Trantham, 1994), but mismatches between recorded seismic data and synthetic traces constructed from well-log data occur very frequently (Edgar and Van der Baan, 2011).

The deconvolution is a well known process that compresses the wavelet in the recorded seismogram in order to attenuate reverberations and short-period multiples, thus increasing temporal resolution and yielding a representation of subsurface reflectivity (Yilmaz, 2000). Classical deconvolution methods such as the Wiener filtering for the predictive and spiking deconvolution are based on the classical premises about the convolutional model of the earth, which assumes, among other factors, a stationary minimum phase wavelet and a random process reflectivity. Herrera and Van Der Baan (2012) used the homomorphic deconvolution as a statistical approach to estimate the seismic wavelet, without making any assumptions about the phase of the wavelet. The power of the deconvolution techniques to separate the components of the reflectivity and the wavelet, makes it a valuable tool in the seismic wavelet estimation for well-to-seismic-tie purposes and gets even more interesting if the reflectivity calculated from well logs is available, since it may mitigate the problem of estimate the proper amplitude and phase of the wavelet.

This paper aims to show the results of the application of the deconvolution in time with zero order quadratic regularization to firstly recover the seismic wavelet for the well-to-seismic-tie, and then use the estimated wavelet to recover the reflectivity of the seismic section through the sparse-spike deconvolution, using known stratigraphic markers to check the feasibility of the inversion. The sparse-spike deconvolution can be seen as a least squares

inversion problem with a L1 norm regularization. The L1 norm regularization is the factor that ensures that the response of the deconvolution is a series of sparse spikes. Our examples shows that when we consider the L1 regularization, we assume the sparsity of the solution, which is not a proper assumption to be made for the seismic wavelet, but is a reasonable assumption to be made for the reflectivity series. The same least squares algorithm can be used to estimate the wavelet and to recover the reflectivity, as long as the proper convolutional matrix is calculated and the L1 regularization parameter is set to zero to estimate the wavelet (in order to avoid the sparsity assumption) and is non zero to recover the reflectivity. This method does not require an assumption regarding the phase of the input wavelet and does not require a random reflectivity series, as occurs with a large class of deconvolutions. Both synthetic and real dataset showed reasonable results, the wavelet estimated produced a high quality well-to-seismic-tie and the reflectivity of the seismic section was properly recovered.

## THEORETHICAL BACKGROUND

According to the classical convolutional model of the Earth, a seismogram is the sum of the convolution of the seismic wavelet with the impulse response series and added noise. Thus, the convolution of two time series can be expressed by:

$$s(t) = a(t) * x(t) + n(t) \tag{1}$$

The matrix form of equation A-1 omitting the random noise factor is:

$$\mathbf{Ax} = \mathbf{s}, \tag{2}$$

where  $\mathbf{s}$  and  $\mathbf{x}$  are vectors  $\mathbf{A}$  is the convolution matrix with elements  $A_{ij} = a_{i-j+1}$ . In general, matrix  $\mathbf{A}$  is ill conditioned, the input data  $\mathbf{s}$  is noisy and the solution  $\mathbf{x}$  to the

equation 2 does not exist. A possible approach to solve equation 2 is through least squares minimization,

$$\|\mathbf{Ax} - \mathbf{s}\|^2 \rightarrow \min_{\mathbf{x}}, \quad (3)$$

whose solution  $\mathbf{x}$  is achieved by the normal equations:

$$\mathbf{A}^T \mathbf{Ax} = \mathbf{A}^T \mathbf{s}. \quad (4)$$

Its unconstrained least-squares solution causes enormous oscillations in the estimative of  $\mathbf{x}$ , since the equation system is very sensitive to noise present in the vector  $\mathbf{s}$  (Morháč, 2006), therefore, direct inversion of this system cannot produce a stable solution. Due to the instability of the problem, a small perturbation in the input data  $\mathbf{s}$  may lead to a huge difference in the solution  $\mathbf{x}$ . Therefore, is added a term to regularize the functional 3 aiming to produce a more stable solution  $\mathbf{x}$ . When the term added is quadratic, it configures the Tikhonov regularization:

$$\|\mathbf{Ax} - \mathbf{s}\|^2 + \alpha \|\mathbf{Lx}\|_2^2 \rightarrow \min_{\mathbf{x}}, \quad (5)$$

where  $\mathbf{L}$  is a real squared matrix. The relation expressed in 5 can be rewritten as

$$\|\mathbf{Ax} - \mathbf{s}\|^2 + \alpha \|\mathbf{Lx}\|_2^2 = \|\mathbf{Cx} - \mathbf{h}\|^2, \quad (6)$$

where

$$\mathbf{C} = \begin{bmatrix} \mathbf{A} \\ \sqrt{\alpha} \mathbf{L} \end{bmatrix} \quad (7)$$

$$\mathbf{h} = \begin{bmatrix} \mathbf{s} \\ \mathbf{0} \end{bmatrix} \quad (8)$$

Therefore, minimizing 5 is the same as minimizing

$$\|\mathbf{Cx} - \mathbf{h}\|^2 \rightarrow \min_{\mathbf{x}}, \quad (9)$$

whose solution is given by

$$\mathbf{C}^T \mathbf{C} \mathbf{x} = \mathbf{C}^T \mathbf{h}, \quad (10)$$

that can also be written as:

$$(\mathbf{A}^T \mathbf{A} + \alpha \mathbf{L}^T \mathbf{L}) \mathbf{x} = \mathbf{A}^T \mathbf{s}. \quad (11)$$

The zeroth-order Tikhonov regularization or just zero order quadratic regularization is achieved when the real square matrix  $\mathbf{L}$  is the identity matrix  $\mathbf{I}$ . In this case, the system 11 takes the form

$$(\mathbf{A}^T \mathbf{A} + \alpha \mathbf{I}) \mathbf{x} = \mathbf{A}^T \mathbf{s}, \quad (12)$$

that can be rewritten as

$$\mathbf{x} = (\mathbf{R} + \alpha \mathbf{I})^{-1} \mathbf{g}. \quad (13)$$

It is equivalent to add a perturbation in the diagonal of the autocorrelation matrix  $\mathbf{R}$ . This procedure is also called pre-whitening and is a form to stabilize the deconvolution problem. In this study, in order to distinguish the regularization parameters, we decide to set  $\alpha = \beta$  when the regularization parameter acts as pre-whitening (zero order quadratic regularization), and  $\alpha$  when the regularization acts to control the sparsity of the solution (L1 norm regularization).

Another form to stabilize the solution of the functional 3 is by adding a L1 norm regularization:

$$\|\mathbf{A} \mathbf{x} - \mathbf{s}\|^2 + \alpha \|\mathbf{x}\|_1 \rightarrow \min_{\mathbf{x}}. \quad (14)$$

Sacchi (1997) shows that it is possible to find a solution to the equation 14 in the form:

$$\mathbf{x} = (\mathbf{R} + \alpha \mathbf{Q})^{-1} \mathbf{g}, \quad (15)$$

where  $\mathbf{Q}$  is a diagonal matrix whose elements for a L1 norm regularization takes the following form:

$$\mathbf{Q}_{ii} = \frac{1}{|\mathbf{x}_i|}, \quad \mathbf{x}_i \neq 0. \quad (16)$$

The solution for  $\mathbf{x}$  in equation 15 is achieved through the iteratively re-weighted least squares, which seeks to find iteratively a solution for  $\mathbf{x}$  by updating the diagonal matrix of weights  $\mathbf{Q}$  depicted in equation 16 at each interaction.

The sparse-spike deconvolution is mathematically a least squares minimization with a L1 norm regularization, given the seismic wavelet and the seismic trace as inputs to recover the reflectivity. It seeks the least number of spikes in the input so that, when convolved with the seismic wavelet, it fits the data within a given tolerance (Velis, 2007). Moreover, the L1 norm regularization implies the sparsity of the solution, which is a reasonable assumption for the reflectivity series, since it will enhance the appearance of the main stratigraphic markers and will set to zero the less important ones. However, the same assumption is not reasonable to recover the seismic wavelet, since it is characterized by a smooth finite time pulse. In other words, depending on the formulation of the convolutional matrix depicted in equation 2, the least-squares solution 3 may recover the reflectivity series or the seismic wavelet, given the proper term to regularize the problem for each case: zero order quadratic regularization when one desires to recover the wavelet adding the pre whitening factor  $\beta$ , and L1 norm regularization when one desires to recover the reflectivity adding  $\alpha$  to control the sparsity of the solution of the inversion.

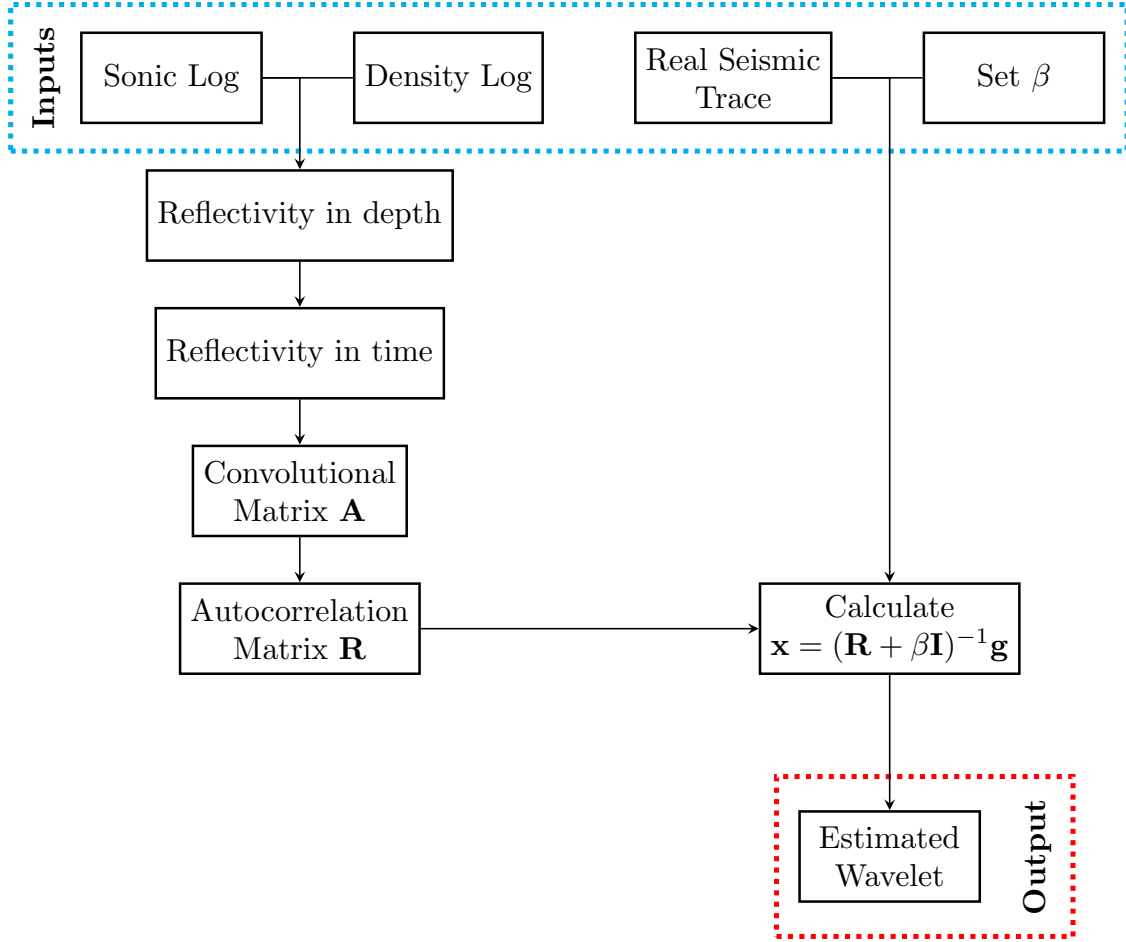


Figure 1: Flowchart for the wavelet estimation procedure through the deconvolution in time, using the zero-order quadratic regularization.

## METHODOLOGY

The objective of applying the theory explained before is to use the deconvolution in time to estimate the wavelet (flowchart on Figure 1) that produces the best match between the real seismic traces and the synthetics, and then use the estimated wavelet on the sparse-spike deconvolution, to recover the reflectivity (flowchart on Figure 2) in the vicinity of the well location. The steps we performed in the algorithm built for this study to perform the well-to-seismic-tie can be summarized as follows:

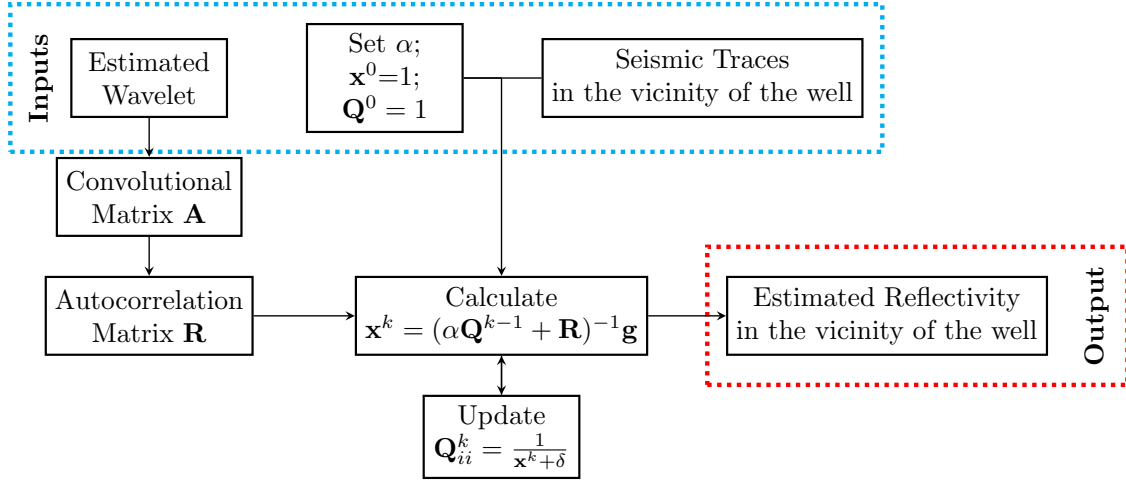


Figure 2: Flowchart for the recovery of the reflectivity in the vicinity of the well location using the estimated wavelet. In this case, the L1 norm regularization is used.

1. Quality control of the inputs and possible edition of them, since the well logs have null e/or noisy values that need to be dealt with.
2. Calculate the reflectivity series in depth through the well logs according to the contrast of impedance:

$$R_i = \frac{\rho_{i+1}v_{i+1} - \rho_i v_i}{\rho_{i+1}v_{i+1} + \rho_i v_i}. \quad (17)$$

3. Apply the time-depth relationship to correctly place the reflectivity in time.
4. Set the sparsity parameter  $\alpha=0$ ; set the pre whitening parameter  $\beta$ .
5. Calculate the convolutional matrix  $\mathbf{A}$  of the normal equations 12 using the reflectivity.
6. Calculate the autocorrelation matrix  $\mathbf{R} = \mathbf{A}^T \mathbf{A}$ .
7. Use  $\mathbf{R}$  and the seismic trace to estimate the seismic wavelet through the zero-order quadratic regularization deconvolution, which is done through the equation 13.
8. Calculate the synthetic seismic trace and compare with the real seismic trace using the correlation coefficient.

To proceed with the recovery of the reflectivity of the seismic section, we use the sparse-spike deconvolution, which is done through the iteratively re-weighted least squares and the relations proposed by Sacchi (1997) for a L1 norm regularization, as shown before. The algorithm is summarized as follow and is illustrated on Figure 2:

1. Define the initial solution for  $\mathbf{x}^0 = 1$  and the initial diagonal matrix of weights  $\mathbf{Q}^0=1$ .
2. Set the sparsity parameter  $\alpha$ .
3. Calculate the autocorrelation matrix  $\mathbf{R} = \mathbf{A}^T \mathbf{A}$ , using the estimated wavelet to build the convolutional matrix  $\mathbf{A}$ .

4. Solve iteratively

$$\mathbf{x}^k = (\alpha \mathbf{Q}^{k-1} + \mathbf{R})^{-1} \mathbf{g}, \quad (18)$$

where  $k$  is represents the index of the number of iterations and  $\mathbf{g}$  is the seismic trace.

5. Update the diagonal matrix of weights  $\mathbf{Q}$  according to Sacchi (1997) (as previously shown in equation 16)

$$\mathbf{Q}_{ii}^k = \frac{1}{|\mathbf{x}_i^k| + \delta}, \quad (19)$$

the term  $\delta = 0.0001$  is added to avoid a division by zero.

6. Find solutions for  $\mathbf{x}$  until the established tolerance.
7. If it is necessary, adjust the parameter  $\alpha$  and repeat the procedure from step 3 to find a new solution for  $\mathbf{x}$ .

Our results shows that the deconvolution in time produced a high quality well-to-seismic-tie. Moreover, the wavelet estimated for the real dataset used in this study was

compared with the wavelet estimated through the deterministic homomorphic deconvolution, explained in the appendix. Both methods estimate the wavelet without making any assumptions regarding the wavelet’s phase or the reflectivity. The wavelets estimated through those essentially different methodologies are quite similar, which suggests their efficiency. The wavelet estimated for the well-tie also recovered the main stratigraphic horizon of the seismic section when used as an input to the sparse-spike deconvolution.

## RESULTS ON THE SYNTHETIC DATASET

Before applying the algorithm built on the real dataset, we tested it on a synthetic data to verify its behavior on the wavelet estimation. Figure 3a shows the synthetic layer model we used to simulate the well log data. Figure 3b shows the causal wavelet with a peak frequency of 20Hz we used to compute our simulated real seismic trace  $\mathbf{s}$ . We created three simulations of the real seismic trace to test our algorithm: a noise-free seismic trace, a noisy seismic-trace, and a seismic trace with a small perturbation. This last was done to verify the stability of the solution: if a small perturbation in the input seismic trace causes a huge change in the estimated wavelet.

We use the deconvolution in time to recover the seismic wavelet following the methodology explained before and then we perform the well-to-seismic-tie to verify the similarity between the real seismic traces and the synthetic ones.

The results shown in Figure 5 infers that the deconvolution in time with zero order quadratic regularization to recover the wavelet might be used for well-to-seismic-tie purposes. A small perturbation in the input (Figure 5c) caused the correlation to decrease, but did not produce a huge change on the wavelet estimated, which suggests that the zero

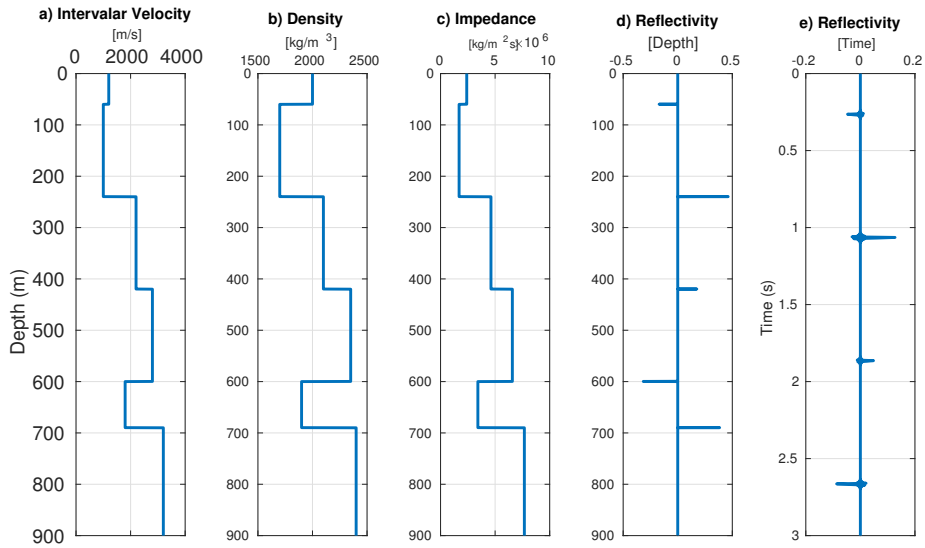


Figure 3: The layer model (constituted of 5 interfaces) used to generate the impedance profile and, therefore, the reflectivity series.

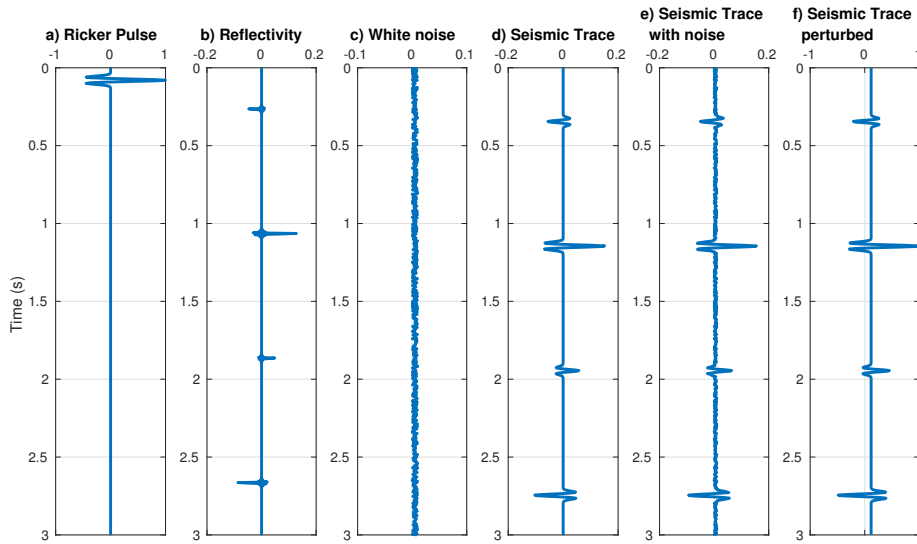
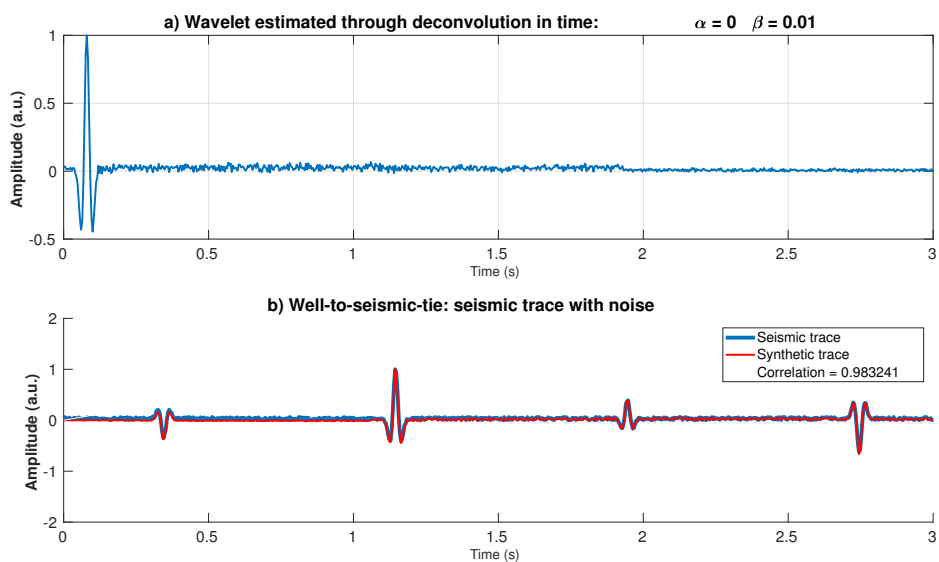
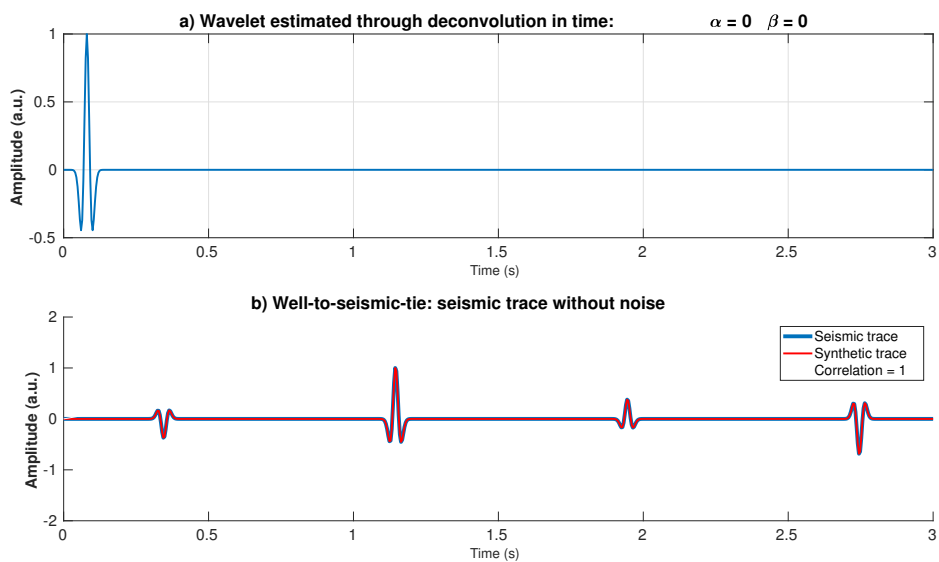


Figure 4: The convolutional model for the synthetic scheme: the reflectivity, the original wavelet (which in this case is a causal pulse), and the real seismic traces generated, with and without the white noise, and with a small perturbation.

(a)



(b)



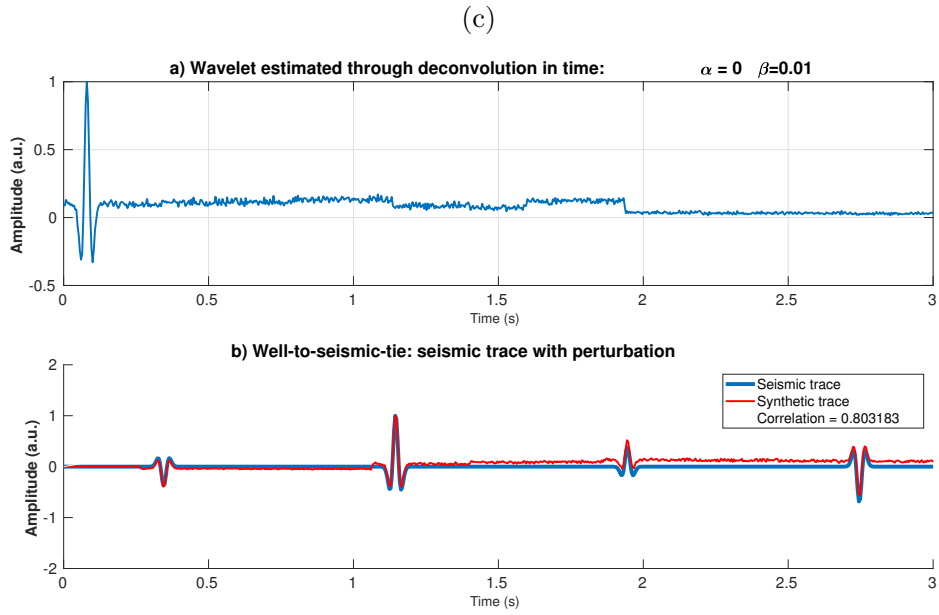


Figure 5: Well-to-seismic-tie performed on the synthetic dataset with three simulations of the real seismic trace. The deconvolution in time was used to estimate the wavelet, therefore, the L1 regularization parameter  $\alpha$  was set to zero. The pre-whitening factor for the noise-free case was  $\beta=0$  and for the other cases was  $\beta=0.01$ . a) Real seismic trace with noise, a correlation of 0.98 was achieved. b) Real seismic trace without noise, a correlation of 1 was achieved and the seismic wavelet was entirely recovered. c) Real seismic trace with a perturbation, a correlation of 0.80 was achieved.

order quadratic regularization might work for the case of wavelet estimation through deconvolution in time. For the cases with and without noise on the real trace, the algorithm was able to estimate a wavelet almost with total accuracy, producing a correlation of 0.98 for the trace with noise, and a correlation of 1 for the noise-free trace.

## RESULTS ON VIKING GRABEN DATA SET

The Viking Graben is located on the northern North Sea basin and was the product of a rifting that happened in the late Permian to the Triassic. A detailed geological background can be found at Madiba and McMechan (2003) and Keys (1998), as well as the informations regarding the acquisition of the seismic and well log data. For the well-to-seismic-tie, we use a 2D seismic line of the Viking Graben dataset, which contains 2142 CMPS with 1501 samples separated by 0.004s each, and 2 wells placed along the seismic section, named as well A (located at CMP 808) and well B (located at CMP 1572).

Keys (1998) highlight that the Jurassic was a period of active faulting in the northern North Sea basin and some hydrocarbon traps are associated with stratigraphic truncations at the unconformity at the base of the Cretaceous. This unconformity - referred as BCU - is located above the Jurassic synrift sediments that are also overlain by Cretaceous and Tertiary basin fill.

According to Madiba and McMechan (2003), the major base Cretaceous unconformity (BCU) is located at approximately 1.97s on well A and at 2.46s on well B. It marks an important known stratigraphic horizon in this dataset that can be used as reference to check if the recovery of the reflectivity in the seismic section, using the estimated wavelet, is coherent.

Figure 6 show the well log data of the Viking Graben dataset used in this study. The well log data was edited to remove noisy spikes and wrong values. There are missing data values on well B density and sonic logs. Those missing data were filled using the Gardner's relation (Gardner, 1974).

The result of the application of the deconvolution in time to estimate the seismic wavelet in the real Viking Graben dataset is depicted in Figure 7. For the estimation of the wavelet, as mentioned before, we used the least-squares minimization with zero order quadratic regularization, which is equivalent to the pre whitening procedure. For both cases, we use  $\beta=0.01$ , and a correlation of 0.90 was achieved for the well A and a correlation of 0.87 was achieved for the well B.

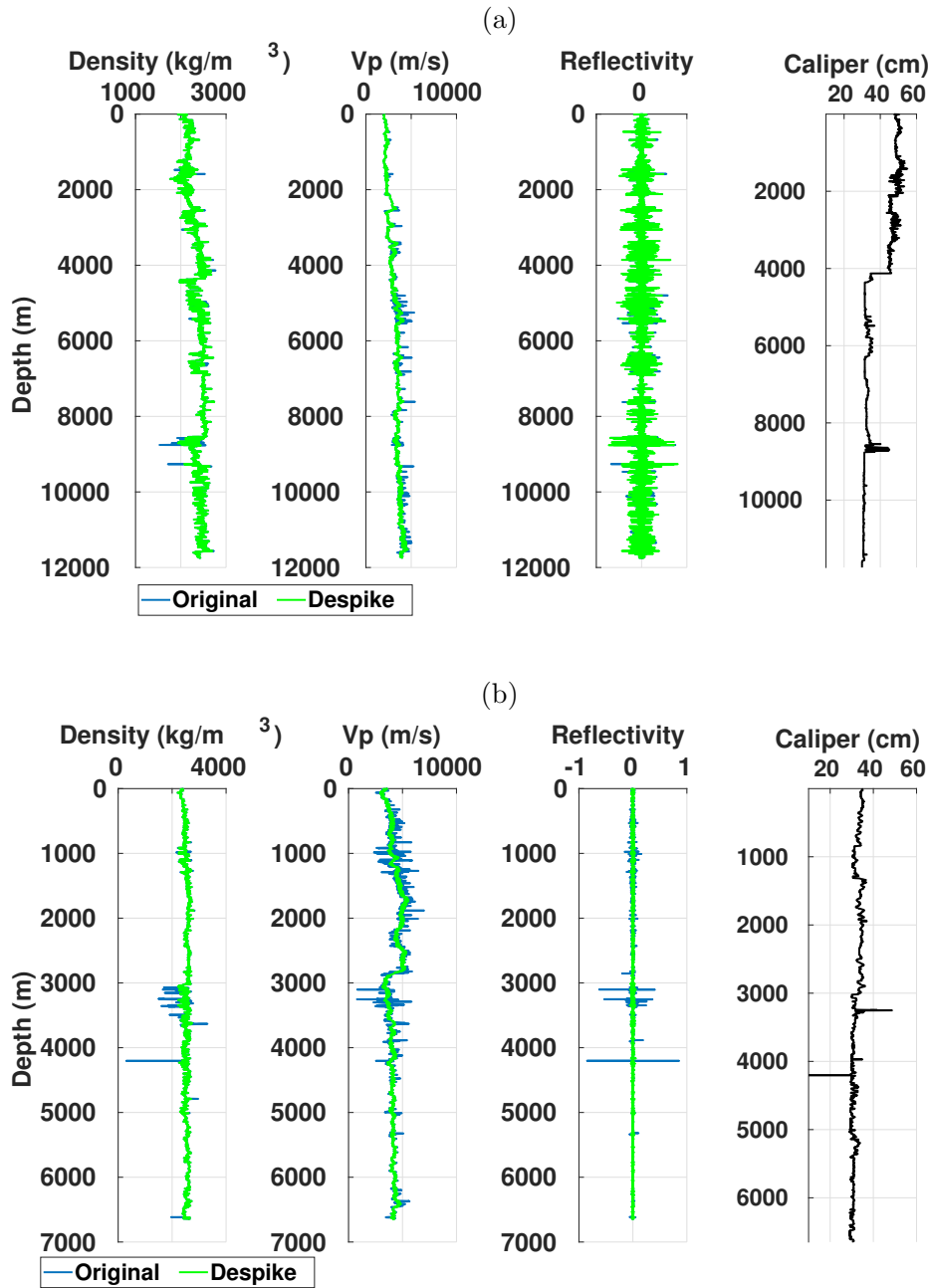


Figure 6: Well log data from the Viking Graben dataset used to perform the well-to-seismic-tie. a) Information from well A, located at CMP 809. b) Information from well B, located at CMP 1573.

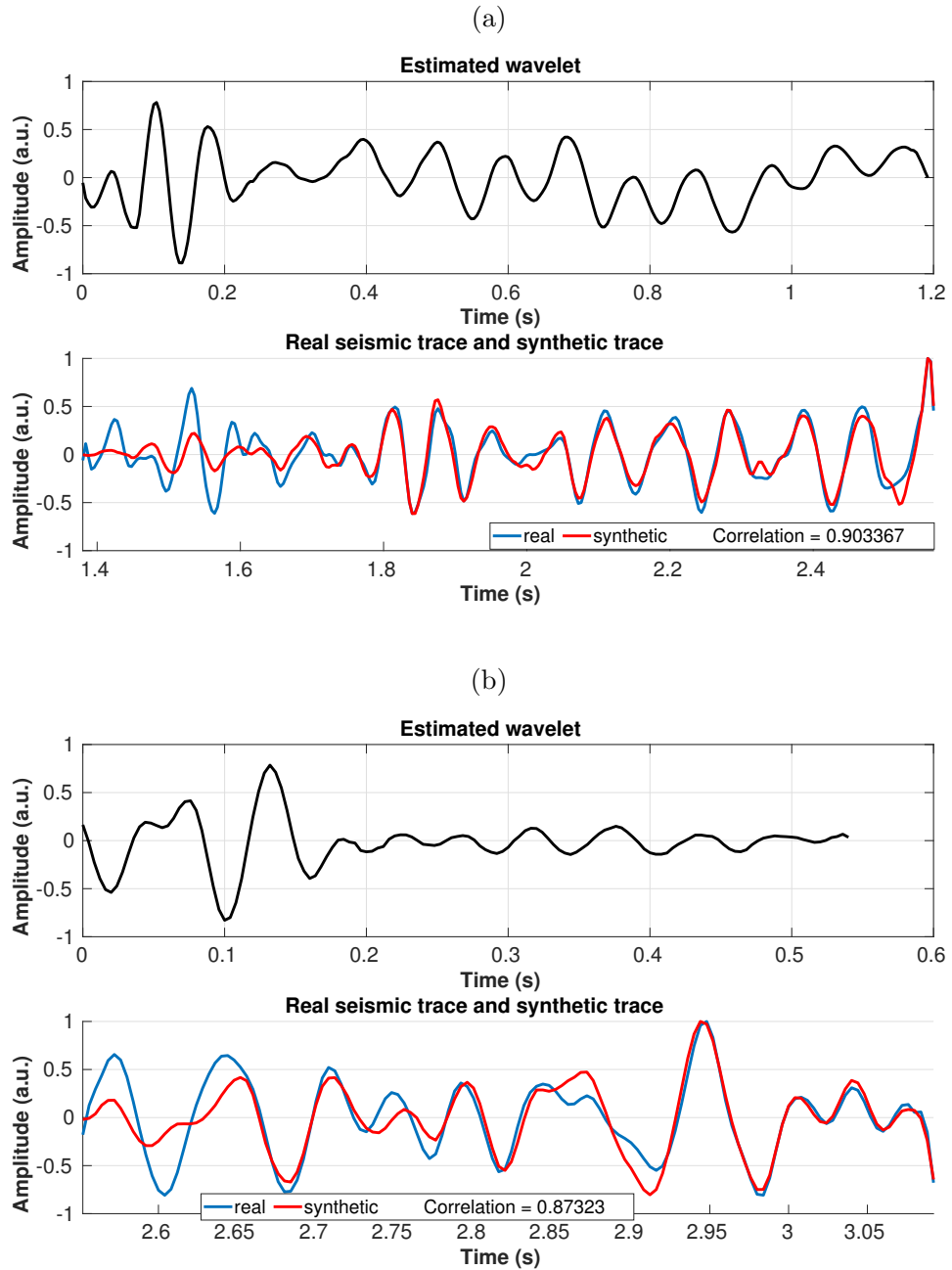


Figure 7: Well-to-seismic-tie performed in the real dataset using the deconvolution in time to estimate the wavelet. a) Well log A located at CMP 809, a correlation of 0.90 was achieved. b) Well B located at CMP 1573 a correlation of 0.87 was achieved.

## Discussion

It is important to emphasize that the well-to-seismic-tie (using a single well and a single trace to estimate the best wavelet), in terms of the correlation, is a valuable tool to check if the estimated wavelet is accurate. We compared the estimated wavelet using the deconvolution in time, with the estimated wavelet using the homomorphic deconvolution, detailed in the appendix. Those deconvolutions are completely different in formulation and they do not make any assumptions regarding the wavelet's phase or the reflectivity: the homomorphic deconvolution perform a separation of the seismogram components in the cepstral domain by the application of a linear filter to estimate the wavelet, and the deconvolution in time estimate the wavelet through least-squares minimization with zero order quadratic regularization. Yet, the estimated wavelet for both wells are similar, as shown in Figure 8, which suggests they might be close to the unknown real wavelet.

As mentioned before, the deconvolution in time requires the establishment of the parameter  $\beta$  to stabilize the solution of the minimization. According to Yilmaz (2000), the optimum pre-whitening factor  $\beta$  depends significantly upon the noise level in the data, and for a noise-free case, in theory, the best choice of  $\beta$  should be zero. However, to avoid exaggeration of numerical round off errors,  $\beta$  should be chosen to be a very small number. The results on Figure 7 were achieved with  $\beta=0.01$ . The number of iterations was 3 to estimate the wavelet on well A and 5 to estimate the wavelet on well B.

If one has the right wavelet, it is possible to recover the reflectivity in a region of the seismic section in the vicinity of the well location. In other words, it is possible to use the estimated wavelet from a single CMP (through the well-to-seismic-tie), to recover the reflectivity for several close CMPs: recovering the reflectivity is a form to identify

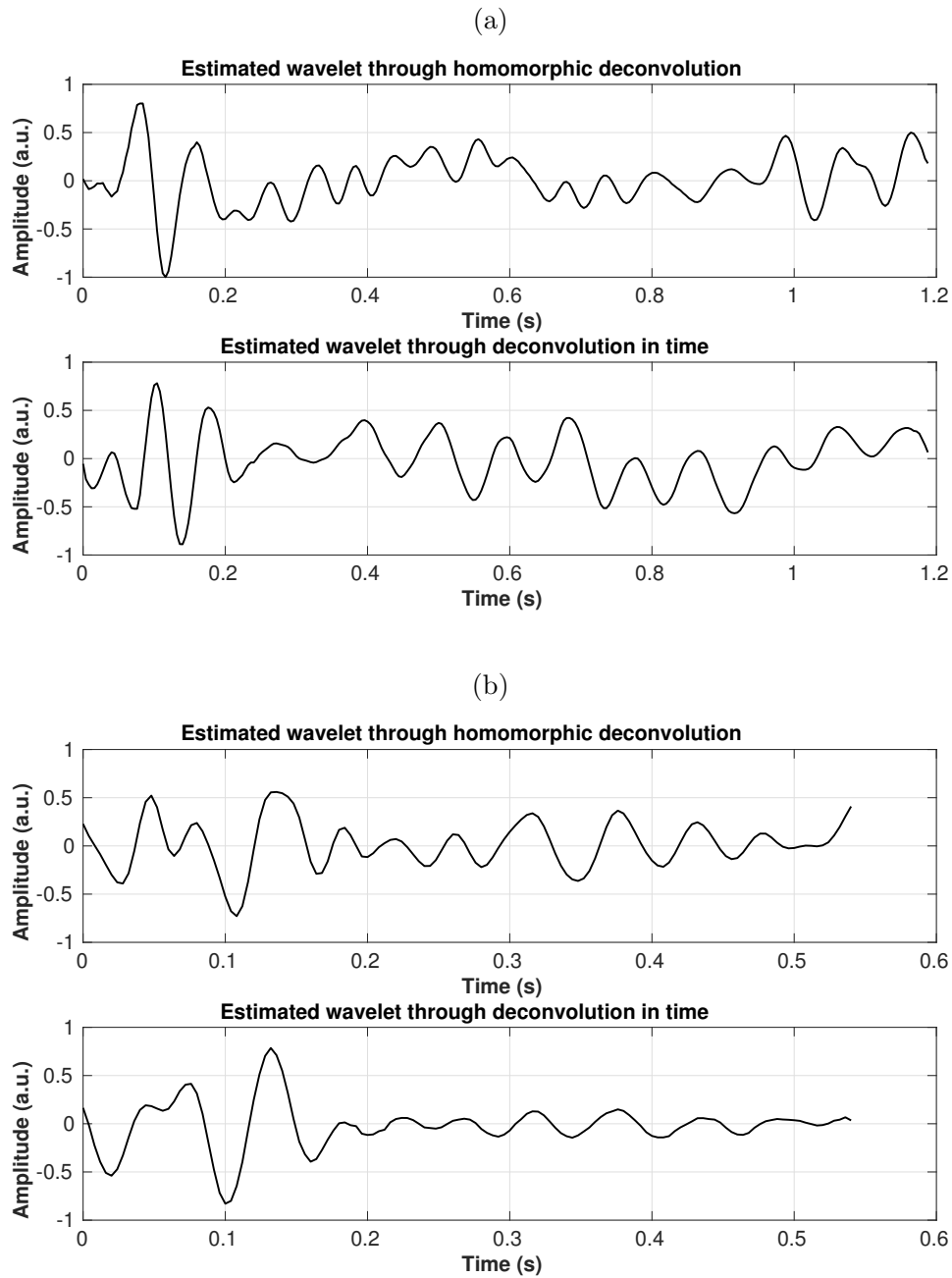


Figure 8: Wavelets estimated using two different methodologies that does not require any assumptions regarding the wavelet's phase or the reflectivity: the homomorphic deconvolution perform the separation of seismogram components in the cepstral domain and the deconvolution in time perform a least square minimization in time domain. a) Wavelets obtained for the well A. b) Wavelets obtained for the well B.

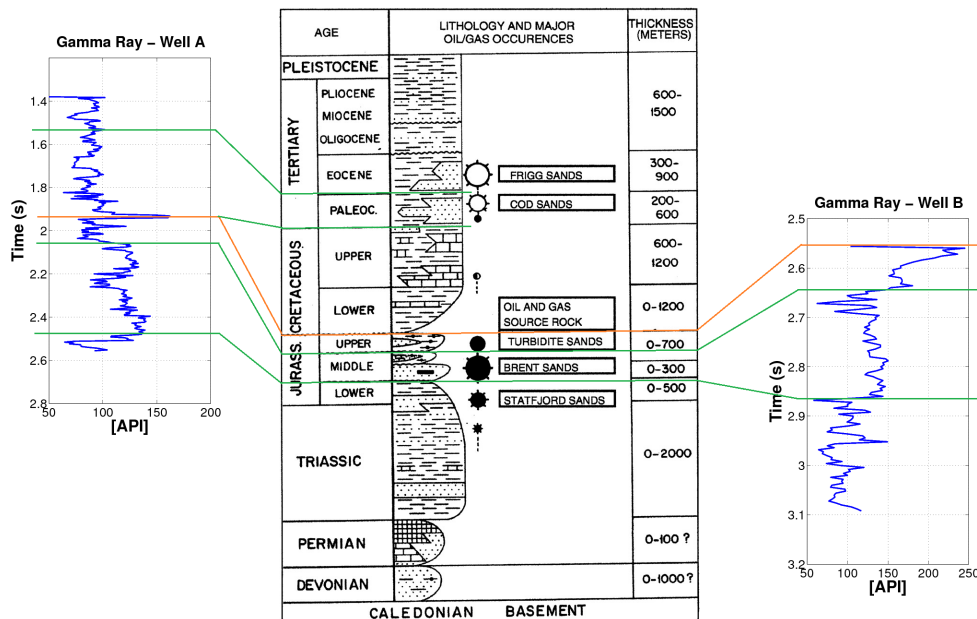


Figure 9: The lithological representation of the Viking Graben dataset (Madiba and McMechan, 2003) and their locations in time on well A and B according to the gamma-ray logs. As mentioned by Keys (1998), the BCU (base cretaceous unconformity) is located on 1.97s on well A. On well B it is possible to note a change in lithology around 2.65s and 2.85s.

stratigraphic horizons in the seismic section. With those recovered reflectivities from the seismic section, one can perform the second tie, which is the seismic-to-well-tie: compare the convolution of the recovered reflectivity and estimated wavelet, with the real seismic section. In this second case, a 'good tie' is an indication of how well the reflectivity was recovered but it is necessary to have geological information to check if the reflectivity is being recovered correctly and not shifted. Because of that, it is important to have known stratigraphic markers in the seismic section so it is possible to have not only a mathematical control of the recovered reflectivity, but also a geological control of them.

Figure 9 shows the main stratigraphic markers we used to check if the recovered reflectivity using the sparse-spike algorithm and the estimated wavelet through the deconvolution in time is coherent: for well A, the marker is the BCU located around 1.97s in time, and for well B the markers are the changing in lithology occurred around 2.65s and 2.85s.

Figures 10, 11, 12 and 13 shows the application of the sparse-spike algorithm to recover the reflectivity for the traces in the vicinity of well A and B, using different values of the regularization parameter  $\alpha$ . When  $\alpha$  is set to zero, the unconstrained least squares minimization is done, which is not recommend since it is unstable, as mentioned before. The parameter  $\alpha$  controls the sparsity of the solution: as its value increases, also increases the sparsity of the solution. For both cases, when  $\alpha=0$  the recovered reflectivity is noisy as shown in 10a and 12a, and the stratigraphic marker for well A is not apparent.

When  $\alpha$  is overestimated, for instance when  $\alpha$  is set to 7, the sparsity of the solution increases, more samples are set to zero, and only the prominent stratigraphic markers appears. As shown in Figure 11b, the reflectivity recovered at 1.973s is consistent with the BCU located at 1.97s, as mentioned by Madiba and McMechan (2003). In Figure 13b, when  $\alpha=7$ , only the marker around 2.85s is apparent, according to the lithology of Figure 9. For this case, it is possible to note that the synthetic traces calculated with the recovered reflectivity and the estimated wavelet does not match the real seismic data. For the case of  $\alpha=0$ , the synthetics match the real seismic data, but the stratigraphic markers are not consistent.

Those results elucidates the importance of having known stratigraphic markers to control the inversion for the reflectivity through the sparse-spike deconvolution, and is also a tool to check if the estimated wavelet is reliable: a wrong wavelet might recover a reflec-

tivity inconsistent with the geology. By establishing a reasonable estimated wavelet and a reasonable value of  $\alpha$  in the sparse-spike deconvolution, one can correctly recover the reflectivity in the position of the stratigraphic markers and have a good fit in the seismic-to-well-tie. It was achieved in the real Viking Graben dataset by using the deconvolution in time to estimate the wavelet and by setting  $\alpha=0.7$  for well A, and  $\alpha=0.1$  for well B, as depicted in Figures 11b and 13a.

## CONCLUSIONS

In this study we propose an approach to estimate the wavelet for the well-to-seismic-tie using least squares minimization with zero-order quadratic regularization and we test the efficiency of the estimated wavelet to correctly recover the stratigraphic markers of the seismic section through the sparse-spike deconvolution. We compare the estimated wavelet in this study with the one estimated through the homomorphic deconvolution, which also does not require any assumption about the wavelet's phase or reflectivity and is essentially different in formulation. However, both methods suggests the stationarity of the wavelet.

Our results shows that the estimated wavelets are similar for both methodologies. Moreover, by using both real seismic and well log data, we perform a deterministic estimation of the wavelet through the deconvolution in time. Our results also shows that a correlation of 0.90 was achieved for the well-to-seismic-tie in the well A, and a correlation of 0.87 in the well B, higher values than the ones obtained with the homomorphic deconvolution (0.74 and 0.86 for well A and B, respectively) and with methods that takes into account the classical assumptions of the convolutional model. We also show that by using the estimated wavelet as an input to the sparse-spike algorithm, the main known stratigraphic markers of the real dataset were recovered, which suggests the feasibility of this approach.

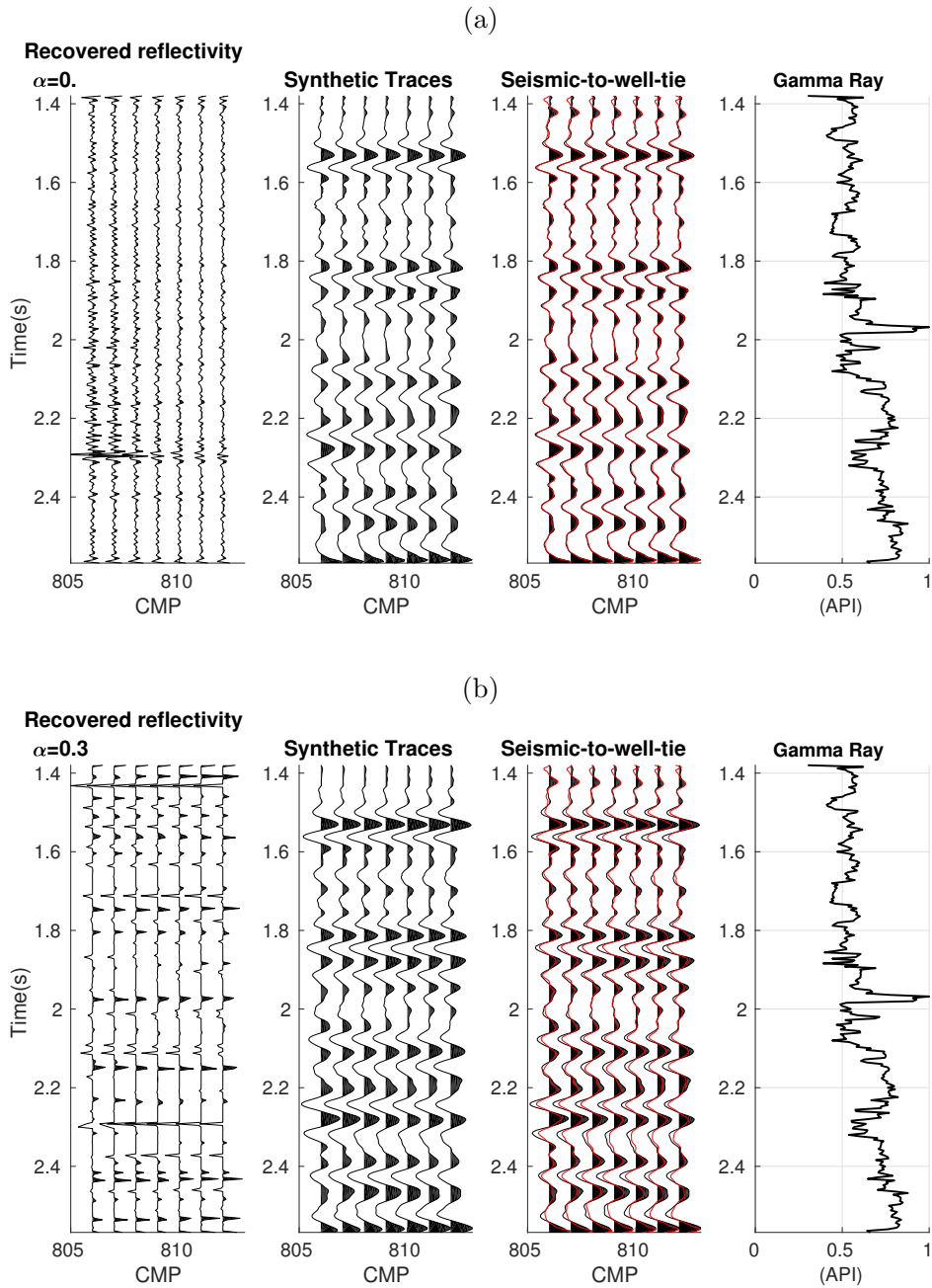


Figure 10: a) Recovered reflectivity near the well A position, using  $\alpha=0$ . b) Recovered reflectivity near the well A position, using  $\alpha=0.3$ . Well A is located on CMP 809. The input wavelet was the one estimated through the deconvolution in time. The first panel shows the recovered reflectivity, the second shows the synthetic traces calculated with the recovered reflectivity and the estimated wavelet, and the third shows the match between this last and the real seismic section in the vicinity of the well location. The gamma-ray log illustrates the similarity between the recovered reflectivity and the stratigraphic markers.

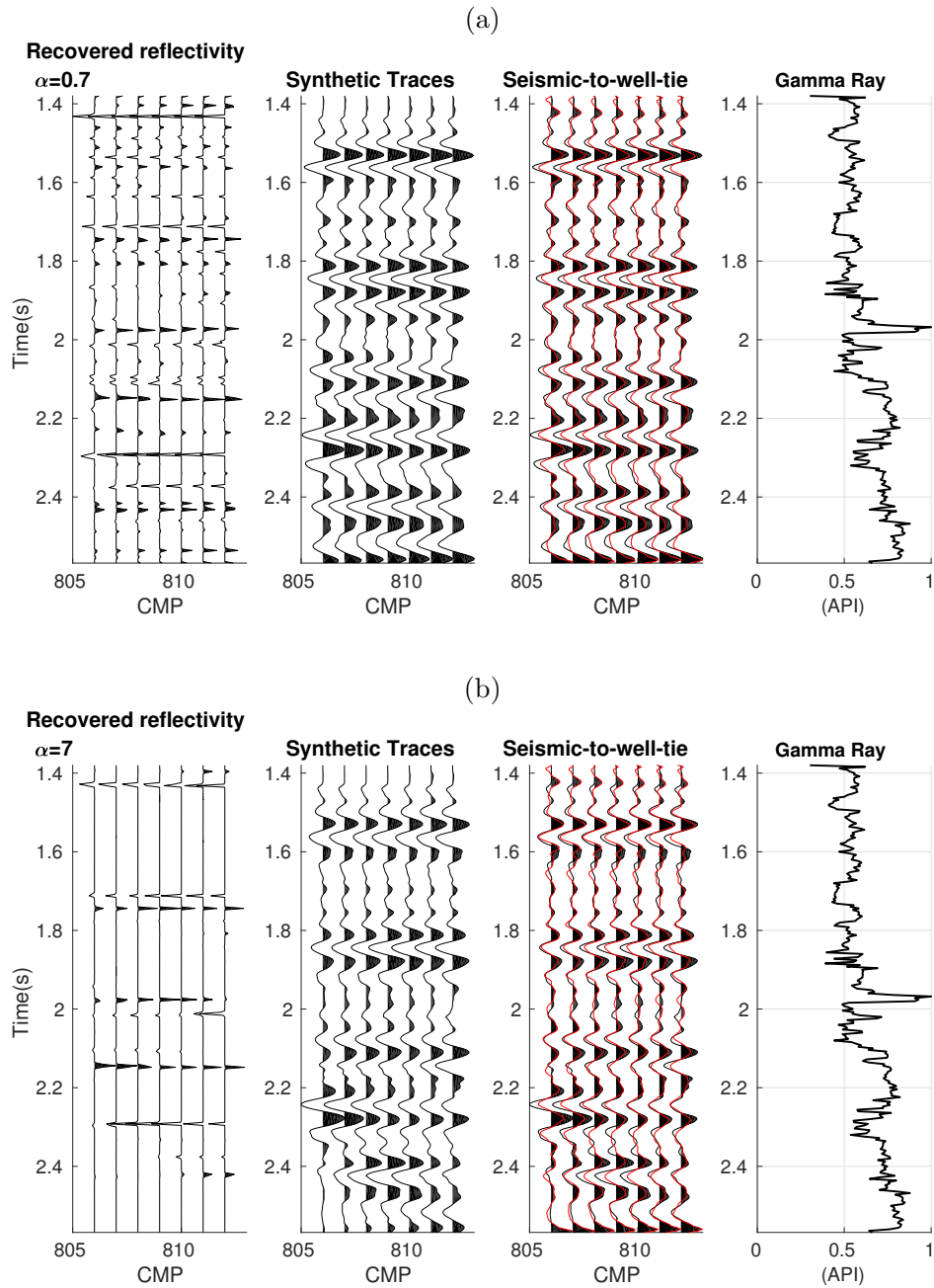


Figure 11: a) Recovered reflectivity near the well A position, using  $\alpha=0.7$ . b) Recovered reflectivity near the well A position, using  $\alpha=7$ . Well A is located on CMP 809. The input wavelet was the one estimated through the deconvolution in time. The first panel shows the recovered reflectivity, the second shows the synthetic traces calculated with the recovered reflectivity and the estimated wavelet, and the third shows the match between this last and the real seismic section in the vicinity of the well location. The gamma-ray log illustrates the similarity between the recovered reflectivity and the stratigraphic markers.

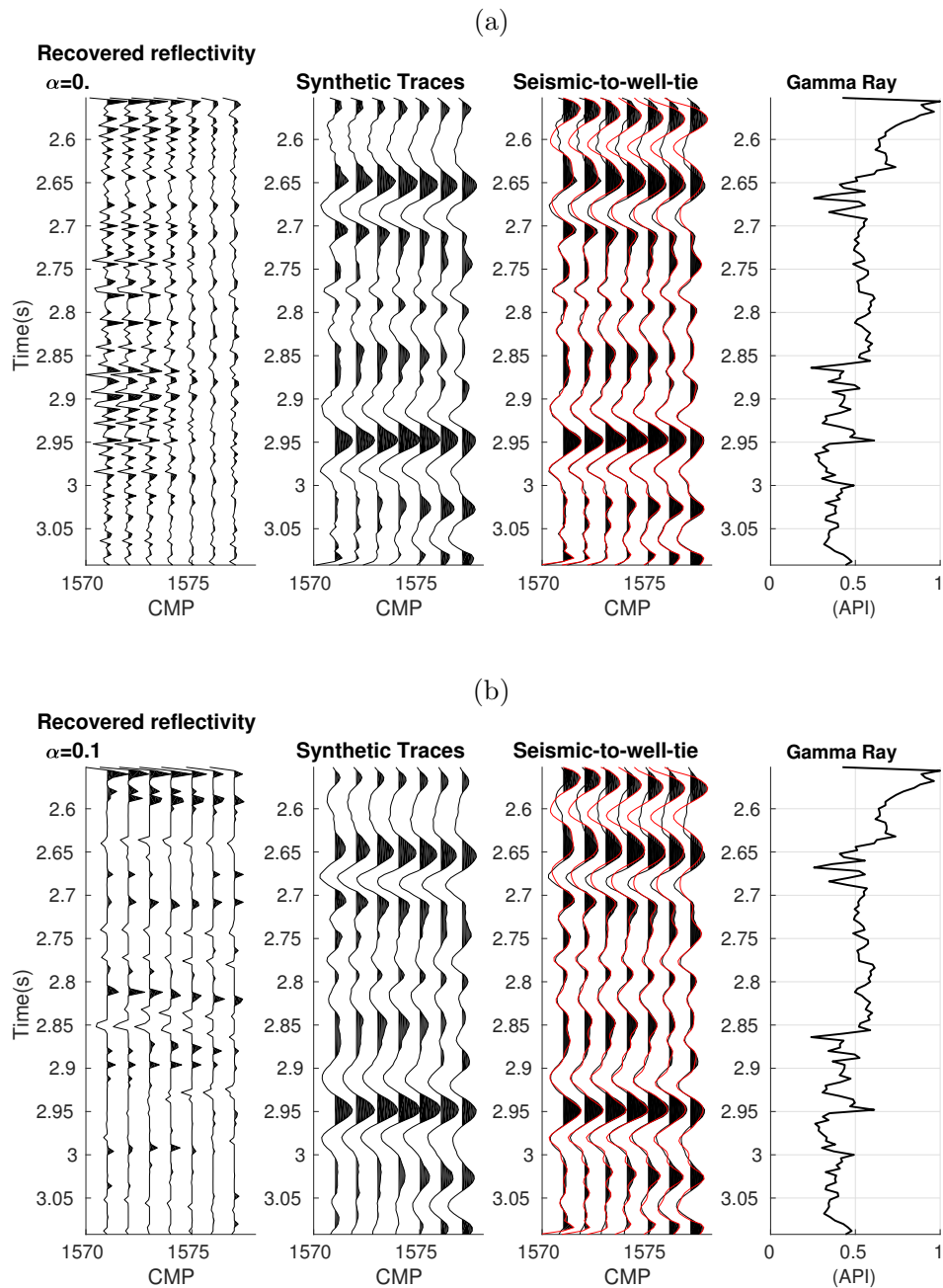


Figure 12: a) Recovered reflectivity near the well B position, using  $\alpha=0$ . a) Recovered reflectivity near the well A position, using  $\alpha=0.1$ . Well B is located on CMP 1573. The input wavelet was the one estimated through the deconvolution in time. The first panel shows the recovered reflectivity, the second shows the synthetic traces calculated with the recovered reflectivity and the estimated wavelet, and the third shows the match between this last and the real seismic section in the vicinity of the well location. The gamma-ray log illustrates the similarity between the recovered <sup>27</sup>reflectivity and the stratigraphic markers.

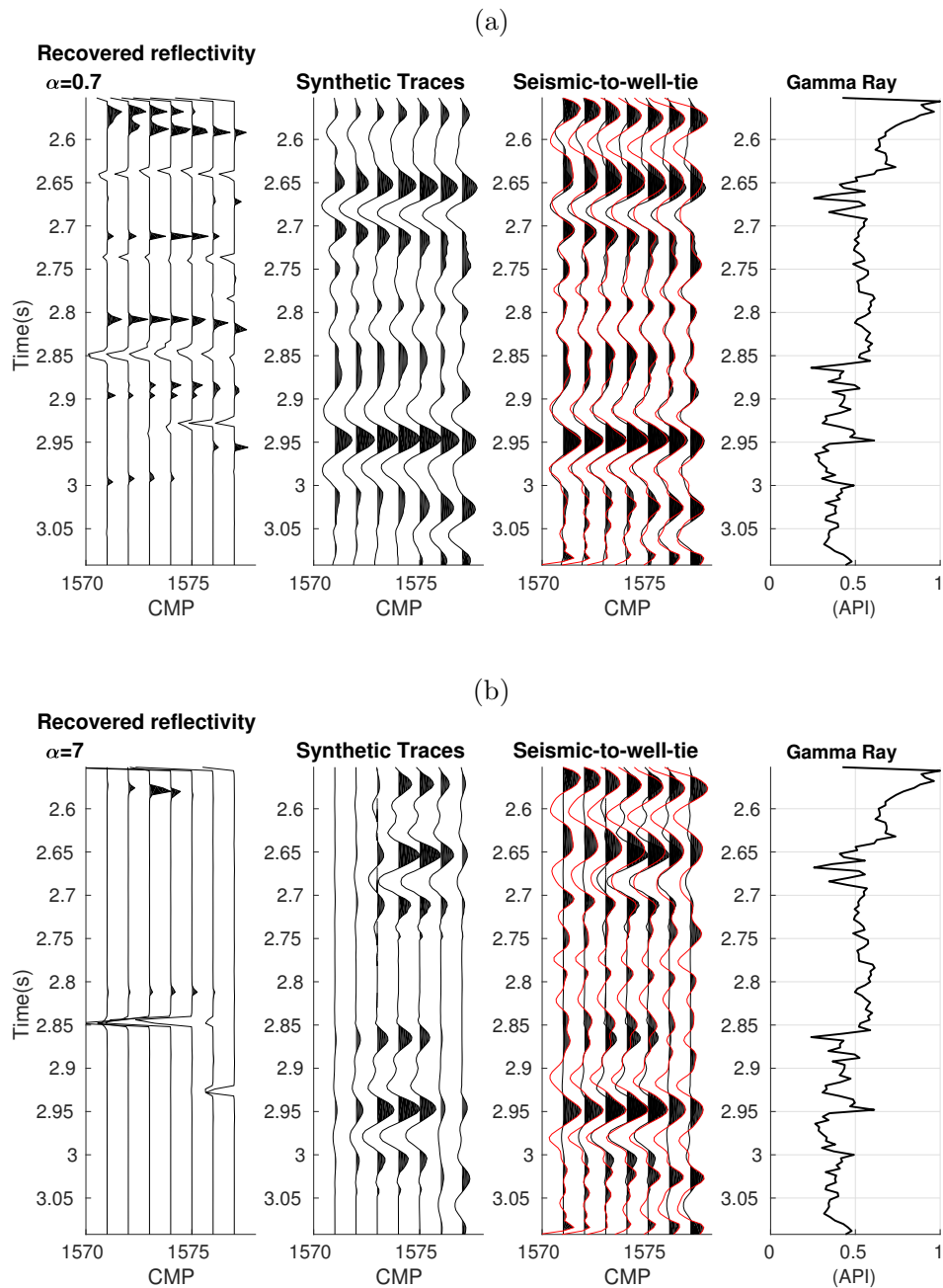


Figure 13: a) Recovered reflectivity near the well B position, using  $\alpha=0.7$ . a) Recovered reflectivity near the well B position, using  $\alpha=7$ . Well B is located on CMP 1573. The input wavelet was the one estimated through the deconvolution in time. The first panel shows the recovered reflectivity, the second shows the synthetic traces calculated with the recovered reflectivity and the estimated wavelet, and the third shows the match between this last and the real seismic section in the vicinity of the well location. The gamma-ray log illustrates the similarity between the recovered reflectivity and the stratigraphic markers.

## ACKNOWLEDGMENTS

The authors would like to thank the Exxon Mobil for providing the Viking Graben dataset.

This work was kindly supported by the Brazilian agencies INCT-GP and CNPq from Brazil and the Geophysics Graduate Program at Federal University of Pará.

# HOMOMORPHIC DECONVOLUTION TO ESTIMATE THE WAVELET

Homomorphic systems are a class of linear systems that satisfy the principle of superposition and are useful in the separation of signals generated by convolutions. The seismic trace ( $x(n)$ ) is generally given as a convolution between the source pulse wavelet ( $w(n)$ ) and the reflectivity series ( $h(n)$ ) of the Earth subsurface. The homomorphic deconvolution configures a statistical filtering process applied to geophysical data to recover the reflectivity or estimate the source signature, through separation of components on the cepstrum domain. The accuracy of the homomorphic deconvolution is determined by the ability of a filter, or other method, to separate the reflectivity and the seismic wavelet components. We propose, for the seismic wavelet estimation, the use of the reflectivity series calculated from well logs to design the filter to separate the components of the convolution, which in the cepstral domain are represented by an addition.

Mathematically, the convolution of two time series can be described by

$$x(n) = w(n) * h(n). \quad (\text{A-1})$$

In the frequency domain, this equation can be expressed as:

$$X(w) = W(w)H(w), \quad (\text{A-2})$$

where  $X(w)$  and  $W(w)$  are the Fourier transforms of  $x(n)$  and  $w(n)$ , respectively. A signal can be transformed from the time domain to the complex-valued cepstral domain by Fourier transformation followed by a log operation Herrera and Van Der Baan (2012):

$$\hat{X}(w) = \log\{X(w)\} = \log\{|X(w)| \exp^{iarg(X(w))}\}. \quad (\text{A-3})$$

The cepstral transform of  $x(n)$  is given by inverse Fourier transform of  $\hat{X}(w)$ , i.e.,  $x(n) =$

$iFFT\{\hat{X}(w)\}$ . The convolutional model described in A-1 can be transformed into an addition in the cepstral domain according to:

$$\hat{x}(n) \approx \hat{w}(n) + \hat{h}(n). \quad (\text{A-4})$$

The output  $\hat{x}(n)$  is called complex cepstrum of the input  $x(n)$  and it contains both informations of phase and amplitude of the seismic signal.

The use of the complex cepstrum of the reflectivity takes place in the process of building a filter in the cepstral domain. The complex cepstrum of a seismogram can be described as:

$$\hat{x}(n) = \hat{w}(n) + \hat{h}(n), \quad (\text{A-5})$$

where  $\hat{x}(n)$ ,  $\hat{w}(n)$ ,  $\hat{h}(n)$  are the complex cepstrum of the real seismic trace, the wavelet, and the reflectivity, respectively. In this domain, we aim to build a filter  $l(n)$  that applied to the real seismic trace, separates the component of the wavelet  $\hat{w}(n)$  from the component of the reflectivity  $\hat{h}(n)$ . Therefore:

$$l(n)\hat{x}(n) = \hat{w}(n). \quad (\text{A-6})$$

Our choice is to build  $l(n)$  as an inverse linear filter. If we have the reflectivity series calculated from the well log data, it is possible to transform it to the time domain by the correct time-depth relationship used on the well-to-seismic-tie, and to calculate a new complex cepstrum of the reflectivity,  $\hat{h}'(n)$ , which transforms the equation A-5 into:

$$\hat{x}(n) = \hat{w}(n) + \hat{h}'(n). \quad (\text{A-7})$$

Therefore, the inverse linear filter  $l(n)$  is described as:

$$l(n)\hat{x}(n) = \hat{x}(n) - \hat{h}'(n), \quad (\text{A-8})$$

$$l(n) = \frac{\hat{x}(n) - \hat{h}'(n)}{\hat{x}(n)}, \quad (\text{A-9})$$

$$l(n) = 1 - \frac{\hat{h}'(n)}{\hat{x}(n)}. \quad (\text{A-10})$$

By applying the filter A-10 in the complex cepstrum of the real seismic trace A-6, we have:

$$\hat{w}(n) = \hat{x}(n) \left\{ 1 - \frac{\hat{h}'(n)}{\hat{x}(n)} \right\}, \quad (\text{A-11})$$

which represents the complex cepstrum of the seismic wavelet isolated in the cepstrum domain. The next step is to bring back the cepstrum of the wavelet to the time domain, in order to estimate the wavelet. Therefore:

$$\hat{W}(w) = FFT\{\hat{w}(n)\}, \quad (\text{A-12})$$

$$W(w) = FFT\{\hat{W}(w)\}, \quad (\text{A-13})$$

$$w(n) = iFFT\{W(w)\}. \quad (\text{A-14})$$

Equation A-14 represents the estimated wavelet in the time domain through the homomorphic deconvolution using the well log data.

## REGULARIZATIONS AND THE ESTIMATIVE OF THE WAVELET

The regularization term is added to the lost function in order to stabilize the solution of the minimization. While the L1 norm is just the sum of the weights, the L2 norm is the sum of the square of the weights. When using the L1 norm regularization, a sparse output is implied, which is not a reasonable assumption for the wavelet, but is for the reflectivity series. Figure 14 shows the results on synthetic data of using the L1 norm regularization for the wavelet estimation and the quality of the well-to-seismic-tie. The sparsity assumption in the minimization does not produce a reliable wavelet, it approaches to a spike. On the other hand, when using a quadratic regularization, the wavelet is very close to the real one.

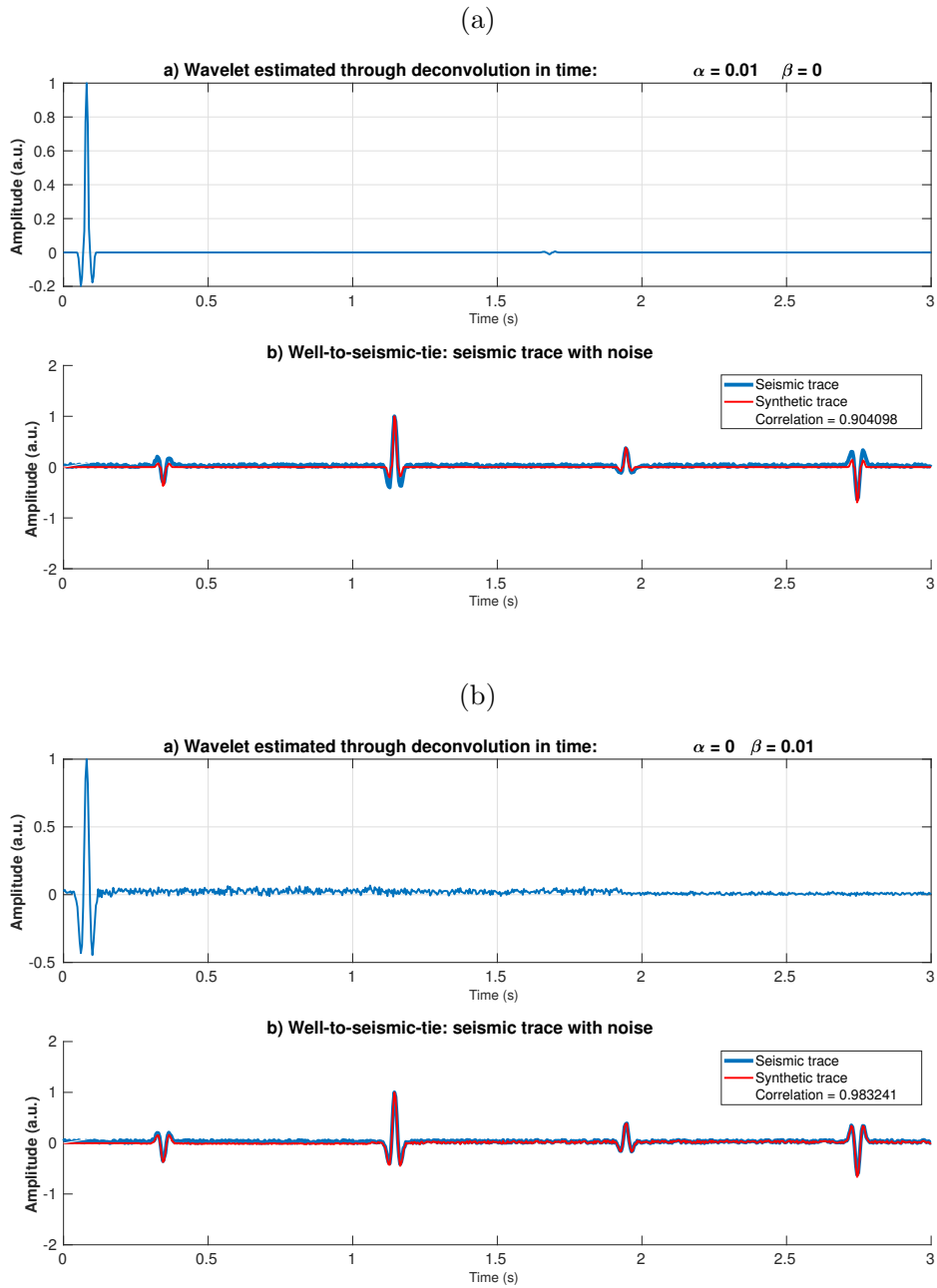


Figure 14: Comparison of regularization effects on the estimative of the wavelet on the synthetic data. a) Wavelet estimated through the deconvolution in time using a L1 norm regularization, setting the sparsity parameter  $\alpha=0.01$ . The sparsity assumption produce a sparse output wavelet that is not reliable. b) Wavelet estimated thorough the deconvolution in time using the zero-order quadratic regularization, setting  $\beta=0.01$ . The wavelet, in this case, is reliable and the correlation of the well-to-seismic-tie increases.

## REFERENCES

- Dey, A. K., and L. R. Lines, 1998, Seismic source wavelet estimation and the random reflectivity assumption, *in* SEG Technical Program Expanded Abstracts 1998: Society of Exploration Geophysicists, 1088–1091.
- Edgar, J. A., and M. Van der Baan, 2011, How reliable is statistical wavelet estimation?: *Geophysics*, **76**, V59–V68.
- Gardner, G. H. F., 1974, Formation velocity and density -the diagnostic basics for stratigraphic traps: *Geophysics*, **39**, 770.
- Herrera, R. H., and M. Van Der Baan, 2012, Revisiting homomorphic wavelet estimation and phase unwrapping: arXiv preprint arXiv:1205.3752.
- Keys, R. G., 1998, Comparison of seismic inversion methods on a single real data set, open file publications: Society of Exploration.
- Madiba, G. B., and G. A. McMechan, 2003, Processing, inversion, and interpretation of a 2d seismic data set from the North Viking Graben, North Sea: *Geophysics*, **68**, 837–848.
- Morháč, M., 2006, Deconvolution methods and their applications in the analysis of  $\gamma$ -ray spectra: *Nuclear Instruments and Methods in Physics Research Section A: Accelerators, Spectrometers, Detectors and Associated Equipment*, **559**, 119–123.
- Sacchi, M. D., 1997, Reweighting strategies in seismic deconvolution: *Geophysical Journal International*, **129**, 651–656.
- Trantham, E. C., 1994, Controlled-phase acquisition and processing, *in* SEG Technical Program Expanded Abstracts 1994: Society of Exploration Geophysicists, 890–894.
- Ursin, B., and O. Holberg, 1985, Maximum-likelihood estimation of seismic impulse responses: *Geophysical prospecting*, **33**, 233–251.
- Velis, D. R., 2007, Stochastic sparse-spike deconvolution: *Geophysics*, **73**, R1–R9.

- White, R., 2003, Tying well-log synthetic seismograms to seismic data: the key factors, *in* SEG technical program expanded abstracts: Society of Exploration Geophysicists, SEG Technical Program Expanded Abstracts, 2449–2452.
- White, R., and R. Simm, 2003, Tutorial: Good practice in well ties: *First Break*, **21**.
- Yilmaz, O., 2000, *Seismic data analysis: processing, inversion, and interpretation of seismic data*: SEG Books.

## 6 DISCUSSION AND CONCLUSIONS

Anomalous caliper readings suggests a borehole enlargement or shrink during drilling, as previously mentioned. On chapter 2 it is shown that the reflectivity calculated from well logs follows the phenomenological Benford distribution and that the conformity decreases on segments of reflectivity that have a corresponding anomalous caliper log. On chapter 3, based on the apparent geometric factor theory, a correction for the borehole enlargement is proposed on the density log to improve the well-to-seismic-tie quality. Figure 6.1 show the result of the application of the Benford's law on the reflectivity calculated with the corrected density log (chapter 3) for the well A from the Viking Graben field, the one we have available data to perform the well-to-seismic-tie.

Figure 6.1 illustrates the Benford distribution for the reflectivity calculated with a density log with and without correction for the borehole enlargement. The correction generated a reflectivity series with a slightly higher conformity with Benford distribution: without correction, the mean absolute deviation from Benford distribution is around 0.0025, and with the correction, the deviation is around 0.0023. Those results are consistent with the proposal of using the Benford distribution to analyze the quality of the density and velocity log for the borehole environment effects.

The Benford distribution was also applied on the output of the sparse-spike deconvolution algorithm, shown in Chapter 5. As well as the reflectivity calculated from well log data, the recovered reflectivity of the seismic section in the vicinity of the well location also follows the Benford trend. Moreover, its conformity with the Benford Law increases when a reasonable regularization parameter is used. Figures 6.2, 6.3, 6.4 and 6.5 show the results achieved for the recovered reflectivity near the well A and the well B from the Viking Graben dataset when the regularization parameter that controls the sparsity of the solution varies.

Table 6.1 summarizes the correlation values achieved for the well-to-seismic-tie on the synthetic data and on the real dataset from the Viking Graben field, and shows the evolution on the improvement on the well-to-seismic-tie response. The statistical estimation of the wavelet through the predictive deconvolution and the deterministic estimation using filtering techniques was done on the same dataset. The results can be seen in Macedo, I. A. S. de et al. (2017). These methodologies requires the classical assumptions of a minimum-phase wavelet and a random process reflectivity. The last two methodologies on table 6.1, deterministic homomorphic deconvolution and deterministic deconvolution in time, does not make those assumptions and produced the best results.

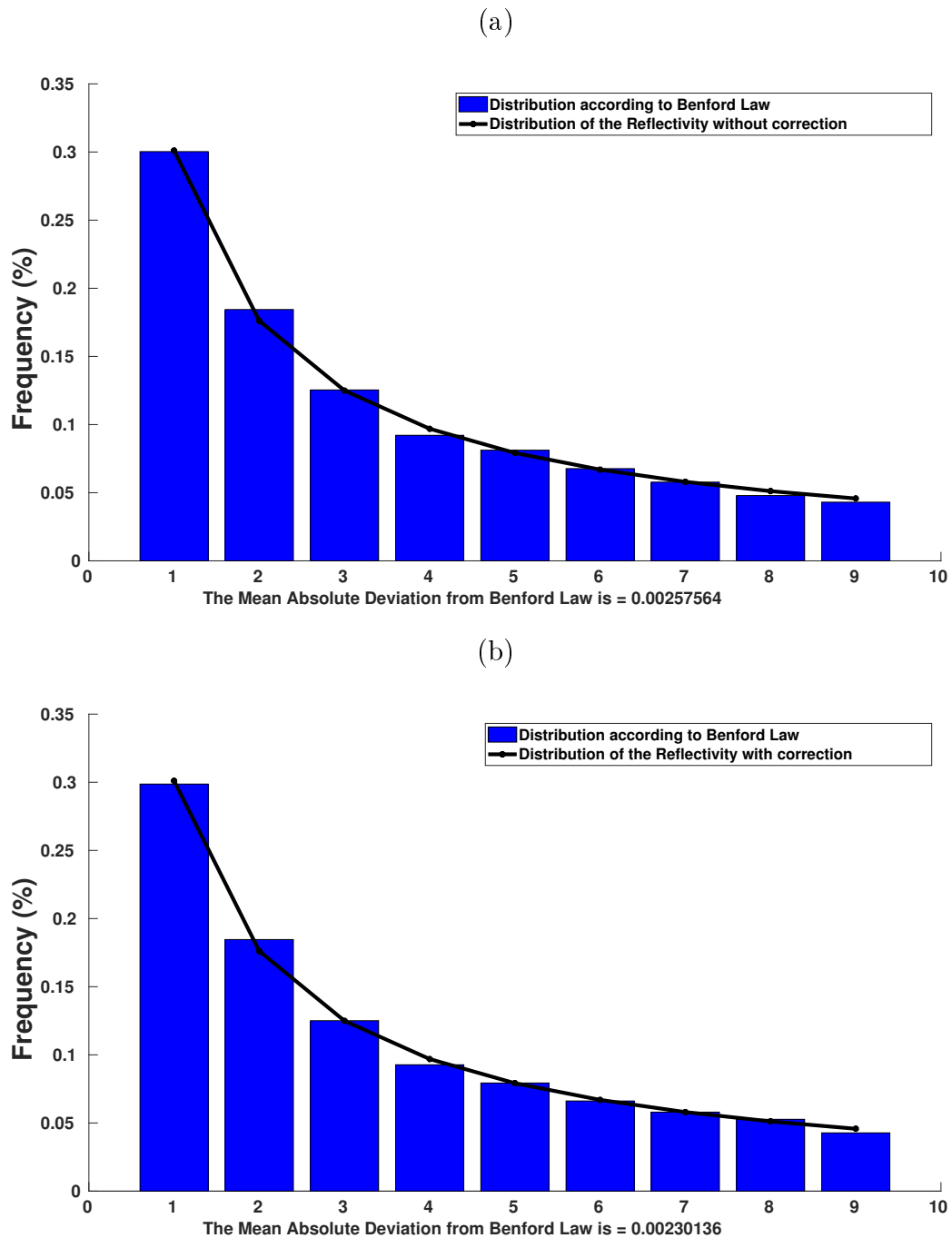


Figure 6.1: Calculated reflectivity from well A, Viking Graben field and its conformity with Benford's law. a) Reflectivity without correction on density log for the borehole enlargement, mean absolute deviation around 0.0025. b) Reflectivity with correction on density log for the borehole enlargement, mean absolute deviation around 0.0023.

<b>METHOD TO ESTIMATE THE WAVELET</b>	<b>SYNTHETIC DATA</b>		<b>VIKING GRABEN DATASET</b>	
	With noise	Without noise	Well A	Well B
Predictive Deconvolution (Macedo, I. A. S. de et al., 2017)	0.91	0.95	0.65	0.74
Average Predictive Deconvolution (Macedo, I. A. S. de et al., 2017)	-	-	0.67	0.73
Predictive Deconvolution with correction on density log (chapter 3)	-	-	0.71	-
Deterministic Filtering (Macedo, I. A. S. de et al., 2017)	0.98	1	0.71	0.81
Deterministic Filtering with correction on density log (chapter 3)	-	-	0.77	-
Deterministic Homomorphic Deconvolution (chapter 4)	0.98	1	0.74	0.86
Deterministic Deconvolution in time (chapter 5)	0.98	1	0.90	0.87

Table 6.1: Correlation values achieved for the well-to-seismic-tie using different methodologies applied to synthetic and real data. The first five methods to estimate the wavelet are based on the classical assumptions of the convolutional model of the Earth. The last two methods of deconvolution does not assume a minimum-phase wavelet or a random process reflectivity.

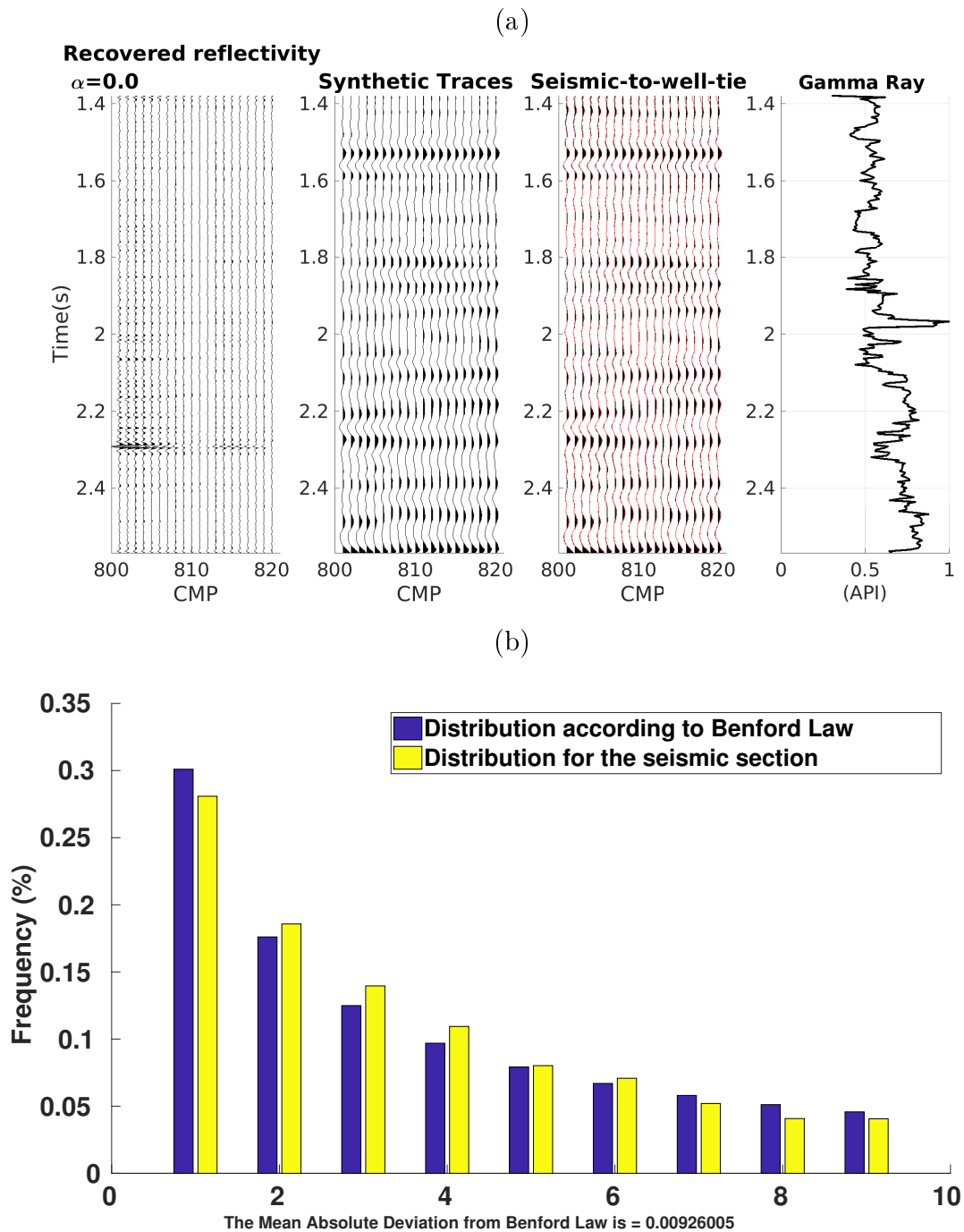


Figure 6.2: a) The recovered reflectivity from the seismic section near the well A when the regularization parameter that controls the sparsity of the solution is set to  $\alpha = 0$  b) The Benford distribution of the estimated reflectivity from the seismic section for  $\alpha = 0$ , a acceptable conformity with BL is achieved with a MAD of 0.0092.

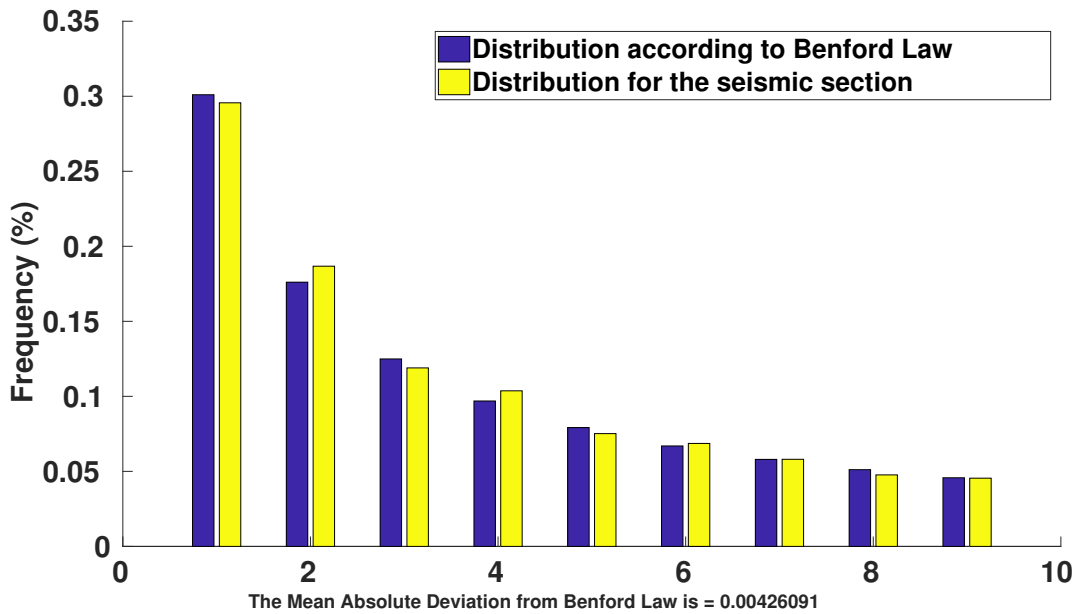
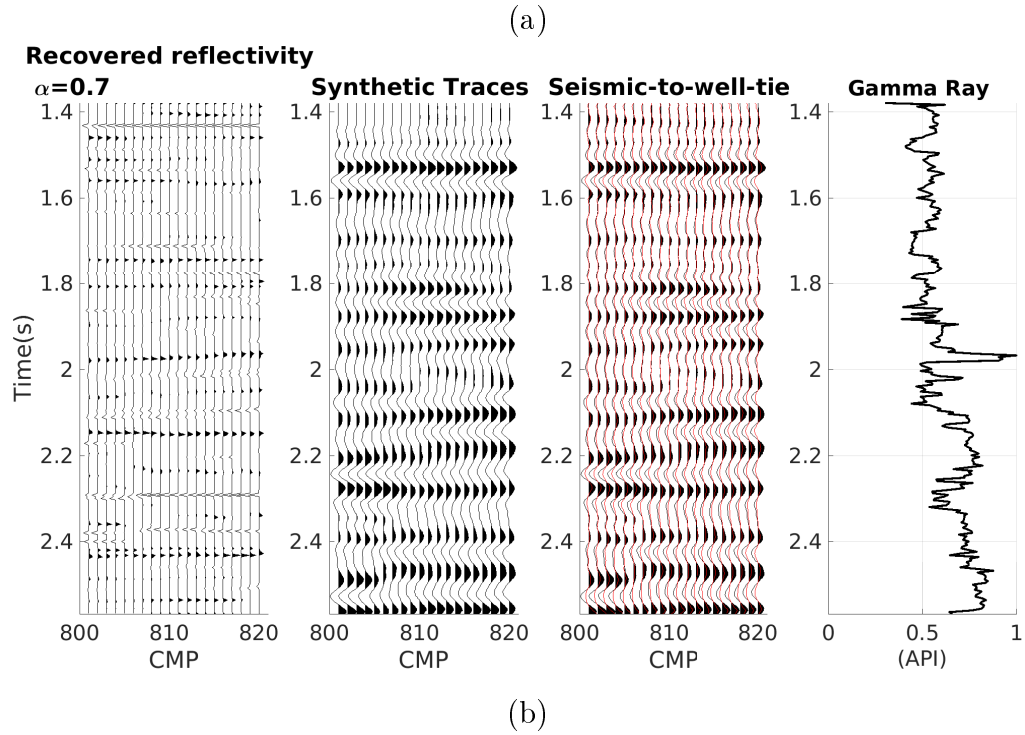


Figure 6.3: a) The recovered reflectivity from the seismic section near the well A when the regularization parameter that controls the sparsity of the solution is set to  $\alpha = 0.7$  b) The Benford distribution of the estimated reflectivity from the seismic section for  $\alpha = 0.7$ , a close conformity with BL is achieved with a MAD of 0.0042.

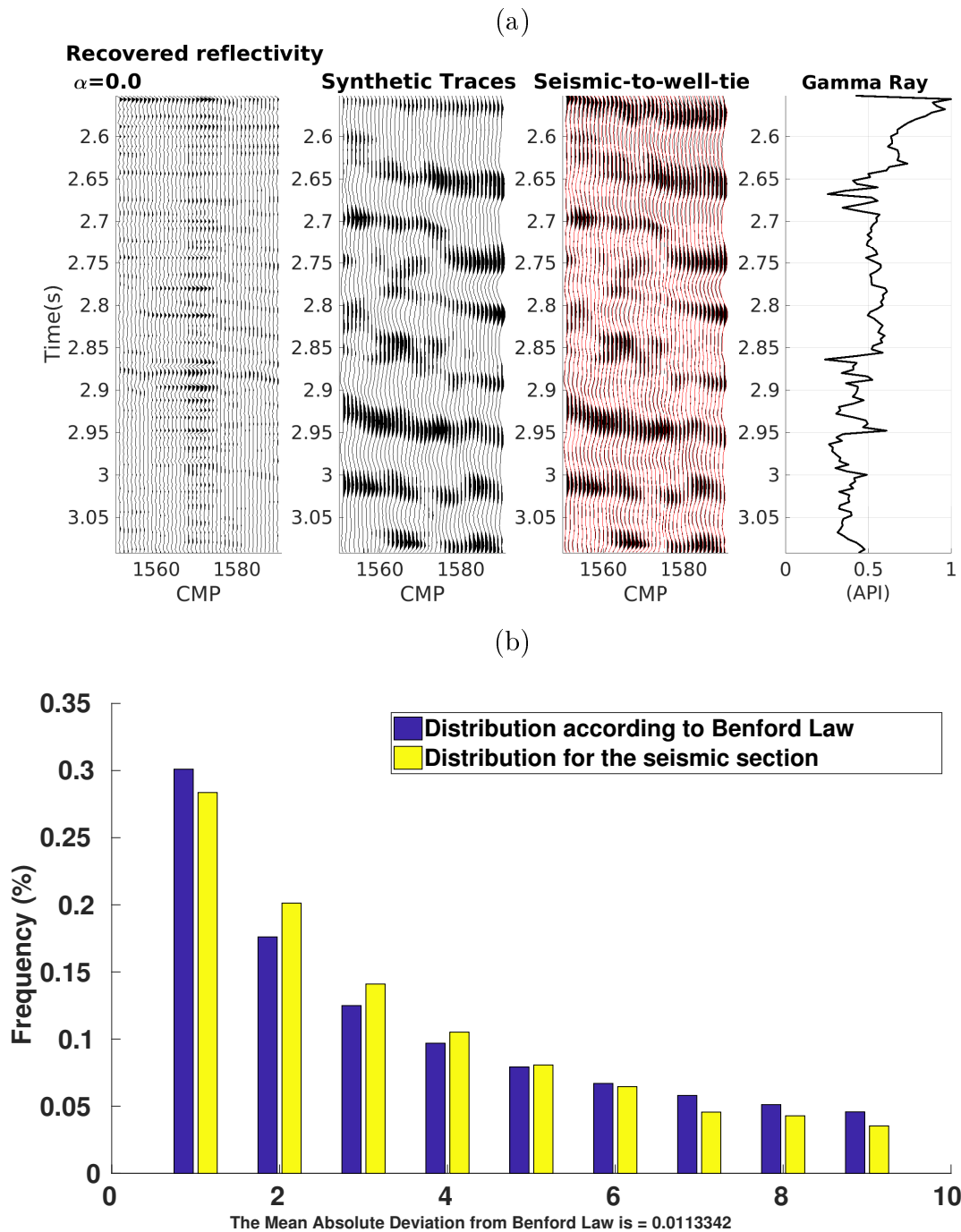


Figure 6.4: a) The recovered reflectivity from the seismic section near the well B when the regularization parameter that controls the sparsity of the solution is set to  $\alpha = 0$  b) The Benford distribution of the estimated reflectivity from the seismic section for  $\alpha = 0$ , a acceptable conformity with BL is achieved with a MAD of 0.011.

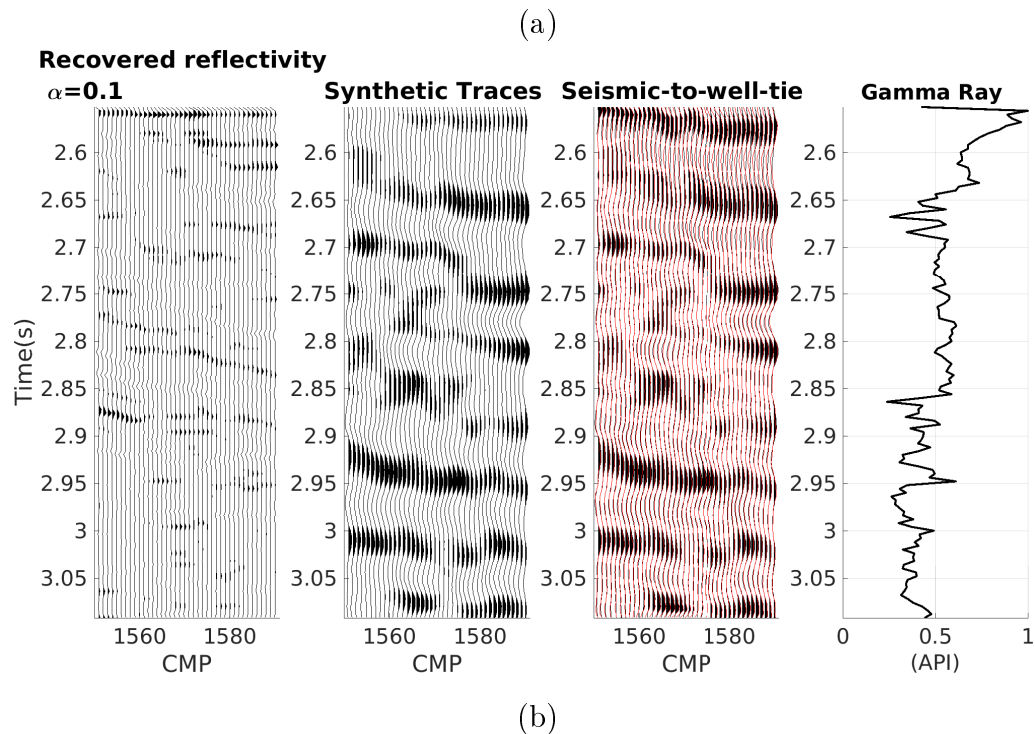


Figure 6.5: a) The recovered reflectivity from the seismic section near the well B when the regularization parameter that controls the sparsity of the solution is set to  $\alpha = 0.1$  b) The Benford distribution of the estimated reflectivity from the seismic section for  $\alpha = 0.1$ , a close conformity with BL is achieved with a MAD of 0.0057.

High correlation values suitable for the exploitation stage were achieved for the well tie in this study, but the methods we proposed are still strongly dependent of a accurate time-depth relationship, since it is used to place the reflectivity in the desired domain (time or cepstral) to perform the wavelet extraction. For both wells, the Viking Graben dataset has VSP data to use as checkshot for the time-depth conversion. Keys (1998) mentioned problems during the acquisition of VSP data for the well A, and VSP data from a well named well C was acquired and attributed to the well A. The report does not mention the distance between the wells. Moreover, although the deterministic wavelet estimation through the homomorphic and in time deconvolution does not require the wavelet's phase, they still assume a stationary wavelet, which does not occur in reality since the seismic pulse is always under attenuation effects as it propagates.

For future studies, we propose the application of the borehole enlargement correction on well tie using a method to estimate the wavelet that does not assume the wavelet's phase. Moreover, it is interesting the investigation of methods capable to correct a damaged time-depth relationship for the well-to-seismic-tie, without using the unrecommended stretch-squeeze to fit the synthetics to the real data, and methods to estimate the wavelet that does not take into account both the minimum-phase and stationarity assumptions.

This research proposed a few tools for some of the objections to the standard well-to-seismic-tie procedure such as the influence of the drilling environment on the quality of well data acquisition; the well log edition considering not only the environmental noises but also the possible errors relative to the well geometry and how methods to estimate the wavelet that are not based on the classical assumptions of the convolutional model affect the quality of the tie. Those factors elucidates that a good wavelet estimation by conventional methods is not the only factor that influences the obtaining of satisfactory well-to-seismic-tie, which is a valuable tool present in seismic processing and interpretation to achieve the main focus of geophysics: a reliable estimate of the physical properties of the Earth.

## BIBLIOGRAPHY

- Geyer, A. and J. Martí, 2012, Applying benford's law to volcanology. *Geology*, **40**(4), 327–330.
- Keys, R.G., 1998, Comparison of seismic inversion methods on a single real data set, open file publications. Society of Exploration, Tulsa, OK.
- Macedo, I. A. S. de, C. B. da Silva, J. J. S. de Figueiredo and B. Omoboya, 2017, Comparison between deterministic and statistical wavelet estimation methods through predictive deconvolution: seismic to well tie example from the North Sea. *Journal of Applied Geophysics*, **136**, 298–314.
- Macedo, I. A. S. de and J. J. S. de Figueiredo, 2018, Using benford's law on the seismic reflectivity analysis. *Interpretation*, **6**(3), T689–T697.
- Margrave, G.F., 2013, Why seismic-to-well ties are difficult. the 25th Annual Report of the CREWES Project.
- Oldenburg, D., S. Levy and K. Whittall, 1981, Wavelet estimation and deconvolution. *Geophysics*, **46**(11), 1528–1542, doi:10.1190/1.1441159.
- Sambridge, M., H. Tkalčić and A. Jackson, 2010, Benford's law in the natural sciences. *Geophysical research letters*, **37**(22).
- Schroeder, W.F., 2006, Lecture notes in well-seismic ties.
- Sottili, G., D. M. Palladino, B. Giaccio and P. Messina, 2012, Benford's law in time series analysis of seismic clusters. *Mathematical Geosciences*, **44**(5), 619–634.
- White, R.E. and Simm, R., 2013, Tutorial: good practice in well ties. *First Break*, **21**(10).
- Yilmaz, O., 2000, *Seismic data analysis: processing, inversion, and interpretation of seismic data*. SEG Books.